Master's thesis

NTNU
Norwegian University of Science and Technology
Faculty of Natural Sciences
Department of Chemistry

Sylvia Weging

Study of trace elements, natural organic matter and selected environmental toxicants in soil at Mitrahalvøya, to establish bias correction for studies of long-range atmospheric transported pollutants in Ny-Ålesund

Master's thesis in Environmental Toxicology and Chemistry
Supervisor: Øyvind Mikkelsen
Co-supervisor: Patricia Aguilar Alarcon
June 2021

NTNU
Norwegian University of Science and Technology

UNIS
The University Centre in Svalbard

Sylvia Weging

Study of trace elements, natural organic matter and selected environmental toxicants in soil at Mitrahalvøya, to establish bias correction for studies of long-range atmospheric transported pollutants in Ny-Ålesund

Master's thesis in Environmental Toxicology and Chemistry
Supervisor: Øyvind Mikkelsen
Co-supervisor: Patricia Aguilar Alarcon
June 2021

Norwegian University of Science and Technology
Faculty of Natural Sciences
Department of Chemistry

NTNU
Norwegian University of
Science and Technology

Abstract

The Arctic archipelago Svalbard is an important receptor for long-range atmospheric transported contaminants. However, local emission sources exist as well, but have been only documented in few studies. Accelerated solvent extraction (ASE) along with gas chromatography (GC) coupled to single quadrupole mass spectromety (MS) has been widely used for the extraction and quantification of PAHs and PCBs in solid environmental matrices, but with the drawbacks in previous methods of e.g. distinct GC separation protocols for PAHs and PCBs, demanding more time and cost for analysis. In this study, surface soil samples were collected in the vicinity of Ny-Ålesund and on two locations remote from the settlement: Kiærstranda and Mitrahalvøya and analyzed for elements As, Cd, Cr, Cu, Ni, P, Pb and Zn, PAH and PCB content as well as total carbon (TC), total nitrogen (TN), biologically labile total organic carbon (TOC400), residual oxidizable carbon (ROC), total inorganic carbon (TIC900). The aim of this study was to to develop an ASE-GC-single quadrupole-MS method for the simultaneous extraction, cleanup, detection and quantification of PAHs and PCBs in Arctic surface soils. With this methodology, current data on the concentration of PAHs and PCBs in Artic soil was reported and related to the profile of inorganic contaminants measured in the Arctic soil to (1) identify possible contamination sources of PAHs, PCBs and trace elements and to (2) examine spatial variations of contaminant concentrations in different areas of the Arctic. Analysis of elements revealed more than 10-fold higher concentrations of Cd in Kiærstranda (4.15-4.49 µg g^{-1}) than the other study areas (0.10-0.51 µg g^{-1}). Together with significantly higher TN and P levels at Kiærstranda, these findings suggest a transfer of Cd by seabirds from the marine food web to terrestrial environments as a potential source. Other elements did not show statistically significant spatial variation. Mean As, Cr, Cu and Ni levels in surface soils from this study were higher than reported values in surface soils from Norway. Different sources may have contributed to found levels in surface soils, such as the local bedrock. The developed method for the simultaneous extraction, cleanup, separation and quantification of PAHs and PCBs proved to be successful with recoveries between 80-106%, precision with RSD < 15% and limits of detection (LOD) between 0.67-6.67 ng g^{-1} for PAH and PCB target analytes. The developed method was applied to analysis of sampled surface soils for 16 U.S. EPA PAHs and 7 indicator PCBs. Levels of PAHs and PCBs were <LOD for samples from Mitrahalvøya. 10 of 16 PAH target analytes were above detection limits in Ny-Ålesund and Kiærstranda with $\sum$PAH levels ranging from 12.4-533.6 ng g^{-1}. An alkylated PAH compound that has been documented to be a dominating compound in Svalbard coal, retene, has been confirmed in soil samples from the vicinity of Ny-Ålesund. Spatial variation of PAH concentrations was noted in samples from Ny-Ålesund area. Moreover, the presence of heavier molecular weight PAHs, could be confirmed in the vicinity of Ny-Ålesund and on Kiærstranda, suggesting that local sources contribute more likely than long-range atmospheric transport to PAH

levels quantified in soils from these study areas. The dominance of PHE, NAP and FLU, the presence of retene as well as PAH indicator ratios point towards a mixture of unburnt coal and combustion of coal and fuel being likely sources for PAHs found in soils from Ny-Ålesund. 5 of 7 PCB target analytes were >LOD in two samples on Brøggerhalvøya with $\sum$PCB levels between 37.9-45.9 ng g^{-1}. The proximity to the shore of the two sampling locations possibly points towards influences from oceanic currents or transfer by seabirds from the marine food web as potential PCB sources to these locations.

Keywords: PAHs, PCBs, trace elements, soil, Arctic, Svalbard

Acknowledgements

This thesis is the final part of the Master's degree programme "Environmental Toxicology and Chemistry" with specialisation in Environmental Chemistry at the Department of Chemistry, Norwegian University of Science and Technology (NTNU). There are many people I would like to thank for their contributions to this master thesis project.

First, I want to thank my first supervisor Øyvind Mikkelsen for giving me the possibility to undertake a very interesting project in a remote region on Svalbard, which is unique itself. I am very thankful for the guidance through the application for the Arctic Field Grant. Moreover, I am thankful for the help during the fieldwork, particularly on Mitrahalvøya and carbon and nitrogen analysis. In addition, I want to express my gratitude for the guidance through later stages of my project and constructive feedback on my thesis.

In particular, I want to thank my second supervisor Patricia Aguilar Alarcon for all the guidance through establishing a methodology for the extraction and analysis of PAHs and PCBs in my soil samples. This part of my project would not have been put into practice without her. Moreover, I want to thank Patricia for the help at later stages of the thesis and the thorough feedback on my thesis.

Another important person for this project was clearly Susana Villa Gonzalez, where I am very thankful for the numerous hours spent and helped out with establishing a GC temperature programme and SIM programme. Moreover, I am thankful for her support during operation of the GC as well as for the help with the analysis of retene.

I also want to thank Anica Simic for the guidance through microwave digestion as well as her contribution to analyze my samples with ICP-MS. This part of my project would not have been possible without her.

I am grateful for the funding for the fieldwork in Ny-Ålesund by the Arctic Field Grant. Furthermore, I am very thankful that I was accepted as a guest master student at UNIS, which enabled me to spend parts of my thesis there in an inspiring environment.

I would like to thank Matthias Henkies for reviewing and for the constructive feedback on my thesis.

I also want to thank my family and friends for their love and support.

Contents

List of Figures

List of Tables

List of abbreviations

ANOVA	Analysis of variance
ASE	Accelerated solvent extraction
DE	diatomaceous earth
EI	Electron impact ionization
GC	Gas chromatography
ICP-MS	Inductively-coupled plasma mass spectrometry
ISTD	Internal standard
K_{OA}	n-octanol-air partition coefficient
K_{OW}	n-octanol-water partition coefficient
LOD	Limit of detection
LLOQ	Lower limit of quantification
LMW PAHs	Low molecular weight PAHs
HMW PAHs	High molecular weight PAHs
LRAT	Long range atmospheric transport
MF	Matrix factor
ME	Matrix effect
MM	Matrix match sample
MS	Mass spectrometry
m/z ratio	mass-to-charge ratio
PAHs	Polycyclic aromatic hydrocarbons
PCBs	Polychlorinated biphenyls
R_{abs}	Absolute recovery
R_{rel}	Relative recovery
ROC	Residual oxidizable carbon
RR	Relative response
RSD	Relative standard deviation
RT	Retention time
SD	Standard deviation
SIM	Selected ion monitoring
SOM	Soil organic matter
SP	Spike sample
TA	Target analyte
TC	Total carbon
TIC900	Total inorganic carbon
TIC	Total ion chromatogram
TN	Total nitrogen
TOC400	Biologically labile total organic carbon
3-F-CHR	3-Fluorochrysene
3-F-PHE	3-Fluorophenanthrene
4-F-BP	4-Fluorobiphenyl
NAP	Naphthalene
ACY	Acenaphtylene
ACE	Acenaphthene
FLU	Fluorene
PHE	Phenanthrene
ANT	Anthracene
FLT	Fluoranthene
PYR	Pyrene
BaA	Benzo[*a*]anthracene
CHR	Chrysene
BbF	Benzo[*b*]fluoranthene
BkF	Benzo[*k*]fluoranthene
BaP	Benzo[*a*]pyrene
IND	Indeno[1.2.3-*cd*]pyrene
DBA	Dibenzo[*a,h*]anthracene
BgP	Benzo[*ghi*]perylene
BDE	Brøggerdalen (east side ofBayelva)
BDW	Brøggerdalen (west side of Bayelva)
GB	Gåsebu
KI	Kiærstranda
NDM	Nordre Diesetvatnet (Mitrahalvøya)

CHAPTER 1

Introduction

Arctic ecosystems are considered to be remote [10], such as the area of Ny-Ålesund, located on Svalbard (74-81°N). However, anthropogenic activities at lower latitudes have shown to markedly influence polar regions through climate change and long-range atmospheric transport of pollutants such as polycyclic aromatic hydrocarbons (PAHs), polychlorinated biphenyls (PCBs) and trace elements, for instance As, Cd and Pb [9, 17, 113]. PAHs, PCBs and trace elements, such as Cd, show adverse health effects on both human health and ecosystems, for instance toxic effects to the kidney, reproductive and nervous systems, as well as mutations and endocrine disruption [9, 97, 120]. Moreover, they have a potential to undergo long-range atmospheric transport [9, 171, 199]. PCBs are highly persistent and have been classified as persistent organic pollutants (POPs) by the Stockholm Convention [159] since 2004. Moreover, the persistent, bioaccumulative and toxic (PBT) properties have been emphasized for PAHs, PCBs and heavy metals such as Pb and Cr in parallel initiatives, for instance for PAHs and PCBs in the 1998 Aarhus Protocol on POPs [124, 190]. Recently, it has been shown that PAH levels in Arctic air are not decreasing despite global reductions of emissions [208]. The increased awareness about these concerns has led to listing PAHs as "chemicals of emerging concern in the Arctic" [21]. Surface soil has been shown to be a suitable matrix for studying atmospheric deposition of long-range atmospheric transported contaminants, since it receives and accumulates contaminants from the atmosphere through wet and dry deposition as well as from melting snow [113, 133]. Moreover, soil organic matter (SOM) shows a high affinity to bind to organic contaminants and metals [82, 133, 171]. Thus, surface soils play an important role in the global cycling of contaminants such as PAHs, PCBs and trace elements, such as Cd and Pb [82, 113, 133, 212].

Svalbard has been selected as a suitable location for studying long-range atmospheric transport due to its remoteness from main industrial areas in Europe and Asia as well as its central location in the high Arctic [17]. However, local sources of pollution on Svalbard such as former coal mining activities in the main settlements Longyearbyen and Ny-Ålesund exist as well [69] and studies on the influence of local pollution that may bias distribution patterns of long-range atmospheric transported pollutants in Svalbard soil are scarce [17, 113, 192]. Efficient extraction procedures and sensitive analytical methods are required to detect and quantify compounds, such as PAHs and PCBs in soils, since they have been reported to occur in low (ng g^{-1}) concentration range on Svalbard [17, 113, 212]. Accelerated solvent extraction (ASE) with gas chromatography coupled to single quadrupole mass spectrometry (GC-MS) has been widely used for extraction, separation, detection and quantification of contaminants such as PAHs and PCBs in solid environmental matrices, for instance in soil and sediment [3, 27, 143]. Past studies have established methodologies for extraction, separation and

quantification of PAHs and PCBs in soil [140, 210, 122]. However, the disadvantages of previous methodologies, such as separate GC separation protocols for PAHs and PCBs [210], which require more time and costs, have highlighted the need for a methodology for the simultaneous extraction, cleanup, detection and quantification of PAHs and PCBs in surface soil, using ASE and selected ion monitoring (SIM) with GC-single quadrupole MS. Therefore, the aim of this study was to to develop an ASE-GC-SIM-MS method for the simultaneous extraction, cleanup, separation and quantification of PAHs and PCBs in Arctic surface soils. With this methodology, current data on the concentration of PAHS and PCBS in Artic soil was reported and related to the profile of inorganic pollutants measured in the Artic soil with the goal of: (1) Identifying possible contamination sources of PAHs, PCBs and trace elements and (2) examining spatial variations of concentrations of contaminants in different areas of the Arctic.

CHAPTER 2

Theory

2.1 Long-range atmospheric transport of contaminants to the Arctic

It is documented that contaminants can reach the Arctic by different pathways, mainly by ocean currents, sea ice, large Arctic rivers, pelagic organisms and migratory birds [10]. An additional pathway, long-range atmospheric transport is of particular importance for the presence of volatile and semivolatile contaminants in the Arctic [10]. The importance of long-range atmospheric transport from lower latitudes differs between winter and summer [203]. In winter, a low pressure over the North (Aleutian Low) and Atlantic Oceans (Icelandic Low) and high pressures over the continents are prevailing (Siberian High) [10]. Consequently, the mean circulation of air masses goes from the northern Eurasia through the Arctic and then towards North America [103, 203]. In summer, the low pressure over the oceans becomes weaker and high pressure cells over the continents vanish. Consequently, the northward transport from low latitudes becomes less [10]. In summer, the mean circulation goes from the North Atlantic Ocean across the Arctic and towards the northern Pacific Ocean [203]. Moreover, the Arctic front, which acts as a meteorological barrier, recedes towards the north in summer [203]. Consequently, transport of contaminants from high latitude sources becomes less important [203]. With atmospheric transport, compounds generally migrate from lower latitudes with higher temperatures, where emission is favored, towards higher latitudes with colder temperatures where deposition is favored [198, 199]. Different mechanisms by that contaminants can reach the Arctic are hypothesized, one of them being global distillation, i.e. the fractionation according to the mobility of a compound in the atmosphere [199]. Measures for the mobility of a compound in the atmosphere can be the octanol-water partition coefficient (log K_{OW}) and octanol-air partition coefficient (log K_{OA}) [60, 200, 199]. The higher the log K_{OW} and log K_{OA}, the lesser will be the mobility of the compound, i.e. it will deposit closer to the emission source and not move further [199]. In general, organic compounds with log K_{OW} being < 6 and a log K_{OA} < 8 are considered to be very mobile in the atmosphere and to reach remote polar regions [5, 199]. Examples are PCBs with 1-4 chlorine atoms (e.g. PCB-28 and 52) and PAHs with lower molecular weight (e.g. fluorene and phenanthrene). Another mechanism, the 'grasshopper effect' is discussed as well [68, 199], where compounds deposit on surfaces such as soil after emission and revolatilize again, migrating by 'multi-hops' towards colder regions, such as the Arctic [199].

Metals, such as Pb, Hg, Zn, Cd and As, can undergo long-range atmospheric transport as well [132, 137, 170]. A large fraction of heavy metals are emitted in the form of aerosols that can be transported to up to a few thousands of kilometers via the atmosphere, depending on the particle size [9, 24]. Larger aerosol particles are deposited closer to their source of origin and have impacts

for the environment on the local scale [9]. Some elements, such as Hg can travel long distances via the atmosphere in gaseous form and can reach remote regions, such as the Arctic where they are frequently measured in air, for instance at Zeppelin station, Ny-Ålesund, svalbard [11, 26]. Although emissions of the major heavy metals including Cd and Pb have been markedly decreasing since the 1980s [25], some elements such as Cd have been detected at elevated levels on remote locations of Svalbard [17]. Strong correlations with soil organic matter as well as elevated levels found in vegetation suggest that metals such as Cd still enter Arctic terrestrial ecosystems through adsorption by soil organic constituents after atmospheric deposition from remote emission sources [17].

2.2 Soil as a suitable matrix to monitor pollution

A soil is a natural three-dimensional entity that which has formed on the surface of the Earth as a result of climate, flora, fauna, relief, parent material and time [156]. A general soil profile from the surface towards deeper horizons consists of an O-horizon, i.e. the surface soil, where soil organic matter (SOM) decomposition processes occur, an A-horizon, where SOM is present in mixture with the mineral fraction, a B-horizon which is characterized by clay accumulation and low SOM content and a C-horizon, which consists of soil parent material [191]. The Arctic environment is characterized by long and very cold winters and short, cold summers with 24 hours of daylight in summer and darkness in winter. For instance, mean temperature in July is ranging between 3-5°C in the more northern part of the Arctic in general [182]. Therefore, development of soils in the Arctic is dominated by cryogenic processes, such as freeze-thaw, resulting in the formation of permafrost-affected soils [182]. A permafrost-affected soil is built up of three layers: (1) the active layer, (2) the transition layer, and (3) the permafrost layer [30]. In general, the thickness of the active layer can vary between 0.1 m (at higher latitudes) and > 10 m at lower latitude regions. The extent of soil formation and content of organic carbon is greater in the active layer [30]. Soils in the Arctic are generally poorly developed, showing a relatively low soil organic matter (SOM) content [182]. The permafrost on Svalbard is continuous, and has a temperature of approximately -2.8°C [32]. The depth of zero annual temperature variation is 5.5 m (1997-2017) [32]. In general, organic matter in soil is characterized by a wide range of chemically and physically variable organic compounds, such as lipids, proteins, polysaccharides, lignin and humic substances as well as combustion-related black carbon or char materials [4]. Humic substances are dominating among organic components in soil [174]. They are very heterogeneous compounds showing a wide range of molecular mass, from a few hundred to several hundred thousand Daltons [174]. Humic substances are operationally clustered into three major fractions: fulvic acids, humic acids, and humin, according to their solubility in e.g. dilute acids [4]. Soils represent an important sink for organic pollutants as well because they receive and accumulate organic contaminants from atmospheric deposition due to the high affinity of SOM to bind to organic contaminants [82, 133]. Moreover, sorption and desorption of less polar and nonpolar organic pollutants by soils are important processes that control their transport and fate in groundwater and surface water systems [82]. Heavy metals can be retained in soils as well through chelation, complexation, and adsorption reactions by the high number of exchange sites of humic substances [171]. Next to the atmospheric net deposition, the concentrations of pollutants in surface soil is determined by losses due to volatilization, biodegradation and burial to deeper layers [133]. Degradation processes of organic pollutants in the surface soil are slow and take decades or more [133]. In particular in the Arctic, persistance of organic compounds is favored due to the cold climate, limited sunlight and less biological activity [133, 198].

2.2.1 Soil and sediment sampling and pretreatment - considerations and limitations

Soil sampling and sample preparation are the first steps in soil analysis as well as the most important steps for a more reproducible and comparable analysis of soil [193, 194]. Sampling of soil should be carried out on representative locations with which a certain area can be characterized [193]. There area three major types of soil sampling: random, stratified random and systematic sampling [139], which are also included in the ISO routines for soil sampling [85]. Random sampling includes collection of samples in a random manner within an area of interest. It is the simplest type and samples can be collected quickly. However, the soil samples obtained from random sampling may be not representative for a study area [139, 205]. Stratified random sampling involves breaking down the population into subgroups and taking a random sample from each subgroup. With this type of sampling, the accuracy and precision of the population estimate can be increased [139]. With systematic sampling, sample collection occurs in a systematic manner, for instance in equal distance from each other within a study area or in a sampling grid [139]. A surface soil sample is usually collected with a spatula and then put in a sample container. For instance, metal-free containers, such as paper bags are recommended as soil sample containers for the analysis of trace elements [152]. Each soil sample should be labelled with a unique number and sampling date and GPS-coordinates of the sampling location should be noted [48]. Once the samples arrive at the laboratory, they have to be spread out on e.g. polyethylene sheets and to be dried [48]. Air drying at room temperature is one possible drying method [48]. Further steps in the sample pretreatment process include homogenization, for instance with mortar and pestle, and sieving and storage until further analysis [48]. Sieving is usually carried out at 2 mm mesh and the resulting 'fine earth' fraction is further processed. Larger particles are removed, such as stones and roots [157]. Importantly, all sources of contamination should be avoided during sampling and sample pretreatment [193]. Contamination can take place at every step within the analytical process and becomes more problematic with decreasing concentration of the analyte to be measured [48]. For instance, contamination with metals can occur from dust, plastics or certain paints in the laboratory [48].

2.2.2 Carbon and nitrogen analysis with automated C/N analyzer

Due to the affinity of SOM to bind organic contaminants and to capacity to retain metallic cations, soils containing a relatively high amounts of SOM show a greater tendency to accumulate organic contaminants and metallic cations [78, 133, 191]. It is expected that with increasing concentration of SOM in soil, the presence of organic contaminants and metallic cations will be more likely, i.e. concentrations will increase [78, 191]. Soil organic matter as well as inorganic fractions can be determined separately as soil carbon and nitrogen fractions with dry combustion techniques. There, organic carbon and nitrogen in samples are oxidised and inorganic carbonates are thermally decomposed by applying heat [45]. Commonly applied dry combustion methods include loss on ignition (LOI) and automated Carbon/ Nitrogen (C/N-) analyzers. While LOI is a semi-quantitative method, estimating a fraction that is combusted at e.g. 550°C as soil organic matter (SOM) by gravimetric mass loss [81], analysis of samples with an automated C/N analyser is a quantitative and a more precise approach [45], measuring C and N directly as CO_2 and N_2, respectively. Moreover, automated C/N analyzer systems allow a higher sample-throughput and necessitate a lower sample amount than LOI [45]. A common dry combustion method for N-determination is the DUMAS methodology which involves the reduction of nitrogen oxides with copper (Cu) to nitrogen (N_2) at 600°C and is usually integrated in C/N-analyser systems [40]. There are individual models of automated C/N analyzer systems commercially available from different manufacturers, one of

them being Primacs^{SNC100} from Skalar Analytical B.V. (Breda, NL) that was used in this study. Fig. 2.1 shows the workflow of the Primacs^{SNC100} for the determination of total carbon (TC) and total nitrogen (TN) in environmental samples. For TC and TN analysis with this model, the sample is first automatically introduced into the a high-temperature oven where full combustion is achieved at 1200°C and oxygen gas (O_2) supply. During the combustion process, C is converted to CO_2 and N is converted to NO, NO_2 and other gaseous N_xO_y compounds. This gas mixture is further transported by helium as a carrier gas towards a splitter where a part of the gas mixture is collected and will be led to the reduction oven. The remaining gas is led towards the nondispersive infrared detector (NDIR) which detects CO_2. In the reduction oven, oxidised nitrogen compounds are reduced to N_2 following the DUMAS methodology. Then, resulting N_2 is detected with a thermal conductivity detector (TCD). As a last step before N_2-detection, the gas stream is led through scrubbers for CO_2 and H_2O removal [162].

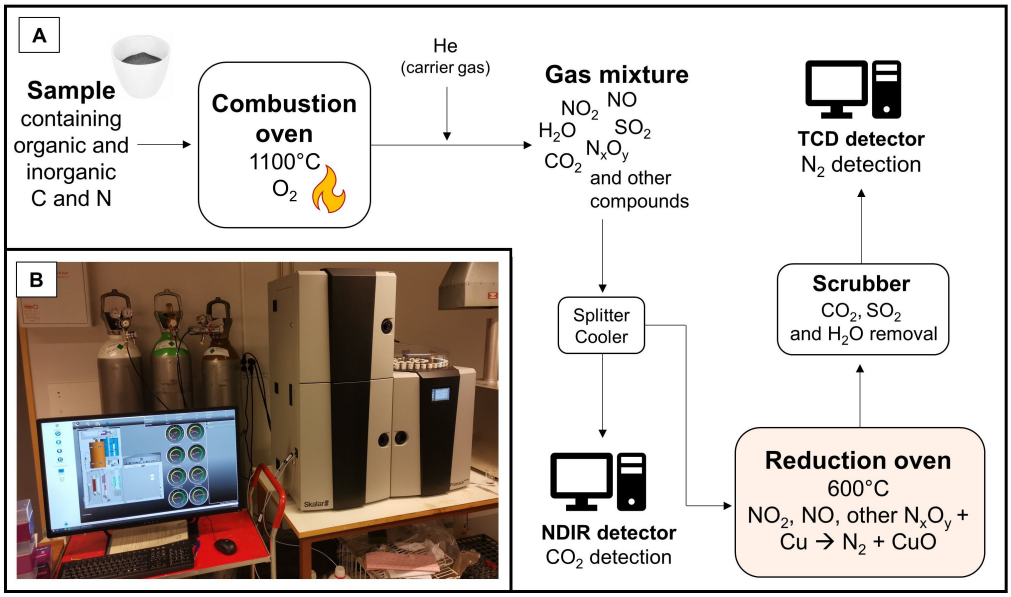

Figure 2.1 – Schematic overview about the workflow of the automated Carbon/ Nitrogen analyser used in this study for the example of total carbon (TC) and total nitrogen (TN) analysis (A) and photograph of the Primacs^{SNC100} instrument at NTNU Trondheim, Department of Chemistry that was used in this study (B).

Next to TC and TN, additional carbon fractions can be determined with the Primacs^{SNC100} C/N analyzer by applying different temperature programmes. For instance, a stepwise combustion of a sample at 400°C, 600°C and at 900°C can be carried out to obtain biologically labile organic carbon (TOC400), residual oxidizable carbon (ROC) and total inorganic carbon (TIC900), respectively [50, 162], which in sum give the TC content (Eq. 2.1).

$$TC = TOC400 + ROC + TIC900 \tag{2.1}$$

2.3 Trace elements

This study investigated the presence of selected elements in surface soil from Svalbard: arsenic (As), cadmium (Cd), chromium (Cr), copper (Cu), nickel (Ni), phosphorus (P), lead (Pb) and zinc (Zn). The elemental composition of surface soils in remote regions is influenced by the local bedrock, but also by interactions with biota and the atmosphere [172]. Next to natural sources, such as volcanic eruptions and soil erosion [130], anthropogenic activities have been significantly contributing on a global scale to concentrations of elements found in environmental compartments [130, 137]. Fossil fuel combustion, non-ferrous metal production, and waste incineration have been identified as the three major anthropogenic sources of heavy metals to the atmosphere [9]. For elements, such as Pb, Hg, Zn, Cd and As, long-range atmospheric transport from anthropogenic releases has been documented to be an important contributor to levels found in environmental compartments such as soil and moss in Norway [132, 170]. However, local sources of pollution of metals to terrestrial ecosystems such as former coal mining activities and coal combustion in the vicinity of Arctic settlements have to be considered as well [37, 80]. Elevated concentrations of iron (Fe), aluminium (Al) and magnesium (Mg), but also Zn, Ni, Co and As can occur in proximity to mining sites [37].

2.3.1 ICP-MS

The analysis of the elemental composition in soil samples with instrumental atomic spectrometry techniques such as inductively-coupled plasma mass spectrometry (ICP-MS) has widespread application in environmental studies [46, 132, 172]. It aids the study of elemental distribution profiles in soils, in order to gain further knowledge on their geochemical status and to identify potential pollution sources of heavy metals in a study area of interest [17, 72]. In comparison to other atomic spectrometry techniques, the most important benefits of ICP-MS are the capacity of analysing multiple elements in a single analysis and to achieve detection limits up to ppt levels [204]. An ICP-MS instrument comprises the following compartments: (I) sample introduction, (II) plasma source, (III) interface region, (IV) ion focusing, (V) mass analyser and (VI) detector. Fig. 2.2 shows the compartments II-VI.

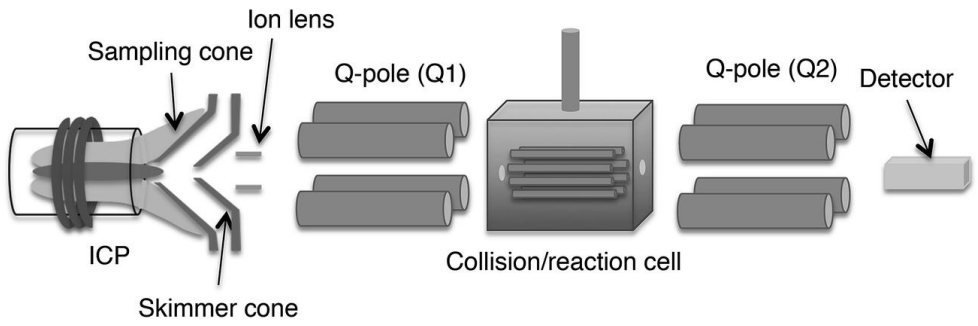

Figure 2.2 – Schematic overview of an ICP-MS system with a triple quadrupole mass analyser. Adopted from Ref. [134].

In order to analyze solid samples such as soils with ICP-MS, it is required that the sample is dissolved or leached, since the nebulizer, that is used for sample introduction to the ICP, requires the sample in most cases to be liquid [138]. Preparation of solid samples for ICP-MS is usually carried out

using microwave-assisted digestion with strong acids such as HNO_3. It is a fast technique and uniform heating of samples is achieved, since microwave energy is directly absorbed by the solution. High pressure can be applied and using closed vessels for samples during digestion minimize the cross-contamination risk [48].

When a sample is analyzed with ICP-MS, it is introduced into a spray chamber with a nebulizer first which creates droplets in mixture with argon gas. Larger droplets are filtered out in the spray chamber and the resulting fine aerosol is injected into the plasma torch. Small enough droplets are important for achieving sufficient ionization in the plasma [158]. The plasma results from the argon gas being in tangential flow in the plasma source region and interaction of argon gas with a strong magnetic field that is induced by a high frequency current [183]. This current is supplied through a copper coil that is connected to a radio frequency (RF) generator (coil and torch illustrated in Fig. 2.2. Through the interaction, argon atoms get ionized and when a high-voltage spark is applied, a high temperature plasma discharge ($\sim$10,000 K) results [183, 204]. A plasma is a gaseous mixture of electrons and positively charged ions. For the majority of ICP-MS instruments, argon is used as gas for plasma generation [204]. Due to interaction of argon gas with a strong electromagnetic field originating from induction in the region surrounded by a copper coil (illustrated in Fig. 2.2) that is supplied with radio frequency power and application of a high-voltage spark at the plasma source, multiple collisions between accelerated electrons, argon atoms and ionized argon atoms occur [204]. As a consequence of friction between these species, it becomes very hot in the plasma area ($\sim$10,000 K) and a lot of energy is available for these species to collide with analyte compounds [119, 204]. This serves as the basis for vaporization of analyte compounds into molecules, following atomization and ionization, once the aerosol with sample arrives at the plasma source [126]. Moreover, excitation of electrons in analyte atoms occurs [126]. In the interface region, ions formed in the hot dense plasma at atmospheric pressure conditions are extracted and accelerated towards the mass analyzer with the help of a sampler cone, a skimmer cone, applying vacuum and focusing the ions with electrostatic lenses [204]. These ions are then further accelerated towards the mass analyzer through the interface region which consists of two cones: a sampler cone and a skimmer cone, each of them having a small orifice in the center [48]. At the mass analyzer ions get separated according to their mass to charge (m/z) ratio [158]. High vacuum in this part of the ICP-MS is important, since it prevents collisions between ions. Collisions would negatively influence the capacity of separating ions with different m/z ratio [158]. One of the mass analysers commonly used for ICP-MS is the triple quadrupole mass analyser. It consists of a collision cell and two quadrupoles. A quadrupole contains four parallel cylindrical metallic rods that are positioned in parallel to each other forming a square array [116]. To these rods, radio frequency alternating current (AC) and direct current (DC) potentials are applied. Consequently, a time-varying electric field in the centre of the four rods is created [116]. Depending on the combination of AC and DC potentials, only ions with the appropriate m/z ratio move along stable trajectories in this electric field and reach the detector which converts the arriving ions into an electric signal [204, 183].

2.4 Organic pollutants: polycyclic aromatic hydrocarbons (PAHs) and polychlorinated biphenyls (PCBs)

Polycyclic aromatic hydrocarbons (PAHs) are organic compounds, composed of at least 2 fused benzene rings (Fig. 2.3) [22, 97]. They are a subgroup of polycyclic aromatic compounds (PACs) to which a high number of different compounds belong to [22]. In comparison to PACs, PAHs contain only carbon and hydrogen [1].Table 2.1 describes some physico-chemical properties for 16 PAH compounds shown in Fig. 2.3 that were classified as priority pollutants by the United States

Environmental Protection Agency (U.S. EPA) in 1976 [93]. They are commonly used in environmental monitoring studies, for example in [113, 140, 192], and were selected as well as target analytes for the current study. PAHs detected in the environment can originate from natural and anthropogenic releases [97]. There are three major processes that lead to the formation of PAHs and that categorize them into (I) pyrogenic, (II) petrogenic and (III) biogenic PAHs [175]. Pyrogenic PAHs form through pyrolysis or incomplete combustion of organic material. Natural sources of pyrogenic PAHs include volcanoes and combustion of plant matter during wildfires [97]. Combustion of fossil fuels such as coal and exhaust fumes from cars are examples for anthropogenic sources of pyrogenic PAHs [105]. Petrogenic PAHs originate from the formation of petroleum products by geological processes [175]. Their release into the environment can take place through anthropogenic oil spills as well as natural oil seeps [6]. Biogenic PAHs result from biological precursor compounds that are transformed by chemical or biological processes in the environment [175]. It has been documented that fossil fuel combustion and biomass burning are the major sources for PAHs found in the environment [147, 105, 208].

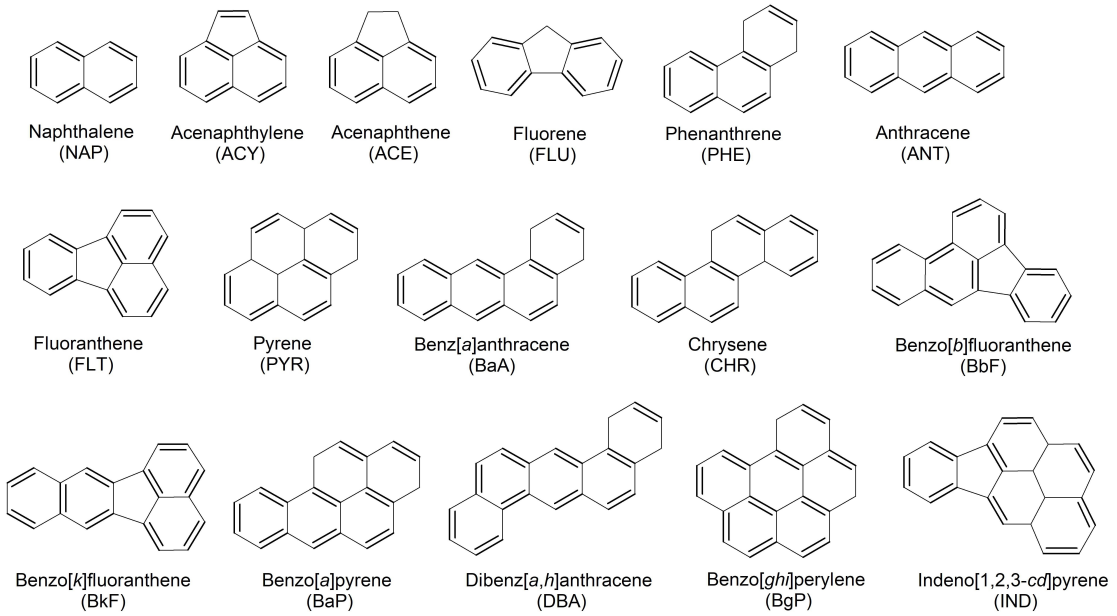

Figure 2.3 – Structural formulas of the 16 US-EPA priority PAHs [93] with Systematic IUPAC name and abbreviation (in brackets) below the respective structural formula. The compounds are ordered according to molecular mass with the lowest at the top left corner and highest in the bottom-right corner See Tab. 2.1 for further compound details.

Polychlorinated biphenyls (PCBs) are a compound class that is characterized by a biphenyl main structure with varying position and degree of chlorine substitution [83, 141].There are 209 individual chlorinated compounds in total, also referred to as congeners [141]. Initially proposed by Ballschmiter and Zell, each congener is numbered from 1 to 209 in a systematic manner, following the IUPAC rules for characterizing the chlorine substitution pattern for biphenyl structures [20]. PCBs were used in mixtures from 1929 until the 1970s as flame retardants, dielectric fluids, and other applications due to their advantageous physico-chemical properties [181] which are mentioned

in Sec. 2.4.1. Common PCB mixture trade names were e.g. Arochlor (United States), Chlophen (Germany), Sovol (U.S.S.R.) and Kanechlor (Japan) [83]. The total global historical PCB production was estimated to roughly 1.3 million tonnes [38]. With time, increasing concern evolved about PCBs because of their high persistence and lipophilicity [120]. As a consequence, PCB production stopped in the U.S. in 1977, in countries within Europe in 1984, while the production continued in Russia until 1993 [39]. Despite their phase-out, PCBs are still detected in environmental compartments, such as the atmosphere [206]. Old electrical equipment such as capacitors, contain PCBs which contaminate waste handling facilities when not properly managed and contribute to PCB emissions to date [13]. There are seven PCB congeners, also referred to as 'indicator-PCBs' (IUPAC numbers 28, 52, 101, 118, 138, 153 and 180) whose concentrations were investigated in this study. They are widely used in environmental monitoring studies (e.g. Refs. [13, 17, 164, 212]), since they occur at higher concentrations than other congeners in environmental samples [181]. It has been estimated that these PCBs account for roughly 18% of total global historical PCB production [39].

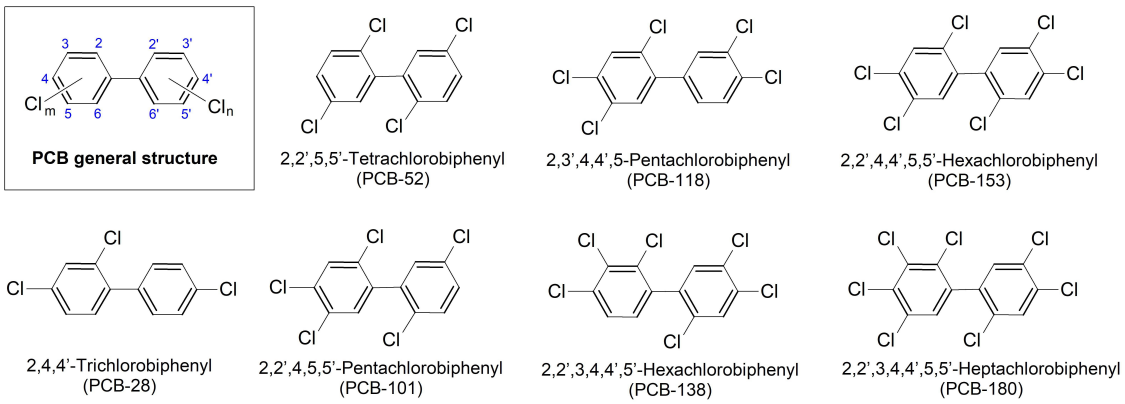

Figure 2.4 – Structures of the 'Dutch Seven' PCBs that were investigated in this study with nomenclature and abbreviation (in brackets below). The compounds are sorted with increasing number according to Ballschmiter and Zell [20] from left to right.

2.4.1 Properties and environmental fate

PAHs exhibit different physico-chemical properties, depending on their molecular mass and structure [97]. An overview is given for selected compounds in Tab. 2.1. According to the number of aromatic rings, PAHs are grouped into (I) low-molecular weight (LMW) PAHs with 2-3 rings and (II) high-molecular weight (HMW) PAHs, having 4 or more fused aromatic rings [179, 97]. In general, PAHs are considered to be hydrophobic and semi-volatile [22]. With increasing molecular mass (M), vapor pressure (given as P_L in Tab. 2.1) is decreasing [97, 135]. Solubility in water (S_{WL} in Tab. 2.1) markedly decreases with increasing number of fused aromatic rings and ring angularity [97, 135] while the n-octanol-water partition coefficient (log K_{OW}) as well as the n-octanol-air partition coefficient (log K_{OA}) increase [2, 155, 127].

Table 2.1 – List of 16 US EPA PAHs, containing name, abbreviation (Abbr.) and respective physico-chemical properties. Number of fused aromatic rings is written over each group of PAH compounds. M is molecular mass. Values for S_{WL} and P_L were adopted from Ref. [135]. S_{WL}, P_L log K_{OW} and log K_{OA} are given at 25°C

	PAH-type & compound name	Abbr.	CAS-number	M (g mol^{-1})	S_{WL} (mol·L^{-1})	P_L (Pa)	Log K_{OW}	Log K_{OA}
LMW-PAHs	**2-ring PAHs**							
	Naphthalene	NAP	91-20-3	128.17	0.42	40	3.35[1]	5.10[4]
	3-ring PAHs							
	Acenaphthylene	ACY	208-96-8	152.20	0.24	1.95	3.94[2]	
	Acenaphthene	ACE	83-32-9	154.21	$5.4 \cdot 10^{-2}$	1.51	3.92[1]	
	Fluorene	FLU	86-73-7	166.22	$1.7 \cdot 10^{-2}$	0.72	4.18[1]	6.68[3]
	Phenanthrene	PHE	85-01-8	178.23	$1.1 \cdot 10^{-2}$	0.11	4.52[1]	7.45[3]
	Anthracene	ANT	120-12-7	178.23	$4.2 \cdot 10^{-4}$	$8.9 \cdot 10^{-2}$	4.50[1]	7.34[3]
HMW-PAHs	**4-ring PAHs**							
	Fluoranthene	FLT	206-44-0	202.26	$2.9 \cdot 10^{-3}$	$7.4 \cdot 10^{-3}$	5.20[1]	8.60[3]
	Pyrene	PYR	129-00-0	202.26	$2.0 \cdot 10^{-3}$	$1.5 \cdot 10^{-2}$	5.00[1]	8.61[3]
	Benz[*a*]-anthracene	BaA	56-55-3	228.29	$8.5 \cdot 10^{-5}$	$5.4 \cdot 10^{-4}$	5.91[1]	9.54[3]
	Chrysene	CHR	218-01-9	228.29	$1.2 \cdot 10^{-5}$	$5.9 \cdot 10^{-5}$	5.86[1]	10.44[3]
	5-ring PAHs							
	Benzo[*b*]-fluoranthene	BbF	205-99-2	252.32	$1.9 \cdot 10^{-5}$	$1.3 \cdot 10^{-6}$	5.78[1]	
	Benzo[*k*] fluoranthene	BkF	207-08-9	252.32	$6.2 \cdot 10^{-6}$	$4.2 \cdot 10^{-6}$	6.11[2]	11.19[3]
	Benzo[*a*]-pyrene	BaP	50-32-8	252.32	$4.5 \cdot 10^{-5}$	$1.5 \cdot 10^{-5}$	6.35[1]	10.77[3]
	Dibenz[*a,h*]-anthracene	DBA	53-70-3	278.35	$1.3 \cdot 10^{-7}$	$9.1 \cdot 10^{-8}$	6.75[1]	
	6-ring PAHs							
	Benzo[*ghi*]-perylene	BgP	191-24-2	276.33	$7.6 \cdot 10^{-6}$	$1.9 \cdot 10^{-6}$	6.63[2]	
	Indeno-[1,2,3-*cd*]pyrene	IND	193-39-5	276.33	$5.8 \cdot 10^{-7}$	$2.3 \cdot 10^{-7}$	6.70[2]	

[1] = according to Ref. [155]
[2] = according to Ref. [127]
[3] = according to Ref. [60]
[4] = according to Ref. [200]

PAHs have a widespread occurrence in the environment and have been detected and quantified in compartments, such as in air, soil, sediment and water from industrial areas [123, 210] as well as regions considered to be remote from local pollution sources [151, 196]. The transport via the atmosphere is the most important pathway for the distribution of PAHs in the environment as well as their occurrence in areas that are remote from emission sources, such as polar regions [63]. When

PAHs are emitted to the atmosphere, they can undergo dry deposition via aerosol particles and wet deposition via snow and rain onto surfaces, such as soil [101].

The importance of deposition processes for the different PAHs depend on their physico-chemical properties, such as vapor pressure (P_L , Tab. 2.1) [95]. Another comprehensive measure to describe the mobility of these compounds in the atmosphere is the n-octanol-air partition coefficient (log K_{OA}). It has been shown to have a good agreement with the gas particle partition coefficient for various compounds, suggesting similar sorption properties of octanol compared to aerosol particles [60]. Moreover, it takes into account the potential of compound retention by surfaces of the terrestrial environment, such as soil and vegetation [199]. LMW PAHs, such as NAP, are predominantly present in the gas phase and undergo reactions there [101], e.g. with nitrogen oxides and ozone, forming nitro-PAHs and quinones, respectively [95]. In particular, compounds with log $K_{OA} < 6$ are considered to be very mobile in the atmosphere and show rather no deposition [200]. At the other hand, HMW-PAHs with 4 or more fused aromatic rings mainly adsorb to the particulate phase, e.g. to aerosols [51, 101]. Among them, compounds with log $K_{OA} > 8$ show rather low mobility and they deposit at lower latitudes close to their emission sources [200]. There are also PAHs that are considered to be semivolatile with log K_{OA} being between 6 and 8 [200]. They usually have 3-4 rings and can distribute between the gas and particulate phase and have the potential to revolatilize from ground surfaces such as soil and to reach polar regions [95, 200]. Soils and sediments are important reservoirs for organic pollutants such as PAHs in the environment due to the hydrophobic nature of PAHs [97]. For instance, Wild and Jones (1995) estimated that more than 90% of total PAHs in the environment of the UK is stored in soils [202].

PCBs are hydrophobic compounds with high lipophilicity [83]. Water solubility of the sub-cooled liquid (S_{WL}) decreases with increasing chlorination degree [160]. Congeners with a high number of chlorine atoms, such as PCB-138 and PCB-180 (Tab. 2.2), are poorly soluble in water [66]. The n-octanol-water partition coefficient (log K_{OW}) increases while the vapor pressure of the sub-cooled liquid (P_L) decreases with increasing chlorination in the biphenyl structure [160] (Tab. 2.2). It is notable that the n-octanol-air partition coefficient (log K_{OA}) increases with increasing chlorine substitution (Tab. 2.2) [104]. In general, PCBs are very resistant to reactions with acids, bases and other chemicals as well as to oxidation [55]. They have great electrical insulation properties [83], high thermal conductivity, are highly resistant to thermal breakdown and show low flammability [55]. .

Table 2.2 – Physico-chemical properties of the Dutch Seven PCBs that were investigated in this study. Vapor pressure of supercooled liquid (P_L) water solubility of supercooled liquid (S_{WL}). Values for Log P_L, Log S_{WL}, Log K_{OW} and Log K_{OA} were acquired from [104] and are given for 25°C (final-adjusted values).

Compound	Abbr.[1]	CAS-number	M (g mol^{-1})	S_{WL} (mol L^{-1})	P_L (Pa)	Log K_{OW}	Log K_{OA}
2,4,4'-Trichloro-biphenyl	PCB-28	7012-37-5	257.54	0.23	$2.7 \cdot 10^{-2}$	5.66	7.85
2,2',5,5'-Tetrachloro-biphenyl	PCB-52	35693-99-3	291.99	0.14	$1.2 \cdot 10^{-2}$	5.91	8.22
2,2',4,5,5'-Pentachloro-biphenyl	PCB-101	37680-73-2	326.43	$3.3 \cdot 10^{-2}$	$2.4 \cdot 10^{-3}$	6.33	8.73
2,3',4,4',5-Pentachloro-biphenyl	PCB-118	31508-00-6	326.43	$2.2 \cdot 10^{-2}$	$1.0 \cdot 10^{-3}$	6.69	9.36
2,2',3,4,4',5'-Hexachloro-biphenyl	PCB-138	35065-28-2	360.88	$6.8 \cdot 10^{-3}$	$5.6 \cdot 10^{-4}$	7.22	9.66
2,2',4,4',5,5'-Hexachloro-biphenyl	PCB-153	35065-27-1	360.88	$1.1 \cdot 10^{-2}$	$6.0 \cdot 10^{-4}$	6.87	9.44
2,2',3,4,4',5,5'-Heptachloro-biphenyl	PCB-180	35065-29-3	395.32	$5.2 \cdot 10^{-3}$	$1.1 \cdot 10^{-4}$	7.16	10.16

[1] according to Ballschmiter and Zell nomenclature [20]

Because of their persistence as well as lipophilic properties, PCBs are widely distributed in the environment and are detected and quantified in various environmental matrices, such as soil and air [17, 44]. Their environmental fate differs, depending on the physico-chemical properties of the congeners. In general, PCBs with 1-4 chlorine atoms and with an octanol-water coefficient (log K_{OW}) < 6 (e.g. PCB-28 and 52, Tab. 2.2) are considered to be very mobile in the atmosphere and to reach remote polar regions [5, 199], where they are continuosly monitored in air, e.g. at Zeppelin station, Ny-Ålesund, Svalbard [118, 206]. Lighter PAHs are more susceptible to atmospheric degradation [75], where the reaction rate with OH radicals determines their lifetime in general [7]. PCBs with a higher chlorination degree and log K_{OW}) > 6 show the tendency to adsorb on aerosols in the atmosphere and to soils and sediments [5] and are less susceptible to degradation in the environment [75]. Due to the lower susceptibility to degradation as well as higher lipophilicity of higher chlorinated PCBs, such as PCB-138 and 153, lead to a higher occurrence in humans and biota [75, 153] (see Sec. 2.4.2 for further details).

2.4.2 Adverse health effects

PAHs are known to exert carcinogenic, teratogenic and mutagenic effects [52, 97]. Moreover, they can bioaccumulate in aquatic food webs [6]. Thus, PAHs are of concern for human and ecosystem health [97, 167]. Reactive PAH-metabolites in living organisms, such as epoxides, can bind to proteins in cells and DNA, which can cause cell damage and result in mutations, cancer and developmental malformations [6, 97]. With increasing molecular weight, carcinogenicity increases while acute toxicity decreases [97]. In particular, 7 HMW-PAH compounds are classified by the International Agency for Research on Cancer (IARC) as carcinogenic to humans (group 1), probably carcinogenic to humans (group 2A), or possibly carcinogenic to humans (Group 2B), namely BaP (group 1), DBA (group 2A) and BaA, CHR, BbF, BkF, IND (group 2B) [84]. Despite the lower carcinogenicity of LMW PAHs, compared to the higher molecular weight PAHs, they show greater potential to react in the environment to oxy- and nitro-PAHs [95]. These derivatives are potentially more toxic than their parent compounds [52].

Among the 209 PCB congeners, the ones with five or more chlorine atoms are of great concern due to their lipophilicity and high biological stability [23, 153]. As a consequence, they biomagnify in aquatic and terrestrial food webs [23]. Particularly, congeners with five or more chlorine atoms and meta-*para* chlorine substitution are slowly biotransformed [33] (*para*-positions: 4 and 4', *meta*-positions: 3, 5, 3', 5', shown in the general PCB structure in Fig. 2.4). For instance, PCB-138, PCB-153 and PCB-180 have been found to be the most dominant congeners in human and wildlife tissues [153]. Furthermore, PCBs have been shown to cause adverse health effects in biota and humans, such as endocrine disruption [153], carcinogenity and neurotoxicity [102]. The chlorine substitution pattern in the biphenyl structure is also an important factor in determining the toxicity of PCBs. Based on the mechanism of toxicity, PCBs can be divided into coplanar and noncoplanar PCBs. Coplanar PCBs have chlorine atoms in both *para*-positions, at least one chlorine atom in *meta*-position of both phenyl rings and no chlorine atom in *ortho*-position [154] (*ortho*-positions: 2, 6, 2', 6', shown in the general PCB structure in Fig. 2.4). Due to their structural similarity to polychlorinated dibenzodioxins (PCDDs) and similar behavior as an antagonist of the aryl hydrocarbon (Ah) receptor as PCDDs, they are also referred to as dioxin-like PCBs [154, 173]. Noncoplanar have several chlorine atoms in ortho-position and show different toxicological behavior than PCDDs. They possess limited affinity towards the Ah-receptor and are therefore also named non-dioxin like PCBs [173]. Congeners with 2 chlorine atoms in ortho-position may act as interfering agents with signaling pathways being important for Ca^{2+}-homeostasis, thus potentially exerting neurotoxic effects [99]. In general, noncoplanar PCBs are less toxic than the coplanar ones, but some noncoplanar PCB congeners are more abundant in the environment and therefore used as indicator compounds in environmental studies [31].

2.4.3 Previous studies on PAHs and PCBs levels in terrestrial compartments on Svalbard

Svalbard, an archipelago in the high Arctic, situated between 74° and 81° North and 10°-35° East, has been in the center of focus for studies on long-range atmospheric transport of pollutants [11]. This is due to its unique location at high latitudes and location between the Eurasian and American continent, which makes it to an important receptor of contaminants that are emitted at mid and low latitudes and transported by air and sea currents to this archipelago [11, 90, 72, 136]. However, local sources of pollution on Svalbard exist as well, but data on local sources of pollutants on Svalbard is scarce [51]. The occurence of PAHs and PCBs has been studied at different locations on

Svalbard, including the main settlements Longyearbyen [51], Ny-Ålesund [197], Barentsburg [86] and Pyramiden [113]. Among PAHs and PCBs, the 16 U.S. EPA priority PAHs and seven indicator PCBs are the most frequently monitored analytes (see selection of studies in Tab. 2.3 and 2.4). There are several studies on the occurence of these PAHs and PCBs in terrestrial compartments on Svalbard, including soil, moss, reindeer faeces, snow and plants, which are presented on the following pages.

The 16 U.S. EPA priority PAHs have been found in different compartments of the terrestrial environment from Svalbard with $\sum_{16}$PAHs usually ranging from a few ng g^{-1} to a few hundred ng g^{-1} (Tab. 2.3), but also comparably high levels were noted in some studies, such as levels up to 11,600 ng g^{-1} in soil from Pyramiden [113]. Local sources such as former coal mining and coal combustion have been identified to be important contributors to PAH levels found in the vicinity of settlements as spatial variations of PAH concentrations were observed [87, 113, 192]. For instance, Marquès et al. (2017) found in soils from the former coal-mining town Pyramiden, collected close to coal and diesel power plants, a heliport and a harbor $\sum_{16}$PAHs levels ranging from 186 to 11,600 ng g^{-1} [113]. The $\sum_{16}$PAHs level was notably lower (52 ng g^{-1}) at a background location in their study that was approximately 2 kilometers away from the settlement [113]. Moreover, in another study on coastal and lake sediments from Ny-Ålesund area, spatial variations in PAH levels were noted as well [87]. In general levels of PAHs in lake sediments, collected closer to Ny-Ålesund settlement were higher ($\sum_{16}$PAHs 27-711 ng g^{-1}) than in coastal sediments ($\sum_{16}$PAHs 27-34 ng g^{-1}) [87]. The authors of that study concluded that local sources may be important for the occurrence of PAHs in Ny-Ålesund area [87]. At the other hand, long-range atmospheric transport has been identified as an important source of PAHs on terrestrial compartments on Svalbard as well. In one study on surface soil, moss, and reindeer dung, collected from the vicinity of Ny-Ålesund, proportions of LMW PAHs in the studied matrices from Ny-Ålesund area were higher and that of HMW-PAHs lower than in matrices from non-Arctic regions [197]. These results suggested that global distillation may have contributed to PAHs detected in Ny-Ålesund area [197].

PCBs have been detected and quantified in terrestrial compartments, such as soil, usually at levels ranging from <1 to a few ng g^{-1} (Tab. 2.4). Differences in the distribution of PCBs between different environmental matrices have been noted by some studies. In particular, levels in vegetation were found to be higher compared to levels in soil [17, 212]. These findings may suggest that the PCBs in vegetation occur from aerosol deposition or ice and snow melting, rather than adsorption from soil through the roots [17, 212]. Local sources of PCBs have been identified on Svalbard as well. For instance, Jartun et al. (2009) found pronounced PCB levels in paint in Pyramiden and Barentsburg with $\sum_{7}$PCBs levels being up to 1,290,000 ng g^{-1} and 3,520,000 ng g^{-1}, respectively [86]. High PCB levels were noted for transformer oils and small capacitors in that study as well [86]. Moreover, in soil at Kinnvika very high PCB levels have been found by Kallenborn et al. (2010) with mean $\sum_{7}$PCBs being 2450 ng g^{-1} [91]. However, in a later survey, markedly lower PCB levels were found with median $\sum_{7}$PCBs being 0.415 ng g^{-1} and the authors of the later study concluded that no further need for remediation or monitoring actions at Kinnvika are needed [59]. Also, in Ny-Ålesund notably high levels of PCBs have been found at the old dumpite at Thiisbukta with $\sum_{7}$PCBs being up to 135 ng g^{-1} [37]. However, in a later study on soils in Ny-Ålesund area, the high PCB-levels in Thiisbukta were found to be an isolated case as $\sum_{7}$PCBs were found to be below detection limits in the later study [34].

Table 2.3 – Comprehensive overview of reported single PAH levels from studies on Svalbard, found in different matrices of the terrestrial environment, including, soil, surface and moss. Values are reported in ng g^{-1} (dry weight basis), unless specified otherwise. NA = not analyzed, LOD = limit of detection

Study area, matrix		NAP	ACY	ACE	FLU	PHE	ANT	FLT	PYR	BaA	CHR	BbF	BkF	BaP	DBA	BgP	IND	$\sum_{16}$PAHs	Ref.
Ny-Ålesund																			
Soil	Mean	12	3	0.4	10	59	5	10	10	7	10	10	8	7	0.5	3	3	157	[196]
	Min	2	0.3	0.1	2	11	1	3	2	0.3	1	2	1	2	<LOD	<LOD	<LOD	37	
	Max	42	5	0.9	20	133	13	20	22	21	23	18	14	14	2	7	7	324	
Moss	Mean	41	9	7	38	72	8	7	5	3	5	6	1.3	6	0.4	4	0.7	213	
	Min	13	5	4	24	63	7	4	3	1	2	<LOD	0.3	0.4	<LOD	<LOD	<LOD	158	
	Max	79	14	13	61	81	9	13	9	6	11	21	4	8	1	14	2	244	
Reindeer dung																			
	Mean	65	8	4	31	48	6	4	3	0.8	1.1	0.5	0.4	0.7	0.4	0.1	0.1	175	
	Min	6	2	0.7	12	15	2	1	1	0.1	<LOD	<LOD	<LOD	0.2	<LOD	<LOD	<LOD	49	
	Max	148	16	7	56	80	10	10	7	3	4	2	2	1	1	0.2	0.2	340	
Ny-Ålesund																			
Surface snow (ng L^{-1})																			
	Median	<LOD	0.95	<LOD	0.7	2.3	2.2	2	3.5	0.4	0.35	2.15	5.4	2.4	4.6	4.4	0.4	8.5	[192]
	Min		0.3		0.4	0.8	0.2	0.6	0.6	0.2	0.02	0.9	3.1	1.2	0.8	0.2	0.3	0.8	
	Max		1.7		17	53	6.7	59	62	17	16	5.9	7.7	7.6	8.4	36	3.2	8.4	
Ny-Ålesund																			
Coal dust[1]		1500	80	140	390	1800	1700	180	260	150	260	130	140	130	<20	<20	<20	6900	[34]
Soil	Min	180	83	81	140	150	52	83	94	64	89	190	93	260	260	90	67	760	
	Max	30000	800	770	1500	9000	2600	22000	18000	13000	10000	18000	7600	18000	2600	6100	6600	139930	
Ny-Ålesund																			
Lake Sediment																			[87]
	Median	60.5	2.1	8	7.7	22.3	1.49	5.1	3.1	-	4.5	3.45	1.9	2.55	3	5.1	2.6	127	
	Min	9.9	0.61	1.5	1.8	3	0.18	1.2	0.68	-	1	1.4	0.88	0.69	0.33	1.3	1	27	
	Max	160	14	29	50	150	18	90	45	-	45	51	41	54	19	49	39	711	
Coastal Sediment																			
	Min	11	0.06	0.97	1.1	3.8	0.17	0.66	0.65	-	1	0.19	0.14	0.18	0.24	0.42	0.23	27	
	Max	17	0.14	2.1	2.9	9.9	0.28	2	1.4	-	1.7	0.59	0.4	0.21	0.27	1	0.25	34	
Pyramiden																			
Soil	Median	157.5	12.1	5.88	11.145	147.5	18.7	57.65	52.1	31.25	45.25	69.95[2]		29.8	9.765	42.9	14.3	704	[113]
	Min	31.9	2.79	1.23	0.74	10.3	3.11	0.8	0.95	0.8	1.59	1.95[2]		0.69	0.66	1.68	0.74	52.8	

Table 2.3 – *(continued)*

Study area, matrix		NAP	ACY	ACE	FLU	PHE	ANT	FLT	PYR	BaA	CHR	BbF	BkF	BaP	DBA	BgP	IND	$\sum_{16}$PAHs	Ref.
	Max	2290	333	43.4	134	1840	315	2360	1960	849	1160	1450[2]		846	114	271	132	11600	[113]
Pyramiden, Skottehytta																			
Soil	Min	42	NA	8	10	24	<LOD	1.8	8	<LOD	<LOD	<LOD		<LOD	1	<LOD	<LOD	-	[70]
	Max	48		14	12	45	69	28	109	18	22	19		18	12	9.8	28	-	
Kinnvika																			
Soil	Min	0.015	2.02	4.74	0.324	0.131	0.001	0.021	0.007	0.003	0.003	0.003		4.63	0.077	2.1	2.92	17	[91]
	Max	330	82	188	146	55.3	221	120	20.3	98.6	98.6	131		308	388	4140	151	6380	

[1] values are based on the analysis of one sample
[2] values are reported as sum of BbF and BkF due to coelution

Table 2.4 – Comprehensive overview of reported single PCB levels from studies on Svalbard, found in different matrices of the terrestrial environment, including, soil and vegetation. Values are reported in ng g^{-1} (dry weight basis), unless specified otherwise. Cells for values for single PCB compounds are left empty when not reported in the respective study. LOD = limit of detection

Study area	Matrix		PCB-28	PCB-52	PCB-101	PCB-118	PCB-138	PCB-153	PCB-180	$\sum_7$PCBs	Ref.
Ny-Ålesund	Reindeer dung	Mean	0.068	0.029	0.087	0.023	0.096	0.18	0.044	0.53	[213]
		Range	0.061-0.087	0.024-0.041	0.045-0.172	0.015-0.033	0.049-0.165	0.12-0.28	0.032-0.063	0.34-0.84	
	Soil	Mean	0.016	0.25	0.36	0.001	0.24	0.26	0.13	1.26	
		Range	0.010-0.021	0.15-0.34	0.19-0.65	0.001-0.002	0.058-0.49	0.057-0.59	0.020-0.31	0.49-2.41	
Ny-Ålesund	Soil	Mean								0.56[1]	[212]
		Range								0.07-1.92[1]	
	Sediment	Mean								0.67[1]	
		Range								0.15-1.79[1]	
	Plants	Mean								5.85[1]	
		Range								2.57-9.95[1]	
	Reindeer faeces	Mean								3.12[1]	
		Range								2.42-3.84[1]	
	Bird faeces	Mean								3.76[1]	
		Range								3.21-4.23[1]	
Barentsburg	Soil	Median								268	[86]
		Range								52-28700	
Pyramiden	Soil	Median								172	
		Range								<4-13900	
Longyearbyen	Soil	Median								<4	
		Range								<4-131	
Barentsburg	Paint	Median								621	
		Range								<4-3520000	
Pyramiden	Paint	Median								18	
		Range								<4-1290000	
Longyearbyen	Paint	Median								64	
		Range								<4-695	
Adventdalen	Organic soil	Median	1.1	2.9	<1.0	<1.0	<1.0	<1.0	<1.0	2.9	[17]
		Range		<1.0-5.5						<1.0-5.5	
Ny-Ålesund	Organic soil	Median	<1.0	2.85	<1.0	<1.0	<1.0	<1.0	5.2	4.9	
		Range		<1.0-3.2					<1.0-5.6	<1.0-8.1	
Adventdalen	Vegetation	Median	<1.0	6.1	<1.0	<1.0	<1.0	<1.0	<1.0	6.3	
		Range		2.7-40						4.3-40	

Table 2.4 – *(continued)*

Study area	Matrix		PCB-28	PCB-52	PCB-101	PCB-118	PCB-138	PCB-153	PCB-180	$\sum_7$PCBs	Ref.
Ny-Ålesund	Vegetation	1 sample	6.7	<1.0	<1.0	<1.0	<1.0	<1.0	<1.0	6.7	[17]
Kinnvika	Soil	Mean Range	18.8 0.528-437	360 142-8840	<LOD	14.6 0.201-194	814 52.9-11400	527 213-8855	716 224-34300	2450 0.201-39900	[91]
Kinnvika	Soil	Median Range								0.415 0.08-1.33	[59]
Ny-Ålesund (Thiisbukta)	Soil	Median Range								6.25 4.8-135	[37]
Ny-Ålesund	Soil									<21	[34]
Longyearbyen	Soil	Mean Range								2.1 <0.4-8.3	[35]

[1] values are reported as $\sum_8$PCBs = sum of PCB-28, -52, -101, -105, -118, -138, -153 and -180

2.5 Analysis of PAHs and PCBs in soil

The analysis of organic contaminants, such as PAHs and PCBs in complex solid environmental matrices, such as surface soil, demands efficient extraction methodologies and sensitive analytical techniques due to low concentrations that are to be expected (few ng g^{-1} to several µg g^{-1}) [140]. Extraction and cleanup is necessary before analysis to bring the target analytes in solution and to achieve suitable concentrations for detection [3]. Moreover, cleanup of extracts is required for removing interfering matrix components [140]. Soxhlet extraction is one of the most commonly applied extraction technologies for PAHs and PCBs in environmental sample to date [3, 27]. However, there are alternatives that require less time and solvent, such as accelerated solvent extraction (ASE) [150], which was used in this study and will be further introduced below. Moreover, with in-cell cleanup procedures that can be applied during ASE, time-consuming additional cleanup of the yielded extract such as gel permeation chromatography (GPC) can be circumvented [94, 140]. When the samples are extracted, compounds can be separated by gas chromatography (GC) and detected by mass spectrometry (MS). GC-MS is one of the most common techniques for the analysis of PAHs and PCBs [3, 27, 143].

2.5.1 Accelerated solvent extraction (ASE)

ASE is an automated extraction method for solid and semi-solid samples such as soil using elevated temperatures and pressures [94]. By applying a higher pressure (∼1500 psi) the solvent remains liquid above its boiling point and a better penetration of the sample with solvent can be achieved [150]. Moreover, the higher pressure in combination with higher temperature helps to solubilize air bubbles, weakens strong matrix-analyte interactions such as hydrogen bonds. Consequently, less equilibration time between solvent and sample phase and less amount of solvent is needed [150]. For in-cell cleanup of extracts, the ASE extraction cell (usually stainless-steel) is packed with resins first, such as copper and alumina (Al_2O_3) that were applied in this study. Copper is used for removal of sulphur which shows a similar solubility as organochlorine compounds such as PCBs and may interfere during detection [188]. Alumina aids to remove nonpolar lipids and colored compounds [94]. The sample is usually added in mixture with a dispersant such as diatomaceous earth (DE) which limits the aggregation of sample particles, reduces the cell dead volume and helps to increase the sample surface to the extraction solvent [140]. Fig. 2.5 shows the main components of the ASE system.

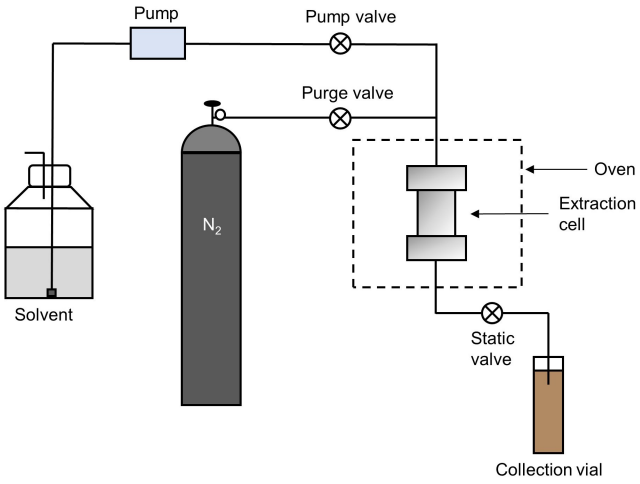

Figure 2.5 – Schematic representation of the accelerated solvent extraction (ASE) system. Redrawn with individual modifications from Ref. [150]

After the cell is packed with sample and resins, it is placed into the oven and the extraction begins with a dynamic extraction step, where the cell is heated and solvent is repeatedly pumped through the sample. Then, the static valve closes which allows pressurization of the cell and a static extraction step begins, i.e. the volume of solvent, temperature and pressure remain constant for a specific time [109]. This step can be repeated once or twice with fresh solvent, i.e. resulting in 1–3 cycles in total. Following the last static extraction cycle, the sample is rinsed with fresh solvent (1–100% of the cell volume) under low pressure [109] and then, remaining solvent is purged out of the cell with N_2. Approximately, 1.5 times the cell size, i.e. 30-40 mL solvent for an extraction in a 22 mL extraction cell is consumed during one extraction [94] and an extraction with 3 static cycles takes 20-25 minutes.

2.5.2 Gas chromatography coupled to mass spectrometry (GC-MS)

Chromatography is a process where components of a mixture are selectively distributed between a mobile phase and a stationary phase [125]. The chromatographic process results from repeated sorption and desorption steps when the analytes are transported along the stationary phase by the mobile phase. Single components get separated from the mixture due to different distribution coefficients [125] (Eq. 2.2, distribution coefficients further explained in Sec. 2.6). In general, a gas chromatograph consists of an a carrier gas with gas filters, of a sample introduction system and inlet, of a oven-temperature-programmed column and of an interface to the detector [169] (Fig. 2.6).

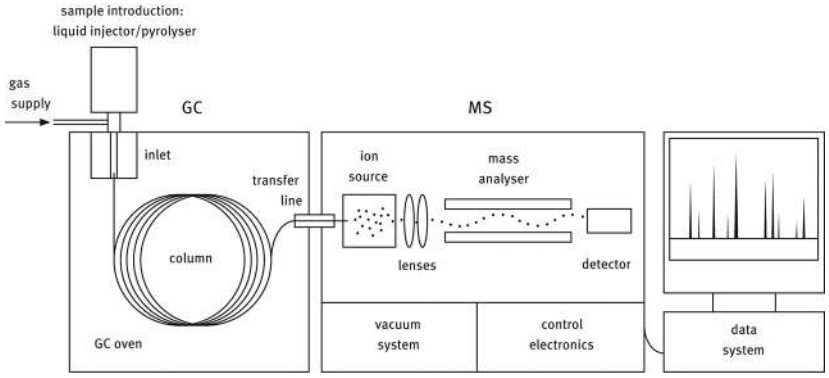

Figure 2.6 – Scheme, displaying the major components of a gas chromatographic system coupled to a mass sensitive detector. Adopted from Ref. [176].

Before the chromatographic separation, the liquid sample gets volatilized in the injector or gases from heating of a solid sample in an inert atmosphere (pyrolysis) are introduced and transferred to the inlet [176] (Fig. 2.6). There are different types of injection, one of them being split/splitless-injection [106]. During split injection which was applied in this study a split valve is open during injection and only a small fraction of the vaporized sample volume enters the column. This type of injection allows the injection of larger sample volumes (e.g. 1 µL) without overloading the GC column [98]. Following evaporation, the sample is transferred towards a column by the mobile phase which is an inert gas such as helium (He) [71]. For efficient separation of components in the gas phase, this type of chromatography requires the analytes to be sufficiently volatile and thermally stable [125]. The column, i.e. the stationary phase, where separation of components occurs, is mostly a capillary column with a length between 15 and 60 m [169]. It is also referred to as an open tubular column that is made of fused silica. The liquid stationary phase is chemically bonded on the inner wall [98]. The choice of the column impacts the quality of a chromatographic separation and should be made based on the physico-chemical properties of the target analytes that are to be separated, the sample type as well as the aim of the analysis [169]. The chemical composition of the stationary phase is one of the major parameter to set for column selection. For instance, columns containing 5% phenyl- and 95% dimethylpolysiloxane as a stationary phase are suited for the separation of non-polar compounds [71]. The column is located in an oven that can be temperature programmed. The temperature should be set high enough to achieve high enough vapour pressure of compounds so that chromatographic separation occurs in a reasonable time window [98]. During an analysis, the temperature can be held constant. This is also referred to as isothermic analysis. However, for separation of a mixture of compounds with a wide range of boiling points it is recommended to set a temperature program. In general, it begins with the optimal temperature for separation of the most volatile compounds, is then increased at a precise rate to a temperature which is suitable for separation of the least volatile components [169]. Once the compounds got separated in the GC, they need to be detected for their identification and quantification. In this study, a mass spectrometer was used as a detector, which is an instrument which registers the mass-to-charge ratio (m/z) of ions in the gas phase and gives a measure of the abundance of each ion with a certain *m/z* ratio [98]. Using a mass spectrometer as detector has the advantage over other GC-detectors that target analytes can be simultaneously quantified and confirmed due to the selective nature of the mass spectrometric detector [71, 143]. Moreover, mass spectrometry enables the detection and identification of non-target compounds in samples [71]. This type of detector requires the analytes

to be ionized, since separation is based on the interaction of charged particles with electrical or magnetic fields [98]. A mass spectrometer is comprised of: (I) an ion source, where neutral analyte molecules get ionized, once they leave the GC, (II) a mass analyzer, where the ions are separated based on their *m/z* ratio, and (III) a detector, which registers and amplifies the arriving ion current [125]. Electron-impact ionization (EI) is one of the most commonly applied ionization techniques within GC-MS [71]. At the ion source, analyte molecules collide with accelerated electrons. These electrons have an energy of 70 eV and originate from a heated metal filament being outside the ion source [142]. They interfere with the outer electron shell of the neutral analyte molecules, leading to removal of outer shell electrons and the formation of positively charged molecular ions and additional free electrons [98]. EI is considered to be a hard ionization technique because the kinetic energy of the electrons is high enough to cause further fragmentation of the molecular ion after collision [76]. At the mass analyzer, ions are separated according to their mass to charge (*m/z*) ratio [125]. The single quadrupole mass spectrometer is most commonly used as a mass analyzer within GC-MS [106, 98]. It has been used in this study for the detection of PAH and PCB target analytes. A single quadrupole MS consists of only one quadrupole mass analyzer in comparison to a triple quadrupole MS that contains two quadrupole mass analyzers as well as a collision cell. The triple quadrupole MS has been used in this study for trace element analysis with ICP-MS and the working mode of the quadrupole mass analyzer is described in detail in Sec. 2.3.1. There are two modes at wich a quadrupole MS can be operated: full scan and selected ion monitoring (SIM) mode [71]. In full scan mode, a broad mass range is monitored, usually between *m/z* ratios of 50–500 which provides additional spectral information for the identification of a compound [142]. In SIM mode, only ions with a certain *m/z* ratio are detected in a selected retention time window [71]. The advantage of SIM over full scan mode is that the sensitivity is increased and lower detection limits can be achieved [125], since less *m/z* ratios are monitored per scan. Thus, more scans per second can occur for an ion with a certain *m/z* ratio [142].

2.5.3 Suspect screening of retene

GC-electron impact-MS has the advantage of achieving reproducible and robust fragmentation patterns for a wide range of compounds [79]. Hence, it enables the comparison of mass spectra from a sample with standard spectra from libraries which provides the basis to screen for potential unknown contaminants [207]. Next to target screening, where reference standards are used to locate, verify, and to quantify analytes, it is possible to carry out a suspect screening with GC-MS [148]. This type of screening is applied in the case when reference standards are not available [148]. Moreover it relies on the prior knowledge to confirm or to reject the presence of a suspect compound in a sample [148]. By obtaining the standard subsequently, the presence of the suspect compound can be confirmed by matching of retention time and mass spectra to that of the reference standard [148].

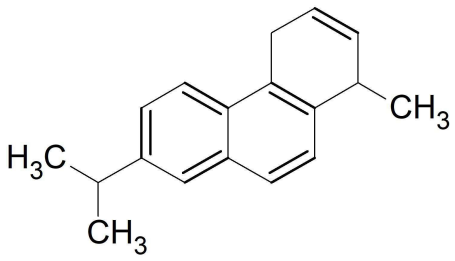

Figure 2.7 – Structural formula of retene.

Retene (1-Methyl-7-isopropylphenanthrene) is considered to be a PAH compound of biogenic origin [2, 175] and derives from the degradation of abietic acid which is a component in plant resins [47, 96]. The structural formula is shown in Fig. 2.7. One typical source of Retene is the release from boreal conifer forest fires [67]. Moreover, it has been characterized as a dominating compound in coals from Svalbard, where Ny-Ålesund was one of the coal-mining settlements [47]. Retene has been applied as an indicator for organic matter derived from coal in sediments from the Kongsfjorden area on Svalbard [96]. Moreover, it has been detected in snow from Ny-Ålesund, a former coal-mining settlement and associated with the presence of coal dust, being a potential source indicator for PAHs detected there [192].

2.6 Quality Control/ Quality Assurance (QA/ QC)

Retention time

Retention time is a measure of the time it takes for a compound from sample injection into the system to elution from the column and detection [169]. For each analyte, the retention time depends on its partition coefficient, also referred to as distribution constant (K_D), between stationary and mobile phase. It can be described by the following equation [61]:

$$K_D = \frac{c_s}{c_m} \tag{2.2}$$

with c_s being the analyte concentration in the stationary phase and c_m being the analyte concentration in the mobile phase. Compounds with higher K_D have more affinity to the stationary phase. They move slower through the chromatographic system. Consequently, their retention time will be longer than that of compounds with lower K_D [169]. By comparing the retention time of a sample to that of an external standard analyzed under the same conditions, this measure can be applied for identification of compounds [125].

Quantification

Quantification of analytes is based on the relationship between the detector signal and concentration of the target analyte in general [142]. The most accurate quantification of target analytes in GC-MS is accomplished by the internal standard method. The internal standard (IS) accounts for losses during sample preparation steps and differences in injected sample amounts to the GC [166]. It is added in a known constant amount to calibration solutions with differing concentration of target analyte as well as to samples. For every target analyte, a calibration curve is established from the relative response ratio ratio, i.e. the ratio of the analyte response to the response of the internal standard in each measured standard solution (Eq. 2.3). The relative response is plotted against the concentration of the analyte [15]. The peak area can be used as a measure for response [166].

$$\mathrm{RR} = \frac{\mathrm{Area_A}}{\mathrm{Area_{IS}}} \tag{2.3}$$

Next to the calibration solutions, the internal standard is added to the sample before extraction in a known amount which should be in the concentration range of target analytes in the sample [166]. It is recommended to mix the sample thoroughly with internal standard before performing the extraction.

In particular for ASE, adding the internal standard on top of the sample being in the extraction cell may lead to overestimation of target analyte concentrations. The reason is that, when the internal standard is added on top of the sample, it has to travel a longer way through the extraction cell during an extraction than target analytes which are more evenly distributed in the sample [109]. The internal standard is a compound that should possess similar physico-chemical properties in comparison to the target analytes. Moreover, it should not be present in the environment and should have a similar retention time to that of the target analytes [143]. For the analysis of PAHs and PCBs with GC-MS, ^{13}C-labelled and perdeuterated analogues are commonly used as internal standards [143]+ citation for PCBs). Less expensive monofluorinated PAHs and PCBs, i.e. F-PAHs and F-PCBs (Fig. 2.8) have been shown to be suitable alternatives [111, 110]. They elute slightly earlier than their parent compound [110, 8] which is advantageous for the analysis of PAHs and PCBs with other techniques than GC-MS, such as analysis of PCBs with GC, coupled to an electron capture detector (GC-ECD) [149]. For the analysis of PAHs with a broad range of physico-chemical parameters, it has been recommended to include three F-PAHs [111].

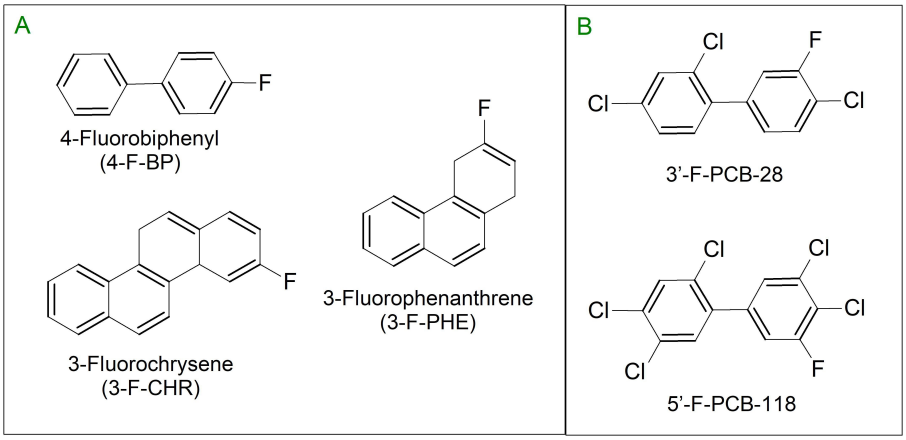

Figure 2.8 – Structures of fluorinated PAH (A) and fluorinated PCB internal standards (B) used in this study.

Linearity

Linearity is defined by the capacity of a method to bring out responses that are directly proportional to the analyte concentration within a given range [178]. In general, linearity is assessed by the characteristics of a calibration function, obtained from procedures used for correlating instrument response to an amount of analyte [117]. For establishing a calibration curve, it is recommended to use six or more calibration standards and to select the concentrations of the calibration standards being evenly spaced within the concentration range of interest [184]. Linear regression can be used to describe the response to a predictor variable with a linear function [163] as follows:

$$y = mx + b \tag{2.4}$$

where x determines the predictor variable, e.g. the concentration in the calibration standard, y determines the measured response, b denotes the y-intercept and m is the slope of the regression line. The linear function, i.e. the regression line, is obtained by the least-squares method for which the

sum of the squares of the residuals (SS_{resid}, Eq. 2.5) are minimized for all data points. The residuals are the vertical deviation from the regression line. SS_{resid} reflects the variation in the values of the response variable that is not explained by the assumed linear relationship between x and y [163]. It is calculated with the following equation:

$$SS_{resid} = \sum_{i=1}^{n} [y_i - (b + mx_i)]^2 \tag{2.5}$$

with x_i and y_i being an individual pair of data. The total sum of the squares (SS_{total}) is a measure of the total variation in the values of the response variable [163] and is obtained as follows:

$$SS_{total} = \sum (y_i - \bar{y})^2 \tag{2.6}$$

where $\bar{y}$ determines the mean value of y for a set number (n) of data points. Based on SS_{resid} and SS_{total}, the coefficient of determination (R^2) can be obtained as a measure for the goodness of fit [62]. It describes the portion of the observed variation in y that is explained by the linear function [163]:

$$R^2 = 1 - \frac{SS_{resid}}{SS_{total}} \tag{2.7}$$

A good fit is indicated by a high R^2 with a value being close to 1 [62].

Instrument and sample limit of detection (LOD) and lower limit of quantification (LLOQ)

The limit of detection is the lowest concentration of an analyte where the chromatographic signal can be reliably detected by the analytical process [112]. It is often based on the signal to noise ratio (S/N) which is the ratio of the intensity of the signal relative to that of the noise [201]. Noise is the fluctuation in the instrument background signal [201]. The range of quantification should be distinctly above the LOD, since signals above the LOD can not be reliably quantified [112]. Therefore, a limit of quantification (LOQ) is applied which is defined as the lowest concentration that is quantifiable with acceptable accuracy and precision [12]. One method for LOQ estimation can be to define a lower limit of quantification (LLOQ) which is set as the lowest concentration that is reliably quantified based on the lowest acceptable chromatographic signal from a calibration standard solution [14, 19]. LOD can be estimated from LLOQ by Eq. 2.8.

$$\text{LOD} = \frac{\text{LLOQ}}{3} \tag{2.8}$$

From the LLOQ and LOD, lower limits of quantitation and limits of detection in theoretical samples (weight/weight, w/w basis) can be estimated by calculations similar to the quantfication of analytes in real samples [19]. The sample LOD is estimated as follows [146]:

$$\text{LOD (Sample, w/w)} = \frac{\text{LLOQ} \cdot \frac{V_{\text{Std. Sol.}}\,(\text{mL})}{m_{\text{Sample}}\,(\text{g})}}{3} \tag{2.9}$$

where $V_{\text{Sol.}}$ is the volume of the standard solution subjected to analysis and m_{Sample} is the theoretical amount of sample which is representative for the amount of all samples that were used for sample preparation within the analytical method.

Precision and accuracy

The accuracy or trueness of a method is the closeness of a test result to the true value [115]. It describes the systematic error of a method [115] and is stated quantitatively as "bias". Recovery studies (Sec. 2.6) as well as certified reference materials (CRMs) can be used for investigating bias [184]. Precision is the closeness between independent test results obtained under specified conditions and can be assessed by analyses of replicates. It describes random error [115] and is used for defining measurement repeatability and reproducibility [117]. Repeatability refers to as the closeness of agreement between independent test results under the same measurement conditions, i.e. within the same analytical sequence [117, 184]. Reproducibility describes the closeness of agreement between independent test results obtained from changed conditions of measurement, i.e. among different analytical batches of the identical sample [117, 184]. In general, precision is expressed by using the standard deviation or relative standard deviation [184]. The standard deviation (SD) describes the dispersion of individual measurements relative to the mean [77] and is obtained as follows:

$$\text{SD} = \sqrt{\sum_i \frac{(x_i - \bar{x})^2}{n-1}} \tag{2.10}$$

where $\bar{x}$ is the mean (Eq. 2.11), x_i refers to individual measurements and n refers to the number of measurements.

$$\bar{x} = \frac{1}{n}\sum_{i=1}^{n} x_i \tag{2.11}$$

The relative standard deviation is the ratio of the standard deviation to the mean [77]. It is the preferred measure for the comparison of the precision of results with different magnitudes or units [115].

$$\text{RSD}\ (\%) = \left(\frac{\text{SD}}{\bar{x}}\right) \cdot 100\% \tag{2.12}$$

Matrix effects

GC-MS has been shown to be a suitable method to analyze PAH and PCB target analytes in complex matrices [143, 121]. However, co-extracted matrix constituents from soil, such as such as lipids, humic and fulvic substances are present in the final extract for analysis as well and can lead to chromatographic signal enhancement or suppression, i.e. to matrix effects (ME) [165].

Consequently, enhancement or suppression due to matrix effects may cause over- or underestimation of analytical results when using standards in pure solvent for calibration [53]. Matrix effects have been considered to a lesser extent in GC-MS than in LC-MS [161]. However, in order to obtain accurate quantitative results, it is important to take matrix effects into account for analyses within GC-MS approaches as well [65]. The source of matrix effects in GC-MS is distinct from that in LC-MS [161]. Matrix effects within GC-MS mainly result from processes within sample introduction into the column and not from mechanisms within the detector [56]. In comparison to LC-MS, where co-eluting compounds affect the ionization process at the interface, a harder ionization technique (electron-impact ionization, EI) is most commonly applied in GC-MS [71]. The ionization energy in EI is high enough to overcome competing ionization mechanisms [161]. The processes behind matrix effects within sample introduction into the column in GC-MS are explained by competition between matrix components and target analytes for active sites in the GC, i.e. inlet and column material. Consequently, when passing the inlet and column, less adsorption of analytes in an extract with matrix constituents takes place, in comparison to analytes being in a pure solvent at the same concentration [56, 57, 161]. Thus, a higher amount of analytes reaches the detector which leads to signal enhancement [57]. Moreover, matrix components act as a protector against decomposition of analytes in the hot injector [56]. In gas chromatography, matrix effects can be evaluated by comparison of the responses (peak areas) of known concentrations of standards prepared in a solvent with standards prepared in a sample extract (post-extraction matrix spikes) [165]. The matrix factor (MF) can be obtained by the following equation;

$$\mathrm{MF} = \frac{(\mathrm{Area}_{\mathrm{A;\,MM}} - \mathrm{Area}_{\mathrm{A;\,MB}})}{\mathrm{Area}_{\mathrm{A;\,STD}}} \tag{2.13}$$

where $\mathrm{Area}_{\mathrm{A;\,MM}}$ is the peak area of an analyte in a post-extraction matrix spiked sample, also referred to as a matrix-matched (MM) sample and $\mathrm{Area}_{\mathrm{A;\,STD}}$ is the peak area of the analyte in a standard solvent. To ensure a comparison based on identical concentrations of the analyte between the matrix-matched sample and the standard solution, the peak area of the analyte in the method blank ($\mathrm{Area}_{\mathrm{A;\,MB}}$) is used for subtraction [15]. A MF being 1 indicates an equivalent response between the sample extract and solvent, i.e. no matrix effect. A value of <1 indicates a response decrease, and will yield a negative % matrix effect (ME). A matrix factor >1 indicates an enhancement of the response, leading to a positive % matrix effect (ME) [15, 161, 165] (Eq. 2.14).

$$\mathrm{ME}\ (\%) = (\mathrm{MF} - 1) \cdot 100\% \tag{2.14}$$

Matrix effects can be reduced by including additional post-extraction cleanup steps, such as gel permeation chromatography (GPC), providing cleaner extracts. However, these steps can be laborious and may lead to further analyte losses [140]. Alternatively, masking active sites in the GC-MS system by continuously adding analyte protectants such as ethylene glycol into the carrier gas help to reduce matrix effects [64]. Another possible solutions for compensating matrix effects include the use of internal standards (Sec. 2.6) as well as alternative calibration methods such as the standard addition method [161]. This method involves the addition of known amounts of analytes to aliquots of sample extracts, accounting for effects due to the presence of coextracted matrix components in the calibration [56]. Single point standard addition calibration has been shown to be a valid approach for compensating matrix effects in GC-MS, for example for pesticide analysis in cucumber and orange, yielding recoveries between 70 and 120% [65].

Matrix effects and interferences occur in ICP-MS as well and can lead to erroneous results [158]. In general, interferences are divided into spectroscopic and non-spectroscopic interferences. Spectroscopic interferences occur when other ions than the analyte ion have the same *m/z* ratio, while non-spectroscopic interferences arise from sample matrix effects or from effects within instrumentation [204]. Common spectroscopic interferences include isobaric interferences, where isotopes from another element have the same *m/z* ratio as the isotope of the analyte element, for example ^{204}Hg and ^{204}Pb. Another spectroscopic interferences can occur from polyatomic ions of other elements which have the same *m/z* ratio as the analyte ion such as ^{35}Cl^{16}O and vanadium (^{51}V) [158]. These types of interferences can be tackled by using a reaction gas in the collision cell within the triple quadrupole mass analyzer (Fig. 2.2). In the collision cell either the interference or the analyte of interest reacts with the gas. An adduct ion forms that has a different *m/z* ratio, by which the analyte ion can be separated from the interference in the second quadrupole (Q2) [49]. Matrix effects occur from other components than the analyte of interest and lead to suppression of ionization, and, thus signal suppression. One strategy to reduce matrix effects is to dilute the sample [204].

Recovery

During different steps of the analytical process, such as evaporation, losses of analytes occur which may bias the results [185]. Therefore, recovery studies are an important part of the validation of analytical methods [185]. The recovery of a method is defined as the relative amount of analyte measured in the final extract in comparison to the actual amount in the original sample [107]. Losses of sample and/or analyte may lead to a lower recovery. Two types of recoveries for a given analyte, referred to as absolute recovery ($R_{abs.}$) and relative recovery ($R_{rel.}$), can be obtained from spike samples (SP) where known amounts of analyte are added to the sample matrix before the extraction procedures (pre-extraction matrix spikes) and from matrix-matched samples (MM) with known fortified analyte amounts to the sample matrix after the extraction procedures (post-extraction matrix spikes) [15, 16]. $R_{abs.}$ is calculated as follows:

$$R_{abs.}\ (\%) = \frac{(\text{Area}_{\text{A; SP}} - \text{Area}_{\text{A; MB}})}{(\text{Area}_{\text{A; MM}} - \text{Area}_{\text{A; MB}})} \cdot 100\% \tag{2.15}$$

with $\text{Area}_{\text{A; SP}}$ and $\text{Area}_{\text{A; MM}}$ being the respective peak areas of analyte in pre-extraction matrix spikes and post-extraction matrix spikes [15]. Possible contamination can be taken into account by subtracting the peak area of analyte being present in the method blanks ($\text{Area}_{\text{A; MB}}$) that undergo the same extraction and cleanup procedures as the samples. By using the analyte signal relative to that of the internal standard (IS) for calculation of the relative recovery, it is accounted for analyte losses during sample preparation and cleanup [15]. $R_{rel.}$ is obtained with the following equation:

$$R_{rel.}\ (\%) = \frac{\left(\frac{\text{Area}_{\text{A; SP}}}{\text{Area}_{\text{IS; SP}}} - \frac{\text{Area}_{\text{A; MB}}}{\text{Area}_{\text{IS; MB}}}\right)}{\left(\frac{\text{Area}_{\text{A; MM}}}{\text{Area}_{\text{IS; MM}}} - \frac{\text{Area}_{\text{A; MB}}}{\text{Area}_{\text{IS; MB}}}\right)} \cdot 100\% \tag{2.16}$$

with Area_{IS} being the peak area of the internal standard in spike (SP), matrix-matched (MM) and method blank (MB) samples.

CHAPTER 3

Materials and Methods

3.1 Study Area

Svalbard is an archipelago in the high Arctic, which is defined as the region north of the 4–6 °C mean July temperature isotherm range [29]. It is situated between 74° and 81° North and 10°-35° East (Fig. 3.2, A). Approximately 34.000 km^2 (i.e. 57%) of its land surface area is covered by glaciers [131]. According to Ref. [42] this archipelago lies within the Continuous Permafrost Zone with $\geq$ 90 to 100% of the land area consisting of permafrost. This study was carried out in August 2020 in the Kongsfjord-Krossfjord area (Fig. 3.2, C), on Spitsbergen (76°-80°N, 10°-21°E), the largest island of Svalbard archipelago. The climate on this archipelago, particularly on the west side, is influenced by the West Spitsbergen Current which is the northernmost extension of the North Atlantic Current and delivers moisture and heat to this area [177]. In Ny-Ålesund, average annual temperature ranges from -6.2 to -1.2°C (based on measurements from a 30-year period, from 1991 to 2020). Based on measurements from the same time period the average temperature within the month where sampling took place (August) lies between 2.5 and 6.2°C. Mean temperature in August 2020 was 6.2°C. Based on measurements from the same time window, the range of total annual precipitation in this area is between 254 to 749 mm and was 434.2 mm in 2020 (data from Norwegian Meteorological Institute). Ny-Ålesund is one of the main settlements in the Kongsfjord-Krossfjord area. It mainly serves research purposes, inhabiting approximately 200 people in summer and 25 people in winter [69]. This settlement is considered to be remote in comparison to Longyearbyen and was frequently used in past studies to investigate long-range atmospheric transport of pollutants to terrestrial compartments [17, 72, 74, 197]. Moreover, air at Zeppelin station is continuously monitored for long-range atmospheric transported pollutants, such as mercury (Hg), PCBs and PAHs [26, 189, 208]. However, the immediate area of Ny-Ålesund is impacted by former mining activities and that occured between 1916-1962, mainly operated by Kings Bay. Moreover, coal combustion has been taking place in Ny-Ålesund [177]. Approximately 1.43 million tonnes of coal in total was exported during that time window [177]. The remains of former coal mining are still visible in the landscape surrounding Ny-Ålesund (Fig. 3.1). Excavated coal waste was left in areas where mining took place and remains untreated to date. Coal dust can blow around the area. Other components of the infrastructure that was necessary for mining still characterize the landscape. As an example, parts of the railway can be seen at different locations of the settlement. It was used to transport the coal from the mines to the harbor for shipping the coal to customers. Local contamination at other locations than mining areas in Ny-Ålesund has been documented, for instance at the old landfill and dumpsites in Thiisbukta, the fuel storage area, the sewage outlet and the airport [34, 37, 69]. Moreover, aerosols from cruise ship emissions during summertime have been documented

to be a local contamination source in Ny-Ålesund air [211]. Some examples for studies on local contamination of PAHs and PCBs in Ny-Ålesund are discussed in Sec 2.4.3.

Figure 3.1 – Photographs of Ny-Ålesund settlement. Top left: aerial image of Ny-Ålesund, seen from the north-eastern side of the settlement. Top right and bottom left: remains of former coal mining activities that can be observed particularly in the south-eastern part of Ny-Ålesund settlement. Bottom right: remains of the railway, on which the coal was transported from the mines to the harbor.

3.1.1 Site description

Two major fjords characterize the Kongsfjord-Krossfjord area, namely Kongsfjord and Krossfjord. The Kongsfjord has a length of approximately 20 km [96] and the Brøgger peninsula (Brøggerhalvøya) is situated on the southwestern side of the fjord. The Krossfjord is 30 km long [96] and the Mitra peninsula (Mitrahalvøya) lies towards the west side of this fjord (Fig. 3.2, C). Soil was sampled from 5 study areas in total: 4 study areas on Brøggerhalvøya and one study area on Mitrahalvøya. The 5 study areas were divided according to distance to the main settlements, local vegetation, local geology, main lithology, landscape and type of superficial deposits: BDE - Brøggerdalen (eastside of Bayelva), BDW - Brøggerdalen (westside of Bayelva), GB - Gåsebu, KI - Kiærstranda and NDM - Nordre Diesetvatnet (Mitrahalvøya) (Tab. 3.1 and Fig. 3.2, C). Three study areas (BDE, BDW and GB) were located in the vicinity of Ny-Ålesund settlement, which is situated on the north side of Brøggerhalvøya. The bedrock in these areas is characterized by the occurrence of sedimentary rocks, mainly dolomite and limestone, originating from the Paleozoic era with an age of 298-300 million years (mega-annum, Ma). Additionally, tertiary rocks from the Cenozoic era (56-66 Ma) occur in proximity to Ny-Ålesund settlement, containing sandstones and shales as well as coal seams from the Van Mijenfjorden Group [18, 177] (Tab. 3.1). Glacifluvial and fluvial deposits as well as marine deposits influence the area. Different plant species occur in this area, for instance from the genus *Dryas*, but also little vegetation with gravel barren communities prevail, particularly in GB (Tab.

3.1). Kiaerstranda (KI) was selected as a background location. It has been considered in a previous study [17] to be unaffected by local anthropogenic activities that took place in Ny-Ålesund, such as mining. Similarly to the study areas BDE, BDW and GB the bedrock in KI is dominated by the presence of dolomite and limestone from the Paleozoic era [18, 177] (Tab. 3.1). Bird guano deposits were observed during sampling in KI, suggesting frequent bird nesting activities in this area (Fig. 3.3). According to Ref. [128], bird cliff vegetation and wet moss tundra communities are dominating this area (Tab. 3.1). The study area in proximity to the lake Nordre Diesetvatnet on Mitrahalvøya (NDM) was chosen as another background location, due to its remoteness and large distance to Ny-Ålesund, in comparison to KI. The average aerial distance of the study area NDM to Ny-Ålesund is approximately 35 km (3.1). Moreover, only few anthropogenic activities haven been taking place, such as the operation of a German meteorological station at Signehamna during World War II [89]. Signehamna is situated on the northeast side of the peninsula (Fig. 3.5). Remains of the former meteorological station are still present (Fig. 3.3). Samples were taken in large distance to this area to avoid possible local contamination affecting the composition of elements and organic contaminants in studied soils. There are only few studies that investigated soil on this peninsula, such as Ref. [96]. The bedrock on Mitrahalvøya is distinct from that of the selected study areas on Brøggerhalvøya. In the area, where samples were taken, the bedrock is characterized by metamorphic rocks, mainly lower dolomite marble, likely originating from the mesoproterozoic and earliest neoproterozoic era with an age of 960-1600 Ma [18, 177] (Tab. 3.1). Large parts of this area show little vegetation [128].

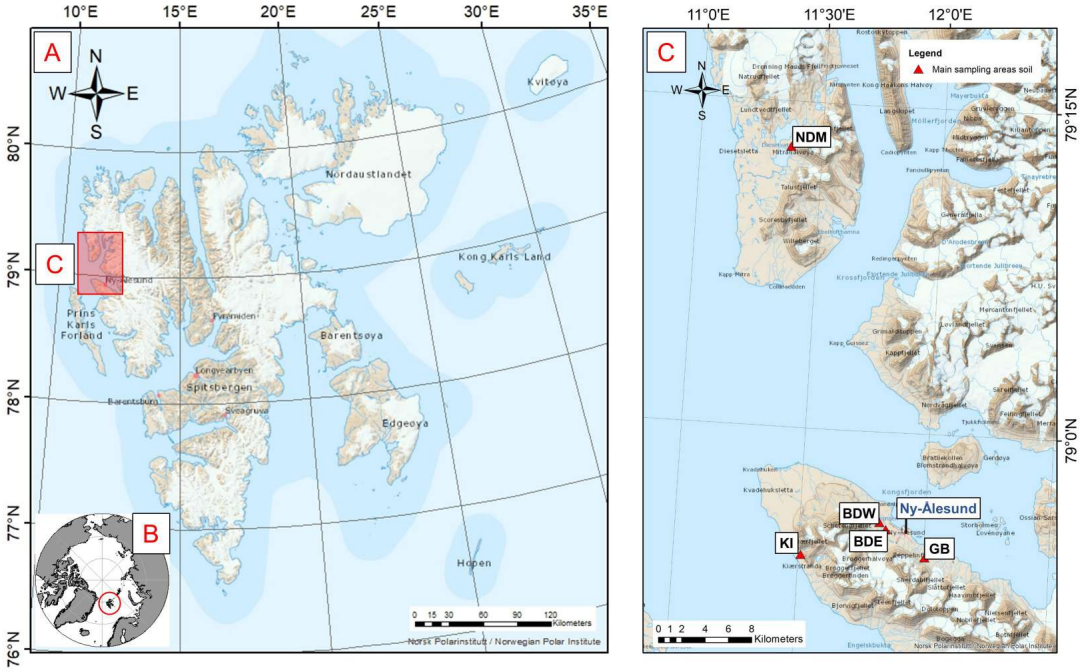

Figure 3.2 – Map (A) shows the islands and main settlements of the Svalbard archipelago. The island Bjørnøya is not included. Svalbard archipelago is highlighted in the circum-Arctic map with a red circle (B). The study was carried out on Spitsbergen, the largest island of Svalbard . Samples were taken on Mitrahalvøya (Krossfjorden area) and Brøggerhalvøya (Kongsfjorden area) (highlighted with a red box in map A and enlarged in map C). The settlement Ny-Ålesund is situated on the north side of Brøggerhalvøya. Main sampling areas on Mitrahalvøya for soil (Nordre Diesetvatnet, NDM) and main sampling areas on Brøggerhalvøya for soil: Brøggerdalen, east of Bayelva (BDE) and west of Bayelva (BDW), Gåsebu (GB) and Kiærstranda (KI) are displayed in map C. See further details on GPS coordinates of single sampling locations for soil in Tab. A.1 and Fig. 3.5.

Table 3.1 – Sampling areas with geological and lithological characteristics. See tables A.1 for exact location of the corresponding soil samples. Study areas are indicated with BDE=Brøggerdalen, east side of Bayelva, BDW=Brøggerdalen, west side of Bayelva, GB=Gåsebu, KI=Kiærstranda and NDM=Nordre Diesetvatnet (Mitrahalvøya). In areas BDE and BDW soil was sampled from areas of distinct geological eras (A and B) [18]. [1] data according to Ref. [128], [2] own observations, [3] data according to Ref. [100].

Sampling area	**BDE, BDW**	**NDM**	**KI**	**GB**
Soil cover/ vegetation	Arctic meadows, dense *Dryas* heaths, open *Dryas* communities [1] Dwarf willow, *Saxifraga* species [2]	Dry, non-vegetated to sparsely vegetated barrens, slopes and ridges [1]	Bird cliff vegetation, wet moss tundra communities, Arctic meadows [1]	Gravel barren communities - Polar deserts, dense *Dryas* heaths, Arctic meadows [1], Dwarf willow [2]
Geology				
Eon	A+B: Phanerozoic	Proterozoic	Phanerozoic	Phanerozoic
Era	A: Paleozoic B: Cenozoic	Meso-proterozoic and earliest Neoproterozoic	Paleozoic	Paleozoic
Period	A: Late Carboniferous, Early Permian, B: Palaeogene	-	Late Carboniferous, Early Permian	Late Carboniferous, Early Permian
Epoch	A: -, B: Paleocene-Eocene	-	-	-
Age (Ma)	A: 298 - 300 B: 56 - 66	960 - 1600	298 - 300	298 - 300
Main lithology	Sandstone, shale, conglomerate, coal	NDM: Lower dolomite marble	Dolomite and limestone	Dolomite and limestone
Superficial deposits [3]	glacifluvial and fluvial deposits	slope deposits, weathering material	slope deposits, marine deposits	glacifluvial and fluvial deposits, marine deposits
Landscape type	coastal lowland and edge-dominated, alpine landscape	coastal lowland and edge-dominated, alpine landscape	plateau mountainous landscape	coastal lowland
Avg. aerial distance to Ny Ålesund (km)	BDE: 1.7 BDW: 2.7	NDM: 34.8	9.2	3.0
Avg. distance to the shoreline (km)	BDE: 0.9 BDW: 1.3	NDM: 4.9	0.5	0.7

Figure 3.3 – Photographs of the different sampling areas chosen in this study. Top left: Kiærstranda. Bird guano deposits (black) can be seen on the left side of the cliff being in the shadow. Top right: view towards the Blåshaugbreen glacier on Mitrahalvøya which is situated in proximity to the sampling locations within the study area NDM. Bottom left: Bayelva river close to Ny-Ålesund settlement. Bottom right: Remains of the meteorological station at Signehamna (Mitrahalvøya) that was operated during WW II.

3.2 Sampling

Surface soil samples (0-15 cm depth) were collected from 15 locations in August 2020 (weeks 33 and 34). The locations can be divided into 5 sampling areas: 3 distinct areas in the vicinity of Ny-Ålesund: Gåsebu (GB) and Brøggerdalen east and west of Bayelva (BDE, BDW); Nordre Diesetvatnet area on Mitrahalvøya (NDM) and Kiærstranda (KI) (Fig. 3.2 and 3.5, Tab. A.1). Three soil samples were taken from each study area. Sampling of surface soil was carried out using a stainless-steel knife and cutting out a (10x10) cm square on each location. Subsequently, the square was divided in two equal samples: one for trace element analysis (collected in a paper bag) and one for organic pollutant analysis (collected in an aluminium box) (Fig. 3.4, B).

Selection of soil samples was carried out according to following criteria:

1. Minimum 300 m distance to current anthropogenic activities.
2. Minimum 500 m distance to the shoreline.

3. Surface soil depth of at least 20 cm.
4. Relatively low amount of rock material in the soil.
5. Relatively low amount of dense moss communities in the vegetation layer.
6. Avoidance of extreme weather events (e.g. heavy rainfall, storm) on sampling days.
7. Avoidance of spots with mineral soil visible on the surface.

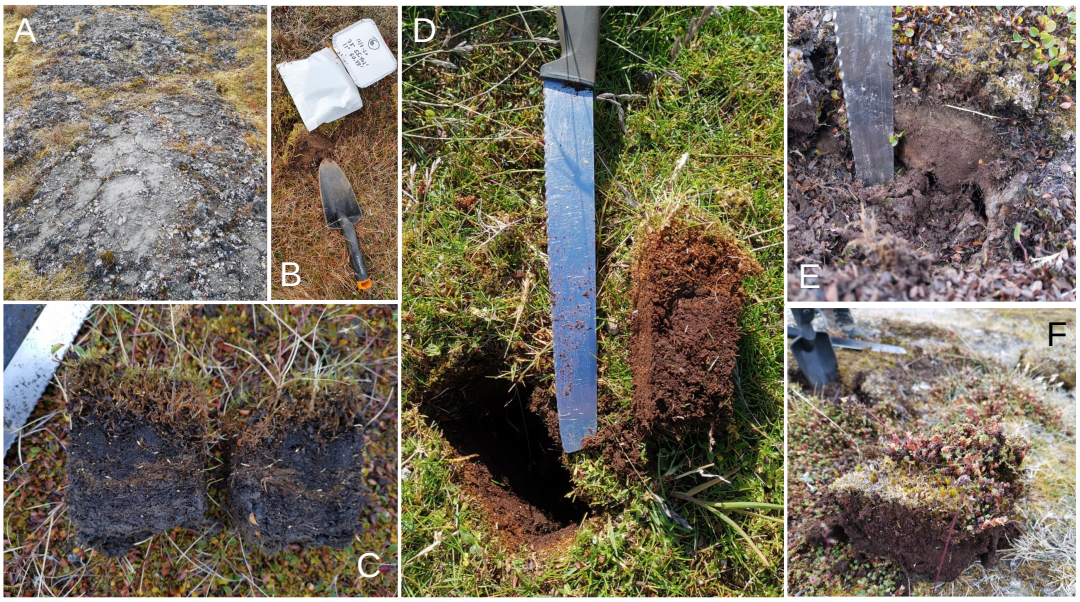

Figure 3.4 – Collection of images illustrating the soil sampling technique and different vegetation cover and surface soil depth in sampling areas Kiærstranda (D), Gåsebu (E) and Brøggerdalen west of Bayelva (C, F). Example for visible surficial mineral soil deposition that was observed in Brøggerdalen (A). Areas with mineral soil appearance were avoided for surface soil sample collection. At each location for surface soil sampling 2 equal samples were collected: one in a paper bag and one in aluminium box (B). Dense moss communities were characteristic for Kiærstranda area (D). Dwarf willow (*Salix herbacea*) visible in the vegetation layer of Gåsebu and of Bayelva (west side) surface soil samples (C, E). In samples from the west side of Bayelva species of the plant genus *Saxifraga* appeared in the vegetation layer. See Tab. 3.1 for further sampling area details.

Sampling in the study areas BDE, BDW and NDM was carried out in week 33. The study area NDM was reached by boat first, landing at the east side of Mitrahalvøya. Then, sampling locations were reached by walking along Trongdalen and along the Blåshaugbreen glacier towards the lake Nordre Diesetvatnet. GB and KI were sampled in week 34. KI was reached by boat. During sampling, a different extent of soil development and vegetation cover was observed. Soils from NDM showed a relatively low development and appeared to be sandy with light color when processing it in the laboratory later. Soils from KI were characterized by the appearance of dense moss communities

(Fig. 3.4), D). Soils from GB seemed to show a relatively low development and lighter color at the location more towards the inland (S7), while samples collected closer to the shore appeared to be more developed (S8, S9). Different plant species in the vegetation layer were observed during sampling, for instance dwarf willow (*Salix herbacea*) was noted on soils from GB and BDW (Fig. 3.4, C and E). Moreover, species of the plant genus *Saxifraga* showed in the vegetation layer in samples from the study area BDE.

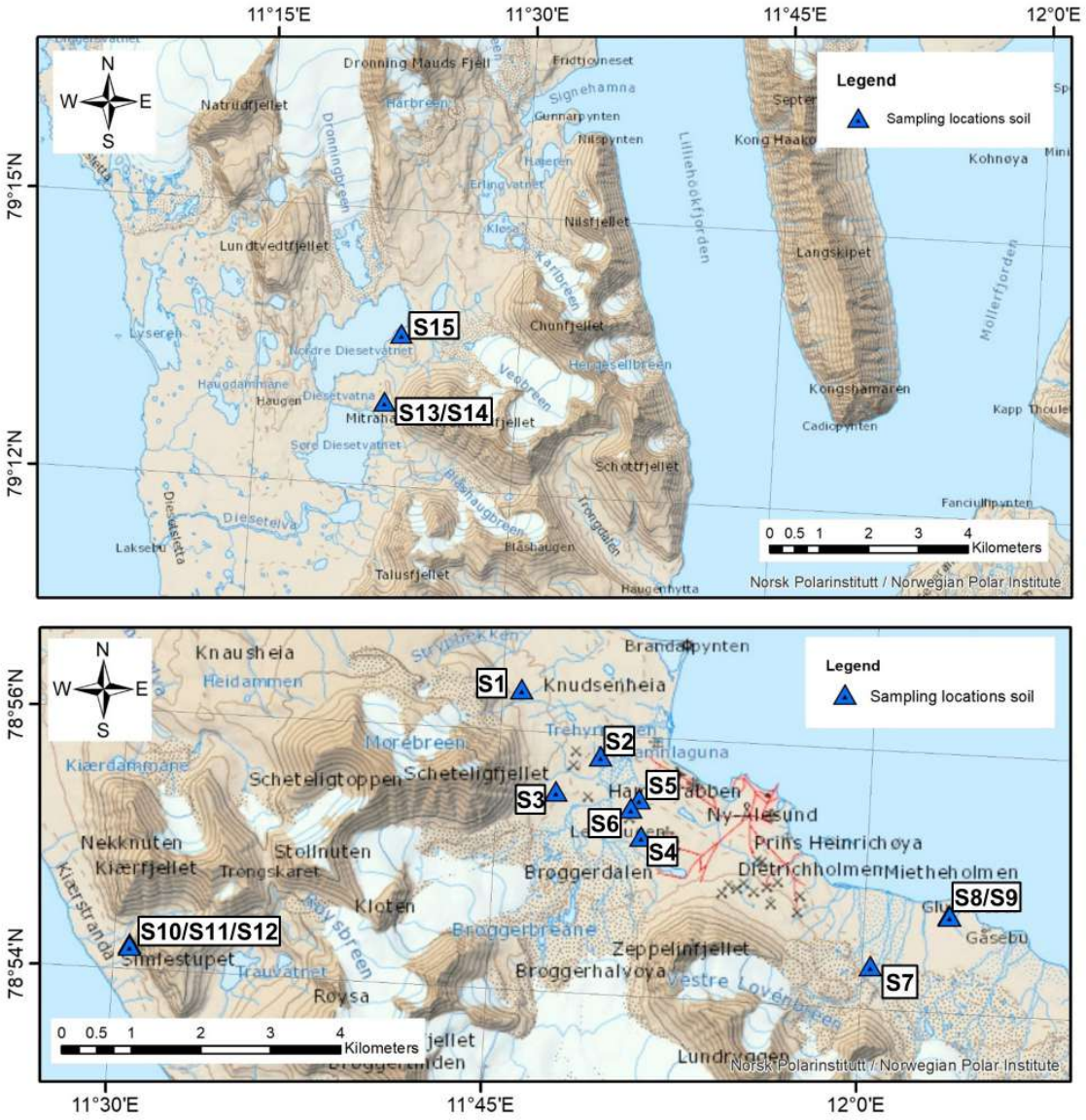

Figure 3.5 – Maps displaying single sampling locations (indicated by dotted triangles) with sample ID's for soil on Mitrahalvøya (upper map) and Brøggerhalvøya (lower map). The sampling points for soil (blue dotted triangles) are grouped into areas Brøggerdalen West of Bayelva (BDW): S1-S3; Brøggerdalen East of Bayelva (BDE): S4-S6; Gåsebu (GB): S7-S9; Kiærstranda (KI): S10-S12 and Nordre Diesetvatnet (NDM): S13-S15. At sampling locations containing more than one sample ID samples were taken within 10-20m distance range. See overview of main sampling areas in Fig. 3.2 and further details on GPS coordinates of single sampling locations for soil in Tab. A.1.

3.3 Determination of TC, TN, TOC400, ROC and TIC900

Surface soil samples (n=15) were dried at 23°C within the first two weeks after sample collection before transfer to NTNU Trondheim, Department of Chemistry. Later at NTNU, samples were further dried at 23-24°C and their weight was monitored. Once the weight loss became insignificant (<5% within three days), samples were further prepared. For further preparation of surface soil samples, the vegetation layer was removed. Approximately 0.5 cm of surface soil material was removed on each side of the sample using a Teflon knife. Later, samples were homogenized using mortar and pestle. Larger roots and stones were removed with a pair of tweezers. Subsequently, samples were sieved (2 mm mesh). To prevent samples from cross-contamination, the first homogenization and sieving fraction was discarded. In addition, mortar, pestle and knife were cleaned and rinsed three times with MilliQ-water and dried with dust-free paper tissues between samples. The homogenized and sieved sample was mixed and transferred to a new paper bag. TC, TN, TOC400, ROC and TIC900 were analyzed in surface soil samples (n=15) with Primacs^{SNC100} Carbon/Nitrogen (C/N) analyzer (Skalar Analytical B.V., Breda, NL) using two distinct temperature programs. For analysis of surface soil with each temperature program, 100-125 mg of a sample was weighed into a ceramic crucible which was preconditioned at 950°C for 15 minutes and cooled to room temperature. Samples were then subjected to combustion in the C/N analyzer. The first temperature program, namely TC/TN-method, involved combustion of the sample at 1200°C. The second temperature program was performed according to the DIN19539 protocol [50] and will be named DIN19539-method in this study. It consisted of three heating steps at 400°C, 600°C and 900°C to quantify thermally labile total organic carbon (TOC400), residual oxidizable carbon (ROC) and total inorganic carbon (TIC900), respectively. Each heating step was held for 480 s. The temperature was increased at a rate of 70°C min^{-1} between combustion stages. Results obtained for TC, TN, TOC400, ROC and TIC900 were corrected for dry mass which was determined gravimetrically by heating 5 representative samples, one from each study area, at 105°C in an oven for at least 16 h following method NS-EN 15934:2012 [168]. For the TC/TN-method, the C/N analyzer was calibrated using glycine standard ($C_2H_5NO_2$, CAS-Nr.: 56-40-6) which is an amino acid with a molecular weight of 75.07 g mol^{-1} consisting of 319.9 mg g^{-1} C and 186.6 mg g^{-1} N. Glycine was dried for 1 h at 105°C and cooled to room temperature prior to weighing into the crucibles. A 7 point calibration was carried out with amounts ranging between 6-120 mg glycine. For the DIN19539-method, the C/N analyzer was calibrated with a standard consisting of separate compounds for TOC400, ROC and TIC. It was prepared according to descriptions in the Skalar method [162]. The composition is specified in Tab. 3.2. A 7 point calibration was carried out with 10-150 mg of standard. Accuracy of the TC/ TN method was verified using glycine standard and that of the DIN19539 method was verified with the DIN19539 standard. Each of these standards were run once between samples for quality control. Accuracy of the TC/ TN method was found to be 99.7% for TC and 101.3% for TN content. With the DIN19539 method, an accuracy of 100% for TOC400, of 99.5% for ROC and of 100.5% for TIC900 was accomplished.

Table 3.2 – Composition of the DIN19539 standard used for TOC400, ROC and TIC900 determination in this study. The mixture consisting of ammonium oxalate, black carbon and calcium carbonate has to be filled up with aluminum oxide to a final amount of 20.0 g.

Compound name	Sum formula	CAS-Nr.	C content in compound (mg g^{-1})	Amount of compound in standard (g)	Amount of respective carbon form in standard
Ammonium oxalate monohydrate	$(NH_4)_2C_2O_4 \cdot H_2O$	6009-70-7	169.0	2.37	20 mg g^{-1} TOC400
Carbon black	C	1333-86-4	1000	0.40	20 mg g^{-1} ROC
Calcium carbonate	$CaCO_3$	471-34-1	120.0	3.33	20 mg g^{-1} TIC900
Aluminum oxide	Al_2O_3	1344-28-1	0	fill up to 20.0 g	-

3.4 Analysis of trace elements

First, surface soil samples (n=15) were homogenized and sieved according to descriptions in Sec. 3.3. Then, samples were prepared for digestion. 250-350 mg of soil was weighed into polymer based vessels. 9 mL of 50 % v/v HNO_3 (Ultra Pure grade, distilled by Milestone SubPur unit) was added to the sample. Then, digestion of prepared surface soil samples was carried out with UltraCLAVE (Milestone Inc.) high-pressure microwave digestion system. After digestion, the solution containing the digested sample was transferred to a new bottle and diluted with MilliQ-water to a total volume of approximately 108 ml. Differences in the final volume were noted by measuring the weight of the sample after dilution. 15 mL of diluted sample was collected in a PP-vial. An additional dilution by a factor of 25 was performed before samples were subjected to analysis with ICP-MS. Trace element analysis was carried out with an Agilent ICP-QQQ 8800 (Agilent Technologies) using two tune modes (O_2 and NH_3). The measurement parameters are listed in Tab. 3.3. For quality assurance/ quality control (QA/ QC), three blanks and one aliquot of the reference material Soil GBW 07408 (GSS-8) (Chinese National Center for Standard Materials) were digested and diluted in one digestion batch, in addition to soil samples. They were treated in the same way as the samples. The obtained concentrations for elements in samples from the ICP-MS analysis were corrected for the concentrations found in blank samples. The quality assurance parameters are listed in Tab. 3.3.

Table 3.3 – ICP-MS acquisition parameters. Parameters were set for both O_2 and NH_3 tune mode, unless stated otherwise.

	Parameter	Value
Plasma parameters	RF power	1600 W
	RF matching	1.80 V
	Sample Depth	8.0 mm
	Carrier gas (Ar)	0.80 L min^{-1}
	Makeup gas (Ar)	0.40 L min^{-1}
Lenses	Extract 1 (O_2 mode)	5.2 V
	Extract 1 (NH_3 mode)	5.0 V
	Extract 2 (O_2 mode)	-80.0 V
	Extract 2 (NH_3 mode)	-95.0 V
	Omega Bias (O_2 mode)	-215 V
	Omega Bias (NH_3 mode)	-210 V
	Omega Lens (O_2 mode)	28.3 V
	Omega Lens (NH_3 mode)	28.1 V
	Deflect	-15.0 V
	Plate Bias	-60 V
Cell	He Flow (O_2 mode)	2.0 mL min^{-1}
	He Flow (NH_3 mode)	1.0 mL min^{-1}
	O_2 Flow	46%
	NH_3 flow	25%
	Oct Bias	-20.0 V
	Oct RF	200 V

Table 3.4 – Quality assurance parameters, listed for the elements that were in the focus of this study. Blank detection limits (BDL) are reported on dry weight (dw) basis. Measured levels are reported with mean and standard deviation (SD) and compared with the certified levels reported for the reference material. Uncertainty of the certified values was reported based on 99% confidence interval (CI). Accuracy (Acc.) and reproducibility was obtained based on 2 analyzed reference material samples.

		Reference material Soil GBW 07408 (GSS-8)				
		Measured		Certified		
Element	BDL ($\mu g\ g^{-1}$)	Mean ($\mu g\ g^{-1}$)	SD ($\mu g\ g^{-1}$)	Mean $\pm$ 99% CI ($\mu g\ g^{-1}$)	Acc. (%)	RSD (%)
P	0.330	685	13	775 ± 25	88	1.9
Cr	0.053	54.4	0.1	68 ± 6	80	0.2
Ni	0.035	27.5	0.2	31.5 ± 1.8	87	0.6
Cu	0.094	19.3	0.01	24.3 ± 1.2	79	0.04
Zn	0.112	59.1	1.21	68 ± 4	87	2.0
As	0.017	10.5	0.16	12.7 ± 1.1	83	1.5
Cd	0.0037	0.122	0.01	0.13 ± 0.02	93	4.7
Pb	0.025	13.91	0.08	21 ± 2	66	0.6

3.5 ASE sample preparation

Extraction of samples was carried out following a protocol established by Pintado-Herrera et al. (2016) [140] with individual modifications. Surface soil samples collected in aluminium boxes were used for the analysis procedure. First, surface soil samples were first dried at room temperature (left with the lid open (few mm) for air exchange) within the first two weeks after sample collection. After transfer to NTNU Trondheim, Department of Chemistry, these samples were stored at -22°C. Before further sample preparation, samples were subjected to room temperature for ∼20 hours. Then, the vegetation layer was removed. Samples were then homogenized and mixed and transferred to CC-cups for freeze drying. Subsequently, samples were freeze-dried for 30 hours with Alpha 1-2 LDplus by Martin Christ. Samples were then sieved with a 2 mm mesh and collected in 50 mL Falcon tubes. To prevent samples from cross-contamination during homogenization and sieving, the first homogenization and sieving fraction was discarded. In addition, mortar, pestle and sieve were cleaned and rinsed three times with soap and MilliQ-water and dried with dust-free paper tissues between samples.

Table 3.5 – Purchased chemicals and materials for determination of PCBs and PAHs in soil. See compound abbreviations for PCBs in Tab. 2.2 and for PAHs in Tab. 2.1.

Chemicals and Materials	Concentration, Specifications	Supplier
For extraction and further sample preparation:		
Dichloromethane	GC- capillary grade	VWR Chemicals (Radnor, PA, US)
Acetone	Analytical grade	VWR Chemicals (Radnor, PA, US)
Ethyl acetate	Analytical grade	VWR Chemicals (Radnor, PA, US)
Acetone (for cleaning)	Technical Grade	VWR Chemicals (Radnor, PA, US)
Hydrochloric acid	37% AnalaR® NORMAPUR® Reag. Ph. Eur. analytical reagent.	VWR Chemicals (Radnor, PA, US)
Ottawa sand	General purpose grade	Fisher Scientific (Loughborough, UK)
Aluminum oxide, activated	Basic brockmann I, standard grade, ca. 150 mesh	Sigma-Aldrich (St. Louis, MO, US)
Copper powder	$<425\,\mu m$, 99.5% trace metals basis	Sigma-Aldrich (St. Louis, MO, US)
Diatomaceous earth		Sigma-Aldrich (St. Louis, MO, US)
ASE extraction filters (cellulose)	For 1, 5, 10, 22 mL Dionex™ ASE 350/150 extraction cell	Thermo Scientific
Nylon syringe filter	$0.45\,\mu m$ pore diameter	VWR Chemicals (Radnor, PA, US)

Table 3.5 – *(continued)*

Chemicals and Materials	Concentration, Specifications	Supplier
Standard reference materials:		
Standard Reference Material 1941b "Organics in Marine Sediment"	-	National Institute of Standards and Technology, NIST (Gaithersburg, MD, US)
Calibration standards:		
3′-F-PCB-28 (internal standard)	100 µg mL^{-1} in isooctane	CHIRON AS (Trondheim, NO)
5′-F-PCB-118 (internal standard)	10 µg mL^{-1} in isooctane	CHIRON AS (Trondheim, NO)
'Dutch Seven' PCBs, ISO 10382 multicomponent stock solution	7 compounds (PCB-28, PCB-52, PCB-101, PCB-118, PCB-138, PCB-153, PCB-180), each 100 µg mL^{-1} in isooctane	CHIRON AS (Trondheim, NO)
16 U.S. EPA priority pollutant PAHs	NAP, ACY, ACE, FLU, PHE, ANT, FLT, PYR, BaA, CHR, BbF, BkF, BaP, DBA, BgP, IND, each 100 µg mL^{-1} in toluene	CHIRON AS (Trondheim, NO)
F-PAHs 'All in One Cocktail, Window 1-4'	1-Fluoronaphtalene, 4-Fluorobiphenyl, 3-Fluorophenanthrene, 1-Fluoropyrene and 3-Fluorochrysene, each 200 µg mL^{-1} in toluene	CHIRON AS (Trondheim, NO)

Equipment used for ASE was rinsed after each use at the following order: water and soap, MilliQ water, acetone. Rinsing was carried out three times with each solvent. Prior to extraction, diatomaceous earth and Ottawa sand were purified following U.S. EPA method 3545A [187]: 5-20 g of the respective resin was transferred into a porcelain crucible and heated at 400 °C for 4 hours in an oven (Carbolite ELF 11/6). Copper was activated before extraction according to U.S. EPA method 3660B [188] by treating the powder with different reagents on a Büchner funnel that was connected to a vacuum stream. Firstly, concentrated hydrochloric acid (HCl, 37%) was used, in order to remove oxides. Roughly, 5 mL acid was applied on 1 g of powder. Secondly, the powder was rinsed with distilled water until it was free of acid. This was tested by using colorimetric pH indicator strips (Sigma, St. Louis, MO, U.S.). Finally, it was rinsed with acetone, allowed to dry and transferred to a reagent bottle. For extraction, 0.5 g soil sample were weighed into a glass beaker and spiked with 50 µL of a 1000 ng mL^{-1} F-PAH and 50 µL of a 1000 ng mL^{-1} F-PCB internal standard solution, each dissolved in acetone. The spiked internal standard solutions were allowed to dry on the soil. 2

g diatomaceous earth was added and thoroughly mixed with the soil using a glass rod. A 22 mL stainless steel cell was sealed hand tight with one end-cap and equipped with two cellulose filters (pore size) at the bottom. Activated copper powder, alumina (Al_2O_3) and sample mixed with DE were sequentially added to the cell. The individual layers were separated each by a cellulose filter. Then, the mixture of soil sample and diatomaceous earth was transferred to the extraction cell with the help of a stainless steel funnel. Finally, Ottawa sand was added to fill void volumes as suggested in U.S. EPA method 3545A [187] and the cell was closed with another end cap and sealed hand tight.

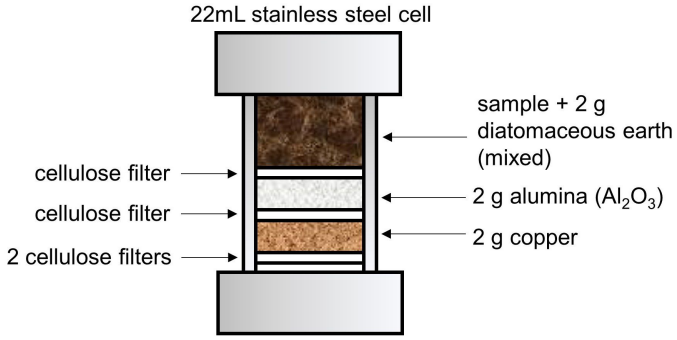

Figure 3.6 – Schematic representation of the cell loading with sample and resins for the ASE procedure.

Accelerated solvent extraction (ASE) was performed with a Dionex™ (Sunnyvale, CA, USA) ASE 150 accelerated solvent extractor using 22 mL stainless-steel cells and 60 mL amber collection vials. The extraction conditions were set as specified in Tab. 3.6. Between extraction of different sample types (e.g. study samples and matrix match samples), the ASE system was rinsed 3 times with the solvent and using an extraction cell that was filled with resins only.

Table 3.6 – Selected ASE conditions for extraction of PAHs and PCBs in soil samples.

System parameter	Value
Oven temperature	100°C
System pressure	1500 psi
Static time	5 min
Number of static cycles	3
Purge volume	60%
Nitrogen purge time	60 s
Cell size	22 mL
Solvent	Dichloromethane
Total time per sample	24 min
Total solvent per sample	∼35 mL

The extract obtained from ASE (∼35 mL) was concentrated to 2 mL with a Biotage TurboVap Classic LV evaporator with vial racks for ASE vials (Biotage, Charlotte NC, USA) at water bath temperature of 35°C and a gentle nitrogen (N_2) gas stream at 5 psi. To minimize analyte loss to the walls, the inner wall of the collection vial was rinsed with 10 mL ethyl acetate. Subsequently, the solution was

filtered through a 0.22 µm nylon syringe filter and concentrated to 1 mL final volume. Finally, the concentrated solution was transferred to amber vials and subjected to GC-MS analysis.

3.6 GC-MS analysis

GC-MS analysis of sample extracts was carried out following a protocol established by Pintado-Herrera et al. (2016) [140] with individual modifications. Analysis of samples was performed with an Agilent 7890A gas chromatograph with a GC Pal autosampler (CTC Analytics, Zwingen, CH) coupled to an Agilent 5975 single quadrupole mass spectrometer. Separation of target compounds was performed on a Thermo Scientific™ TraceGOLD™ TG-5MS GC Column (5% diphenyl/95% dimethyl polysiloxane, 30 m x 0.25 mm inner diameter x 0.5 µm film thickness), keeping the carrier gas flow (helium) at 1 mL min^{-1}, and the transfer line and the injection port temperatures at 290 °C. The temperature programme was set as follows: starting at 50°C for 2 min, followed by a temperature increase at a rate of 25°C min^{-1} to 250°C and held for 1 min, then temperature increase by 3°C min^{-1} to 286°C, and held for 3 min, followed by an increase by 8°C min^{-1} to 308°C and held for 1 minute and finally, 1°C min^{-1} to 310°C and held for 3 min. The overall analysis time for one sample with the selected temperature programme was 34.75 min. Injection volume was 1 µL in split mode with a ratio of 2:1 and the solvent delay was set to 6 min. The mass detector was operated in selected ion monitoring (SIM) mode using electron impact ionization (EI) set at 70 eV. The SIM programme with *m/z* values for the different PAH and PCB target analytes (TA) and internal standards (ISTD) is listed in Tab. 3.7. Retention times of PAHs sharing similar *m/z* and RT, i.e. PHE+ANT, FLT+PYR, BaA+CHR, BbF+BkF+BaP and DBA+BgP+IND, were verified by GC-MS analysis of single compound standards, i.e. standards of ANT, PYR, BkF, BaP, BgP and IND, respectively. Calibration solutions at concentrations ranging between 0.2-200 ng mL^{-1} were prepared from 'Dutch Seven' PCB standard and 16 U.S. EPA priority pollutant PAH mixture (specified Tab. 3.5), each dissolved in ethyl acetate and containing 50 ng mL^{-1} F-PAH and F-PCB internal standard. Lower limit of quantification (LLOQ) was set as the lowest acceptable value from the calibration solution. Instrumental limit of detection (LOD) was calculated with Eq. 2.8. To improve sensitivity of the the MSD, only 3 of 5 compounds from the F-PAH internal standard mixture (Tab. 3.5), namely 3-FBP, 3-FPHE and 3-FCHR were selected for the calibration curves and TA quantification.

Table 3.7 – Selected ion monitoring programme with *m/z* ratios for each time interval for the detection of PAH and PCB target analytes (TA) and internal standards (ISTD). See sections XX and XY for compound abbreviations.

Start time (min)	*m/z* window	Calc. nr. of cycles s^{-1}	Compound	Type	RT (min)	Molecular mass (g mol^{-1})	Ion(s) (*m/z*)
0	128	8.3	NAP	TA	7.76	128.17	128
8.25	172	8.3	4-F-BP	ISTD	8.87	172.2	172
9.25	152, 154	4.5	ACY	TA	9.38	152.2	152
			ACE	TA	9.57	154.21	154
9.8	166	8.3	FLU	TA	10.08	166.22	166
10.8	178, 196	4.5	3-F-PHE	ISTD	11.06	196.22	196
			PHE	TA	11.22	178.23	178
			ANT	TA	11.29	178.23	178
11.5	255.9, 273.9	4.5	3'-F-PCB-28	ISTD	11.62	275.53	273.9
			PCB-28	TA	11.69	257.54	255.9
11.9	289.90	8.3	PCB-52	TA	12.14	291.99	289.90
13	202, 325.8	4.5	FLT	TA	13.36	202.26	202
			PCB-101	TA	13.62	326.43	325.80
			PYR	TA	13.92	202.26	202
14.2	343.9, 345.9	4.5	5'-F-PCB-118	ISTD	14.49	344.42	343.9, 345.9
14.8	325.9	8.3	PCB-118	TA	15.00	326.43	325.9
15.4	359.8	8.3	PCB-138	TA	15.53	360.88	359.8
			PCB-153	TA	16.31	360.88	359.8
17	246	8.3	3-F-CHR	ISTD	17.47	246.3	246
17.7	228	8.3	BaA	TA	17.82	228.29	228
			CHR	TA	17.99	228.29	228
18.2	393.8	8.3	PCB-180	TA	18.32	395.32	393.8
19	252	8.3	BbF	TA	22.74	252.32	252
			BkF	TA	22.86	252.32	252
			BaP	TA	24.37	252.32	252
26	276, 278	4.5	IND	TA	30.13	276.34	276
			DBA	TA	30.27	278.35	278
			BgP	TA	31.33	276.34	276

Quality assurance/ quality control (QA/ QC) was performed with surface soil sample S1 as matrix standard. Pre-extraction matrix spikes (will be referred to as spike samples in this thesis) and post-extraction matrix spikes (will be referred to as matrix-matched, MM, samples) were prepared using 0.5 g sample and following the extraction procedures described in Sec. 3.5. 0.5 g surface soil matrix was pre- and post-extraction spiked with 50 and 100 ng PAH and PCB target analytes, i.e. 50 and 100 µL of a solution containing 1000 ng mL^{-1} analyte, achieving fortification levels of 50 and 100 ng mL^{-1} PAH and PCB target analytes in the final extract, i.e. 100 and 200 ng g^{-1} amount in samples respectively. Spike and matrix-matched samples were used to examine extraction recoveries, matrix effects and precision of target analytes at 50 and 100 ng mL^{-1} fortification level. Three replicates of spike samples and two replicates of matrix-matched samples were prepared

for each fortification level. Recoveries of target analytes were examined by comparison of the chromatographic signal of a pre-extraction matrix spike sample with that of a post-extraction matrix spike sample for each fortification level. Two types of recoveries were investigated: absolute and relative recoveries (Eq. 2.15 and 2.16). Matrix effects were evaluated for target analytes by comparison of the chromatographic signal from a post-extraction matrix spike sample with that from a standard in ethyl acetate solvent being at the same concentration (Eq. 2.13 and 2.14). Precision of the method for target analytes was assessed by the relative standard deviation between absolute chromatographic peak areas as well as peak areas relative to that of an internal standard, obtained from analysis of pre-extraction matrix spike samples at the two fortification levels. Possible contamination resulting during sample treatment was assessed. Method blanks were prepared according to the same extraction protocol as the soil samples without adding any sample matrix. Solvent blanks (ethyl acetate) were frequently analyzed in the GC-MS sequence between samples to record possible carry-over and cross-contamination in the instrument.

3.6.1 Suspect screening of retene in surface soils

Total ion chromatograms (TICs) of sample extracts from GC-MS analysis were examined for the presence of retene. Tentative identification of TIC peaks was carried out using the NIST (National Institute of Standards and Technology) Mass Spectral Library (NIST mass spectral search program, version 2.0). Subsequent verification of compound identity was performed by the analysis of an external standard. Only peaks present in the TICs of the samples and not in the method blanks were considered.

3.7 Data Treatment

Processing of chromatograms obtained from GC-MS analysis was performed with ChemStation2 (Agilent Technologies). Data processing and visualization of chromatographic data was carried out using Microsoft Excel Version 2105. Spatial distribution of PAH concentration data was displayed using ArcMap 10.3 [58]. Topographic basemap services were provided by the Norwegian Polar Institute [129]. Statistical analyses were performed with R version 4.1.0 [145]. Significance level for all tests was set as $p<0.05$. Variables were tested for normal distribution of residuals with a Shapiro-Wilk test. Homogeneity of variances was tested with Levene's test. For normal-distributed data with homogeneous variances, means between study areas were compared by a one-way ANOVA followed by Tukey's post-hoc test. Non-normal distributed data and data with heterogenous variances was analyzed with a Kruskal-Wallis test, followed by a Dunn's post hoc test with Bonferroni correction.

CHAPTER 4

Results and discussion

4.1 Variations in the nitrogen and carbon content in the topsoil of Ny-Ålesund

Surface soil samples (n=15) were analyzed for the following parameters: total carbon (TC), total nitrogen (TN), biologically labile organic carbon (TOC400), residual oxidizable carbon (ROC) and total inorganic carbon (TIC900) to investigate possible influences of these parameters on the composition of metals and organic pollutants as well as to gain more information on the soil characteristics of the study areas. These parameters were compared between the five study areas using a one-way Anova or Kruskal-Wallis test and post-hoc test, depending on the normality of the distribution of residuals of the respective variable (Shapiro-Wilk test, $p<0.05$). Comparison between study areas revealed only for TN a significant difference ($p<0.05$). Significantly elevated levels for TN were found at the study area Kiærstranda (KI) (Tukey's post-hoc test, $p<0.05$), shown as boxplots in Fig. B.1, supplementary material. It can be observed, that the mean TN content in surface soils from KI is approximately 2-fold higher than from other study areas (Tab. 4.1). Although no statistical significant difference was found for TC, TOC400 and ROC levels, it was observed that the mean TC, TOC400 and ROC content was the highest at KI, among study areas. Mean TIC900 level was highest in the study area NDM, despite no statistical significant difference.

Table 4.1 – Mean ± SD of TC, TN, TIC900, TOC400 and ROC composition in surface soil, divided by study area (each study area n=3). Study areas are indicated with BDE=Brøggerdalen, east side of Bayelva, BDW=Brøggerdalen, west side of Bayelva, GB=Gåsebu, KI=Kiærstranda and NDM=Nordre Diesetvatnet (Mitrahalvøya).

	Unit	BDE Mean ± SD	BDW Mean ± SD	GB Mean ± SD	KI Mean ± SD	NDM Mean ± SD
TC	mg g^{-1}	125.7 ±19.1	188.1 ±98.8	199.7 ± 149.6	311.8 ±17.7	201.8 ±69.9
TN	mg g^{-1}	8.9 ± 2.4	11.8 ±5.6	11.2 ± 7.8	26.1 ±2.8	8.6 ±4.6
TOC400	mg g^{-1}	104.9 ±19.4	168.8 ± 100.7	136.7 ± 108.8	255.4 ±17	113.5 ±59.1
ROC	mg g^{-1}	12.1 ±4	15.9 ±5.2	14.5 ±9.2	21.2 ±4	17.7 ±9.6
TIC900	mg g^{-1}	0.7 ±0.5	1.8 ± 1.7	1.6 ± 1.4	4.7 ±2.4	56.4 ±51.2

The pronounced levels of TOC400, ROC and TN in surface soils from KI might be attributable to bird guano deposits and dense moss communities that were observed during sampling in this study

area. Moreover, soils appeared to be darker and soil depth was greater than that of soils from the other study areas, which possibly indicates a higher extent of soil development. The geological background at NDM might have contributed to elevated TIC900 levels in surface soils from that area. Moreover, soils appeared to be less developed, had a lighter color and appeared to be sandy. It has been documented in geological studies on Svalbard that lower dolomite marble is dominating in this area, which is a carbonate mineral [18].

4.2 Profile of trace elements in Svalbard soils

Mean, standard deviation (SD), median, minimum (min) and maximum (max) concentrations of trace elements in studied surface soils (n=15) are given for As, Cd, Cr, Cu, Ni, P, Pb and Zn in Tab. 4.2. The concentrations for the 9 selected elements for each sample are listed in Tab. B.2 in the supplementary material. Mean concentrations of selected elements in soils from this study were found to be with decreasing order as follows: P > Zn > Cr > Ni > Cu > Pb > As > Cd. It was observed that concentrations of some elements in surface soils varied considerably, for instance Ni concentrations ranged between 4.5 and 99.9 µg g^{-1}, while the concentration range of other elements, such as Pb was smaller.

Table 4.2 – Mean, median, SD, min and max of 9 selected elements in surface soil from Svalbard (in µg g^{-1}), based on total number of samples (n=15) in this study. All samples contained levels above LOD.

	Unit	Mean	SD	Median	Min	Max
As	µg g^{-1}	6.19	8.35	3.89	1.59	35.42
Cd	µg g^{-1}	1.09	1.68	0.32	0.10	4.49
Cr	µg g^{-1}	36.4	18.7	42.9	8.5	65.3
Cu	µg g^{-1}	16.2	9.7	15.8	3.1	35.6
Ni	µg g^{-1}	26.6	23.9	21.4	4.5	99.9
P	µg g^{-1}	1118	660	904	234	2372
Pb	µg g^{-1}	15.1	5.8	13.6	8.2	29.6
Zn	µg g^{-1}	65.7	17.0	69.7	32.3	84.0

Mean concentrations of investigated surface soils in this study (n=15) were compared to two previous studies where surface soils from Ny-Ålesund were analyzed at NTNU as well [17, 72]. For a further assessment of concentrations in surface soils from the present study, the values were compared to background values reported in surface soil from Norway [132]. Values for As, Cd, Cr, Cu, Ni, Pb and Zn from the three aforementioned studies are listed in Tab. 4.3. The concentration order of selected elements in surface soils was found to be similar to the study of Aslam et al. (2019) [17]. In general, it can be seen that the mean levels of selected elements in the present study are elevated, compared to that of the two previous studies from Ny-Ålesund [17, 72]. For instance, mean As and Ni levels are 2-3 fold higher in this study than in the two previous studies. But there are also concentrations of elements that show good agreement. For example, Zn is at similar levels as observed in Aslam et al. (2019) [17]. It can be observed as well that the median levels of elements are closer than the mean levels to the concentrations found in the two previous studies. In comparison to the profile of trace elements reported in surface soils in Norway, mean concentrations of Pb in surface soils from the present study on Svalbard are lower than the mean concentrations of Norwegian surface soils [132]. The levels of Zn in surface soils from the present study are similar to levels reported

in Norwegian surface soils, while the mean concentrations of As, Cd, Cu, Cr and Ni on Svalbard are higher than in Norwegian surface soils [132]. Zn, Cd and As have been identified as elements where long-range atmospheric transport is a predominant source in surface soils [132, 170], while it is of lesser importance for Ni and Cu [132]. For Cr, the local bedrock has been identified as a major source in Norwegian surface soils [132].

Table 4.3 – Measured levels of elements in surface soils in Ny-Ålesund from two previous studies at NTNU [17, 72] as well as levels in Norwegian surface soils [132] with given sample size (n).

		Ny-Ålesund (n=21) Ref. [72]	Ny-Ålesund (n=13) Ref. [17]	Norway (n=464) Ref. [132]	
	Unit	Mean ± SD	Mean ± SE	Mean	Range
As	$\mu g\ g^{-1}$	2.54 ± 1.22	3.22 ± 0.24	1.44	<0.03-19.2
Cd	$\mu g\ g^{-1}$	0.57 ± 0.18	0.25 ± 0.03	0.57	0.047-6.7
Cr	$\mu g\ g^{-1}$	19.9 ± 9.4	26.70 ± 1.99	7.86	<0.05–191
Cu	$\mu g\ g^{-1}$	10.5 ± 3.6	10.54 ± 0.74	11.6	3.9–222
Ni	$\mu g\ g^{-1}$	12.9 ± 5.9	12.52 ± 0.85	7.46	0.30–309
Pb	$\mu g\ g^{-1}$	14.3 ± 4.5	11.84 ± 0.89	46.4	7.05–345
Zn	$\mu g\ g^{-1}$	73.2 ± 14.9	45.70 ± 3.68	62.4	10.8-931

Concentrations of selected elements were compared between the five study areas using a one-way Anova or Kruskal-Wallis test and post-hoc test, depending on the normality of the distribution of residuals of the respective variable (Shapiro-Wilk test, $p < 0.05$). The mean ± SD concentration of each element for each study area is shown in Tab. 4.4. Comparison between study areas revealed only for P a significant difference between mean levels (one-way anova, $p < 0.05$). Significantly elevated levels for P were found at the study area Kiærstranda (KI) (Tukey's post-hoc test, $p < 0.05$). Cd was slightly above the significance level (Kruskal-Wallis test, $p = 0.083$). However, it was noted that mean Cd levels were more than 10-fold higher in surface soils from KI than from the other four study areas. Despite no statistical significant difference for Cr and Cu, it was noted, that mean levels of Cr and Cu were higher in the study areas BDE, BDW, GB and KI than in NDM. For instance, mean Cr content was 1.5-2.5 times higher in surface soils from the other study areas compared to NDM. Conversely, mean Pb levels were higher in NDM than in the other four study areas. For As, elevated mean concentrations were noted for the study area KI and NDM. Moreover, the location BDE showed higher mean As levels, compared to the study areas GB and GB. Zn did not vary considerably between the three study areas in the vicinity of Ny-Ålesund (BDE, BDW and GB). Levels at Kiærstranda (KI) and on Mitrahalvøya (NDM) were elevated compared to BDE, BDW and GB, with the highest mean level being in surface soils from the study area KI (80.6 $\mu g\ g^{-1}$).

Table 4.4 – Mean ± SD concentrations of elements As, Cd, Cr, Cu, Ni, P, Pb and Zn in collected surface soil samples, given in µg g^{-1} and divided by study area (each study area with n=3). Study areas are indicated with BDE=Brøggerdalen, east side of Bayelva, BDW=Brøggerdalen, west side of Bayelva, GB=Gåsebu, KI=Kiærstranda and NDM=Nordre Diesetvatnet (Mitrahalvøya).

Element	Unit	BDE Mean ± SD	BDW Mean ± SD	GB Mean ± SD	KI Mean ± SD	NDM Mean
As	µg g^{-1}	4.25 ± 0.93	3.12 ± 2	3.36 ± 2.34	7.13 ± 0.15	13.11 ± 19.32
Cd	µg g^{-1}	0.19 ± 0.14	0.37 ± 0.12	0.3 ± 0.1	4.32 ± 0.17	0.26 ± 0.06
Cr	µg g^{-1}	50 ± 11.1	36.3 ± 25.1	29.7 ± 21.3	44.6 ± 3.9	21.6 ± 21.4
Cu	µg g^{-1}	17.8 ± 2.5	14.1 ± 9.7	17.5 ± 13.6	17.3 ± 1.8	14 ± 18.7
Ni	µg g^{-1}	23 ± 4.4	19.5 ± 14	19 ± 18.8	34.5 ± 2.6	36.8 ± 54.7
P	µg g^{-1}	1014 ± 239	906 ± 222	757 ± 182	2250 ± 125	664 ± 622
Pb	µg g^{-1}	16.5 ± 0.7	12.9 ± 7.7	14.8 ± 5.5	11.1 ± 1.5	20.3 ± 8.4
Zn	µg g^{-1}	59.1 ± 10.6	58 ± 25.9	57.1 ± 22.3	80.6 ± 3.1	73.8 ± 5.7

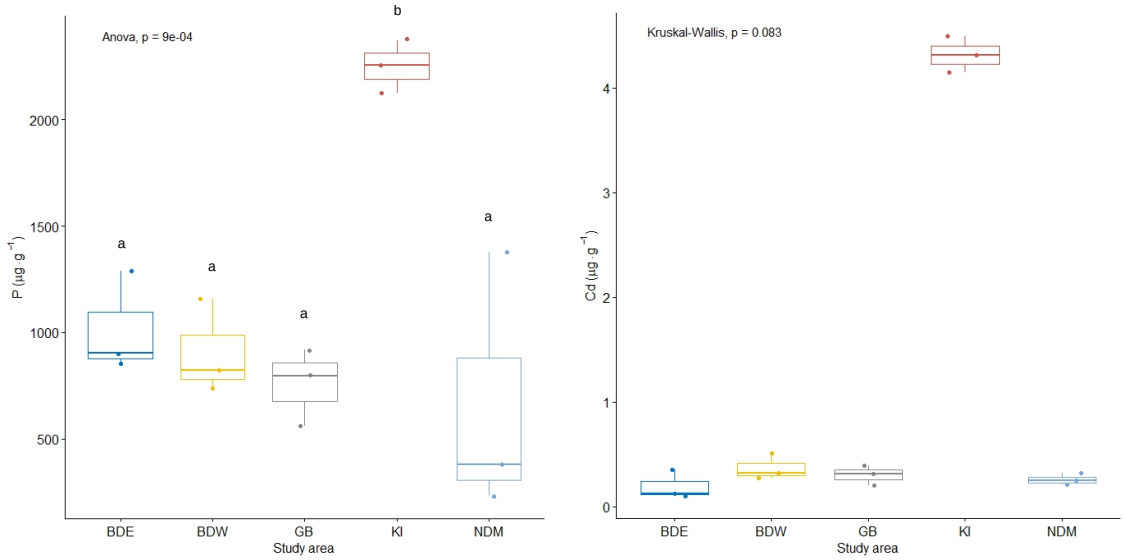

Figure 4.1 – Left panel: Boxplot for P content in soil (mg g^{-1}) at different study areas. Right panel: Boxplot for Cd content in soil (µg g^{-1}) at different study areas. The median is displayed by the line inside the box. The interquartile range (IQR) is displayed as a box. The whisker is determined by the 1st/ 3rd quartile ± 1.5 · IQR. Single data points are visualized as well. There are no outliers due to the low number of data points for each study area (n=3). Study areas sharing the same letter code were not significantly different from each other (one-way Anova and Tukey's post hoc test, $p < 0.05$). Study areas are indicated with BDE=Brøggerdalen, east side of Bayelva, BDW=Brøggerdalen, west side of Bayelva, GB=Gåsebu, KI=Kiærstranda and NDM=Nordre Diesetvatnet (Mitrahalvøya).

The pronounced mean Cd content in surface soils from KI was observed together with significantly higher P and TN concentrations in surface soils at KI than in the other four study areas. During

sampling in KI, bird guano deposits were observed on the cliffs. A previous study in Bellsund area on Svalbard noted significantly elevated Cd levels in an area dominated by seabirds, compared to other areas [214]. Moreover, P has been identified as a bird-derived element [41]. Seabirds as important contributors to elevated levels of metals as well as organic pollutants such as dichlorodiphenyltrichloroethane (DDT) and hexachlorobenzene (HCB) in Arctic terrestrial environments is discussed in the scientific literature [28, 41, 43]. Seabird feed on organisms being at a relatively high position in the marine food chain, where certain metals and organic contaminants biomagnify, for instance mercury (Hg) and polychlorinated biphenyls (PCBs) [41, 43]. Consequently, the pronounced concentrations of metals and organic pollutants in seabird-dominated areas reflect the transport from the marine food web [43]. The findings in this study, concerning the occurrence of elevated Cd levels in a bird influenced study area suggests the importance of potential additional vectors of pollutant transfer in remote locations of Svalbard that may deserve more attention in future studies. At the same time, these findings suggest that local sources of anthropogenic pollution seem to be negligible for Cd in studied soils as levels between the three study areas in proximity to Ny-Ålesund and Mitrahalvøya (NDM) were similar (Tab. 4.4).Variations in the mean As level between surface soils from BDE and BDW and GB may indicate an influence by local sources. Some sampling locations, particularly samples from BDE were in proximity to tertiary rocks that contain sandstones and shales as well as coal seams [18]. It has been documented in a past survey on Svalbard that tertiary rocks show a pronounced As-content [36]. In Longyearbyen, As-content in sediments was reported with levels ranging between 12.6-19.5 µg g^{-1} [37]. Mean As-levels in surface soil from KI and NDM was higher than in the study areas close to Ny-Ålesund (BDE, BDW and GB). At KI and NDM there is no documented presence of tertiary rocks [18]. It has been observed in a previous study that seabirds, such as the northern fulmar (*Fulmarus glacialis*), can transport As into Arctic terrestrial compartments as well [41]. Importantly, a large variation in As-content was noted for surface soil samples from NDM (13.11 $\pm$ 19.32 µg g^{-1}). Mean levels of Cr and Cu were higher in the study areas BDE, BDW, GB and KI than in NDM. It has been documented that the bedrock from the studied area at NDM originates from a distinct geological timescale than that of the other four study areas, leading to the presence of metamorphic rocks such as marble at NDM, while at the other study areas sedimentary rocks prevail, such as limestone [18]. Interestingly, mean Pb levels were higher in surface soils from NDM than from the other four study areas. Moreover, mean Ni levels were higher in surface soils from KI and NDM than from the study areas in the vicinity of Ny-Ålesund. In previous studies, the occurrence of Cr, Pb and Cu as well as Ni in surface soils from Svalbard has been associated with the influence of underlying mineral soil and bedrock [17, 72]. In Norwegian surface soils, the occurrence of Cr has been associated mainly with the bedrock, while for Ni and Cu, local point sources of pollution have been identified to be important [132]. It is possible that the bedrock may have influenced Cr, Cu and Pb levels in this study as well. Local point sources in Ny-Ålesund may have influenced Cu and Ni levels in surface soils in this study as well. However, due to large variation in Cu and Ni concentrations in surface soils from NDM, no clear differences could be observed. Mean Zn levels were higher in surface soils from KI and NDM than from the study areas BDE, BDW and GB, where they were at a similar range. In previous studies, Zn levels in soils from Svalbard have been associated with atmospheric deposition rather than an origin from the bedrock [17, 72, 132]. One study found a significant enrichment of Zn in the vegetation layer compared to the underlying soil [17]. Zn has also been identified as another element being transported to terrestrial ecosystems by seabirds [41, 214]. It is possible atmospheric deposition contributed to Zn levels in surface soils from this study as well and that local sources of pollution in Ny-Ålesund area, such as former mining activities, may play a lesser role to Zn levels in surface soils from Ny-Ålesund.

4.3 Method performance and quality control

This study aimed to develop a time efficient and simple methodology for the simultaneous extraction, detection and quantification of polycyclic aromatic hydrocarbons (PAHs) and polychlorinated biphenyls (PCBs) in soil samples based on the study of Pintado-Herrera et al. (2016) [140]. The time efficiency was achieved by establishing one sample preparation scheme for the extraction as well as a single GC-SIM-MS method for the gaschromatographic separation and subsequent detection of both compound classes. Possible contamination from sample preparation procedures was examined using method blank samples as described in Sec. 3.5. No contamination was found with PCB target analytes. However, 9 of the 16 PAH target analytes, namely NAP, FLU, PHE, FLT, PYR, BaA, CHR, BbF and BkF were found at low but detectable levels in method blank samples. Concentrations in samples were subtracted by the values found in method blanks for these target analytes.

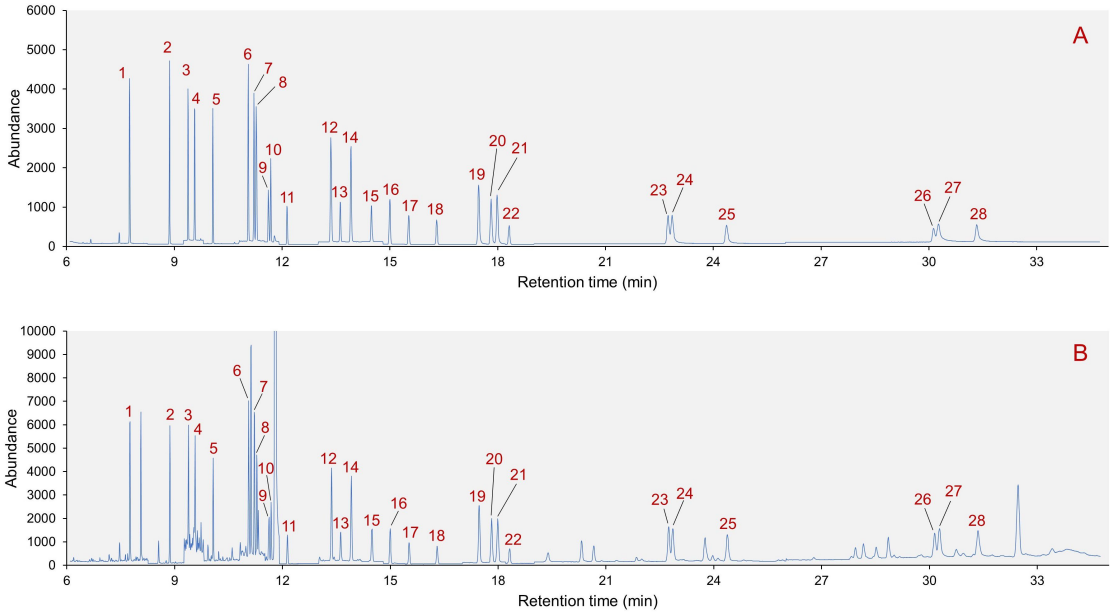

Figure 4.2 – GC-MS SIM chromatogram of a calibration standard containing PAH and PCB target analytes as well as F-PAH and F-PCB internal standards (each compound with a concentration of 50 ng mL^{-1} (A) and of a 50 ng mL^{-1} pre-extraction matrix spike (B). The elution order is as follows (RT for each compound in brackets): 1=NAP (7.76 min), 2=4-F-BP (8.87 min), 3=ACY (9.38 min), 4=ACE (9.57 min), 5=FLU (10.08 min), 6=3-F-Phe (11.06 min), 7=PHE (11.22 min), 8=ANT (11.29 min), 9=3′-F-PCB-28 (11.62 min), 10=PCB-28 (11.69 min), 11=PCB-52 (12.14 min), 12=FLT (13.36 min), 13=PCB-101 (13.62 min), 14=PYR (13.92 min), 15=5′-F-PCB-118 (14.49 min), 16=PCB-118 (15.00 min), 17=PCB-138 (15.53 min), 18=PCB-153 (16.31 min), 19=3-F-CHR (17.47 min), 20=BaA (17.82 min), 21=CHR (17.99 min), 22=PCB-180 (18.32 min), 23=BbF (22.74 min), 24=BkF (22.86 min), 25=BaP (24.37 min), 26=IND (30.13 min), 27=DBA (30.27 min), 28=BgP (31.33 min). See Tab. 2.1 for compound abbreviations.

Simultaneous detection of 16 U.S. EPA priority PAHs and 7 indicator PCBs was achieved by GC–EI-MS in SIM mode and with a Thermo TG-5MS column. The acquired GC–MS chromatograms for the 23 target analytes, 3 F-PAH internal standards and 2 F-PCB internal standards is shown in Fig. 4.2. Individual modifications in the temperature programme that was based on the study of

Pintado-Herrera et al. (2016) [140] improved the chromatographic separation. Sufficient separation of compounds was accomplished within 34.75 min. As it can be seen in the chromatograms in Fig. 4.2, the peaks of all 23 target compounds as well as 5 internal standards were well separated from each other and were clearly visible in standard solutions, dissolved in ethyl acetate, as well as when the soil matrix was present, for instance demonstrated for a pre-extraction matrix-spiked sample at 50 ng mL^{-1} fortification level in Fig. 4.2, B.

Table 4.5 – Instrumental and sample lower limit of quantification (LLOQ) and limit of detection (LOD) (in ng mL^{-1} and ng g^{-1}, respectively) for target analytes. Sample LLOQ and LOD was obtained from 0.5 g sample amount and 1 mL volume of standard solution that was subjected to analysis with GC-MS.

	Instrument		Sample analysis	
Analyte	LOD (ng mL^{-1})	LLOQ (ng mL^{-1})	LOD (ng g^{-1})	LLOQ (ng g^{-1})
NAP	0.33	1	0.67	2
ACE	0.33	1	0.67	2
FLU	0.33	1	0.67	2
PHE	0.67	2	1.33	4
ANT	0.67	2	1.33	4
FLT	0.67	2	1.33	4
PYR	0.67	2	1.33	4
BaA	1.67	5	3.33	10
CHR	1.67	5	3.33	10
BbF	3.33	10	6.67	20
BkF	3.33	10	6.67	20
BaP	3.33	10	6.67	20
IND	3.33	10	6.67	20
DBA	3.33	10	6.67	20
BgP	3.33	10	6.67	20
PCB-28	0.33	1	0.67	2
PCB-52	0.33	1	0.67	2
PCB-101	0.67	2	1.33	4
PCB-118	0.67	2	1.33	4
PCB-138	0.67	2	1.33	4
PCB-153	0.67	2	1.33	4
PCB-180	0.67	2	1.33	4

The lower limit of quantification (LLOQ) was estimated as the lowest concentration that is reliably quantified based on the lowest acceptable chromatographic signal from a calibration standard solution [14]. LOD of the instrument was acquired with Eq. 2.8 and for sample analysis with Eq. 2.9. Estimated LLOQs for sample analysis for PAHs ranged from 2 to 20 ng g^{-1} and for PCBs from 2 to 4 ng g^{-1}. Sample LODs for PAHs were in the range between 0.67 and 6.67 ng g^{-1} and for PCBs between 0.67 and 1.33 ng g^{-1}, which enabled the detection of analytes with appropriate sensitivity in this study. Concentrations detected below the LOD were listed as "<LOD" in the dataset.

Linearity of the method was examined by calibration curves of PAH and PCB standard solutions,

dissolved in ethyl acetate. 5-8 concentration levels (1-200 ng mL^{-1}) were selected, depending on estimated compound limit of quantification. The concentration range was chosen within expected concentration range in environmental samples of the study area (see Sec. 2.4.3 for further details). All compounds showed linear behavior in that range with coefficients of determination (R^2) >0.99. Using 50 ng mL^{-1} F-PAH and F-PCB internal standard proved to be a suitable concentration for calibration.

Table 4.6 – Calibration parameters of the GC-MS analysis of PAHs and PCBs. Parameters are given for PCB and PAH standard solutions, dissolved in ethyl acetate.

Compound class	Analyte	ISTD	Linear range (ng mL^{-1})	R^2	Slope
PAHs	NAP	4-F-BP	1-200	0.999	0.023
PAHs	ACY	4-F-BP	1-200	0.999	0.023
PAHs	ACE	4-F-BP	1-200	1.000	0.019
PAHs	FLU	4-F-BP	1-200	0.999	0.017
PAHs	PHE	3-F-PHE	2-200	1.000	0.020
PAHs	ANT	3-F-PHE	2-200	1.000	0.019
PAHs	FLT	3-F-PHE	2-200	1.000	0.020
PAHs	PYR	3-F-PHE	2-200	1.000	0.020
PAHs	BaA	3-F-CHR	5-200	1.000	0.019
PAHs	CHR	3-F-CHR	5-200	1.000	0.020
PAHs	BbF	3-F-CHR	10-200	1.000	0.015
PAHs	BkF	3-F-CHR	10-200	0.994	0.018
PAHs	BaP	3-F-CHR	10-200	0.992	0.014
PAHs	IND	3-F-CHR	10-200	0.997	0.012
PAHs	DBA	3-F-CHR	10-200	0.999	0.021
PAHs	BgP	3-F-CHR	10-200	0.999	0.016
PCBs	PCB-28	3'-F-PCB-28	1-200	0.999	0.031
PCBs	PCB-52	3'-F-PCB-28	1-200	0.997	0.017
PCBs	PCB-101	5'-F-PCB-118	2-200	0.992	0.018
PCBs	PCB-118	5'-F-PCB-118	2-200	0.995	0.024
PCBs	PCB-138	5'-F-PCB-118	2-200	0.997	0.017
PCBs	PCB-153	5'-F-PCB-118	2-200	0.997	0.015
PCBs	PCB-180	5'-F-PCB-118	2-200	0.999	0.015

4.3.1 Optimization of sample amount

The method for extracting PAHs and PCBs by Pintado-Herrera et al. (2016) [140] was tested for soil samples collected within this study. The optimal sample amount for extraction, detection and quantification of target analytes had to be determined, since the original methodology involved the extraction of marine sediments whose physico-chemical parameters, such as organic carbon content, likely differ to soil samples from this study. Mean TOC in sediment samples from their study ranged from 3.9 to 49.8 mg g^{-1} [140], while in the soils within this study, TOC400 ranged from 21.4 and 272.1 mg g^{-1} and ROC was quantified at levels ranging between 4.2-28.7 mg g^{-1}. It has been documented that organic contaminants such as PAHs and PCBs strongly bind to soil organic matter [114] and that soil physico-chemical properties, such as soil organic carbon content have an influence on the extraction efficiency of organic compounds from soil [82, 109]. On the

basis of these considerations, three different amounts of soil sample (0.5, 1 and 5 g) were tested for extraction efficiencies of PAH and PCB target analytes. Extraction efficiencies between investigated sample amounts were compared based on recovery estimates of PCB and PAH target compounds. For each sample amount to be tested, one pre-extraction matrix spike and one post-extraction matrix spike sample was prepared at a fortification level of 100 ng mL^{-1} for both PAH and PCB target analytes. Extraction was performed according to descriptions in Sec. 3.5. Prior to GC-MS analysis, a visual inspection of the final extracts was carried out. Fig. 4.3 shows the visual appearance of the final extracts obtained from 0.5, 1 and 5 g surface soil sample. Obtained extracts from the tested sample amounts showed the tendency towards a more intensive color with increasing amount of extracted sample. In particular, extracts yielded from 5 g soil showed a dark color and precipitation which indicates the presence of a relatively high amount of co-extracted matrix interferences. As a consequence, the extracts acquired from 5 g soil were excluded from analysis with GC-MS and 5 g as a potential sample amount was not further considered. The extracts from 0.5 and 1 g soil sample were subjected to analysis with GC-MS and absolute and relative recoveries of target analytes were compared between the two sample amounts. Fig. 4.4 shows the absolute and relative recoveries as a bar chart for all 23 target compounds from extraction of 0.5 and 1 g soil. The values are listed in Tab. C.1 in the supplementary material.

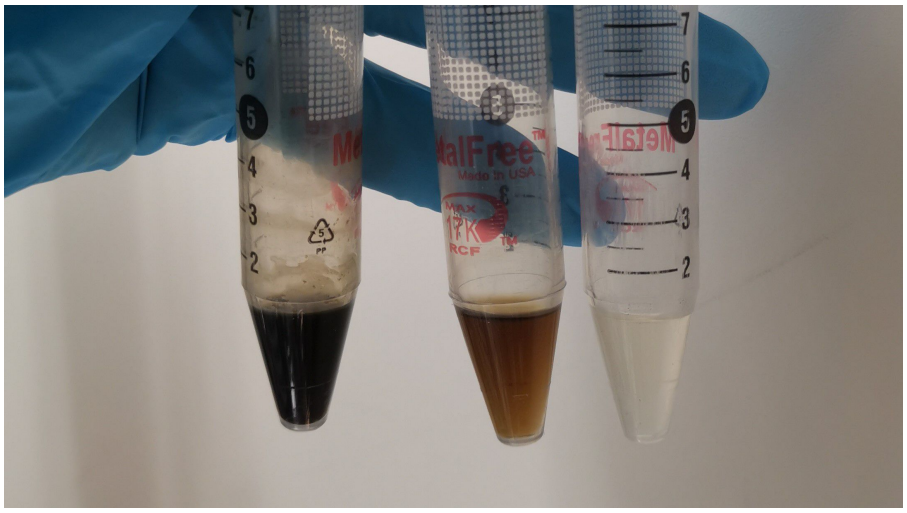

Figure 4.3 – Photograph of the final extract (approx. 1 mL) for subjection to GC-MS analysis, yielded from the ASE and evaporation procedure of different amount of sample 5 g (left), 1 g (center), 0.5 g (right). The procedure is further described in Sec. 3.5.

Comparison of relative and absolute recoveries between sample amounts revealed that the extraction efficiency was affected by the amount of soil used for extraction. For the majority of the 23 target compounds, recoveries were better when 0.5 g soil was used for extraction. The absolute and relative recoveries of all seven PCB target analytes were improved from extraction of 0.5 g soil. For PAHs in 0.5 g soil, relative recoveries improved for 8 (NAP, FLU, FLT, CHR, BbF, BkF, DBA and BgP) and absolute recoveries improved for 12 target compounds (NAP, ACY, FLU, PHE, FLT, PYR, CHR, BbF, BkF, IND, DBA and BgP). On the basis of these results, 0.5 g soil sample was selected as the most optimal amount for extraction, detection and quantification of target analytes as well as for quality assurance/ quality control (QA/QC) procedures.

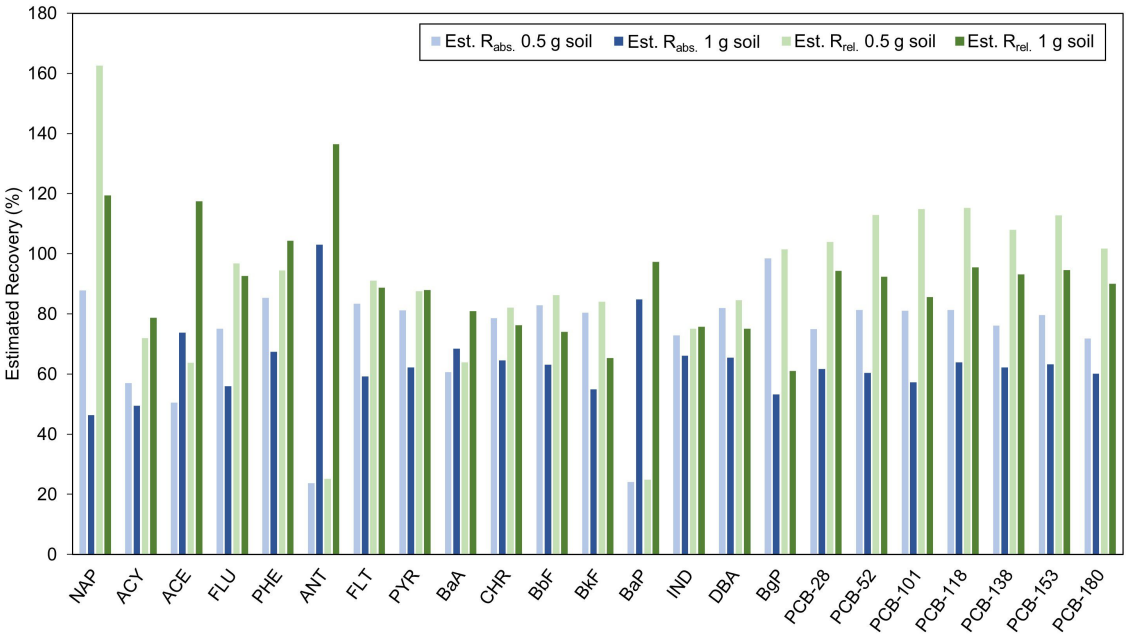

Figure 4.4 – Comparison of estimated relative and absolute recovery between 0.5 g and 1 g extracted sample. The samples were fortified with PAH and PCB target analytes at 100 ng mL^{-1}. The values for estimated absolute and relative recoveries are listed in Tab. C.1 in the supplementary material.

4.3.2 Method precision

Method precision was evaluated by spiking PAH and PCB target analytes into a soil matrix (0.5 g) prior to extraction at two levels, 50 and 100 ng, i.e. at respective fortification levels of 50 and 100 ng mL^{-1} (SP_{50} and SP_{100}) in the final extract. Three replicates were used for each fortification level. The precision is expressed as % relative standard deviation (RSD) between replicates and is shown in Tab. 4.7 for absolute values and values relative to the internal standard (ISTD) (see details for selected ISTDs in Tab. 4.6). Based on the absolute values, precision was acceptable for most PAH target analytes with RSD being <15%. A notable exception from this was naphthalene at lower fortification level where RSD was 35%. During analysis, contamination of method blanks with naphthalene was observed. Although blank subtraction of samples was carried out accordingly, it cannot be ruled out that naphthalene levels from contamination varied and that contamination may have impacted the precision at 50 ng mL^{-1} fortification level. It was observed that precision improved for this analyte at the higher fortification level (100 ng mL^{-1}). For PCBs, precision based on absolute values was appropriate as well and RSD was <15% for all PCB target analytes. Moreover, precision was improved for most PCBs at the higher fortification level (100 ng mL^{-1}) whereas no clear trend for the precision between the two fortification levels could be observed for PAH target analytes. Some PAHs, such as FLT and BgP, had a higher RSD at the higher fortification level while the RSD lowered for other PAHs, such as CHR and BaP. Variations between absolute values may be explained by analyte losses during sample preparation and differences in injected sample amounts to the GC. Internal standards can be used to account for these types of variations and, thus, may improve precision of the analytical results [166]. However, no clear improvement concerning the precision

of relative values, compared to that of absolute values was observable in this study. While some compounds had a lower RSD for the relative values, such as ACY, the RSD of relative values from other compounds increased, such as BkF and PCB-101. In particular, the internal standard method did not improve the precision at both fortification levels for the high molecular weight (HMW) PAHs, where 3-fluorochrysene (3-F-CHR) was used as ISTD, i.e. for BaA, CHR, BbF, BkF, BaP, IND, DBA and BgP.

Table 4.7 – Precision of target analytes in replicates (n=3) of pre-extraction matrix spikes at 50 and 100 ng mL^{-1} fortification levels, SP_{50} and SP_{100} respectively. Mean, STD and RSD of absolute values (peak area) and relative values (peak area of analyte relative to peak area of internal standard) are given for each analyte. See Tab. 2.1 for PAH compound abbreviations and Tab. 4.6 for selected internal standard for the respective analyte.

		Absolute values			Relative values		
Analyte		Mean	SD	RSD (%)	Mean	SD	RSD (%)
NAP	SP_{50}	65357	22726	35	1.07	0.29	27
	SP_{100}	109558	8462	8	1.97	0.20	10
ACY	SP_{50}	53649	5613	10	0.86	0.07	8
	SP_{100}	112463	8428	7	1.95	0.11	6
ACE	SP_{50}	74668	10044	13	1.20	0.16	13
	SP_{100}	117357	4679	4	2.04	0.11	6
FLU	SP_{50}	42990	2676	6	0.69	0.02	2
	SP_{100}	82901	7126	9	1.45	0.12	9
PHE	SP_{50}	86533	9877	11	1.04	0.15	15
	SP_{100}	142822	18969	13	1.95	0.22	11
ANT	SP_{50}	59444	960	2	0.69	0.03	4
	SP_{100}	110294	3898	4	1.47	0.09	6
FLT	SP_{50}	74440	3139	4	0.89	0.02	2
	SP_{100}	132334	7891	6	1.79	0.15	8
PYR	SP_{50}	79541	4046	5	0.93	0.01	2
	SP_{100}	138289	7578	5	1.85	0.15	8
BaA	SP_{50}	62132	5233	8	0.76	0.07	9
	SP_{100}	115494	971	1	1.58	0.10	6
CHR	SP_{50}	64835	5132	8	0.79	0.09	12
	SP_{100}	117325	1650	1	1.60	0.10	6
BbF	SP_{50}	60077	2159	4	0.74	0.10	14
	SP_{100}	102592	3432	3	1.41	0.15	10
BkF	SP_{50}	61519	2002	3	0.76	0.09	12
	SP_{100}	105300	3212	3	1.44	0.15	10
BaP	SP_{50}	53378	2948	6	0.66	0.08	13
	SP_{100}	94490	3920	4	1.29	0.14	11
IND	SP_{50}	48697	1711	4	0.60	0.10	17

Table 4.7 – *(continued)*

Analyte		Absolute values			Relative values		
		Mean	SD	RSD (%)	Mean	SD	RSD (%)
	SP_{100}	85395	852	1	1.17	0.09	8
DBA	SP_{50}	69415	3783	5	0.86	0.15	17
	SP_{100}	122996	3130	3	1.68	0.13	8
BgP	SP_{50}	59636	2912	5	0.74	0.14	18
	SP_{100}	97994	8640	9	1.34	0.11	8
PCB-28	SP_{50}	34901	809	2	1.20	0.05	4
	SP_{100}	66733	2148	3	2.62	0.10	4
PCB-52	SP_{50}	19216	696	4	0.66	0.02	4
	SP_{100}	36659	905	2	1.44	0.03	2
PCB-101	SP_{50}	25129	1706	7	0.80	0.07	8
	SP_{100}	47925	531	1	1.68	0.08	5
PCB-118	SP_{50}	35597	2564	7	1.13	0.04	4
	SP_{100}	68544	2154	3	2.40	0.14	6
PCB-138	SP_{50}	23741	2174	9	0.75	0.01	1
	SP_{100}	46504	1532	3	1.63	0.10	6
PCB-153	SP_{50}	21798	1808	8	0.69	0.02	3
	SP_{100}	42673	1356	3	1.50	0.08	5
PCB-180	SP_{50}	19908	1241	6	0.63	0.03	4
	SP_{100}	38361	746	2	1.34	0.07	5

4.3.3 Recoveries

Extraction efficiency of the method was evaluated by comparing the absolute and relative values between triplicates of pre-extraction matrix spikes and duplicates of post-extraction matrix spikes. Absolute and relative recoveries are presented in Fig. 4.5 and Tab. 4.8.

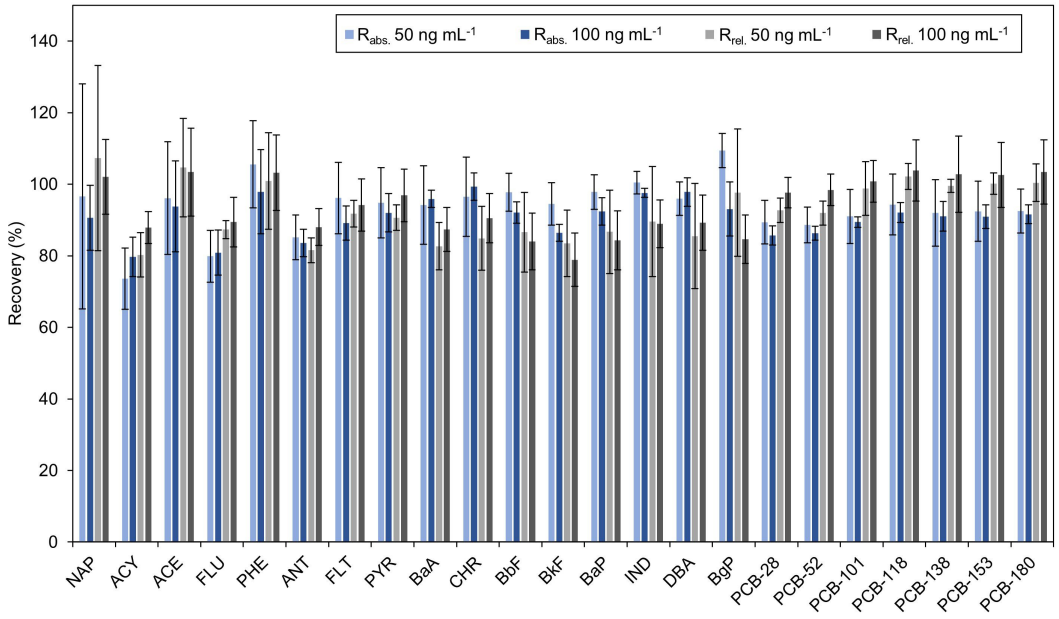

Figure 4.5 – Percent absolute ($R_{abs.}$) and relative recoveries ($R_{rel.}$) of polycyclic aromatic hydrocarbon and polychlorinated biphenyl target analytes at 50 and 100 ng mL^{-1} fortification levels (concentration in the final extract). Values were obtained for each fortification level as averages from pre-extraction matrix spikes (n = 3) and post-extraction matrix spikes (n = 2). Error bars represent the standard deviation.

Mean absolute recoveries were acceptable for the studied target analytes from both compound classes, ranging from 74 to 109 % for PAHs and from 86 to 94 % for PCBs. In general, the absolute recovery for ACY, FLU and ANT were lower than that of other analytes in this study. Similar observations were made by Pintado-Herrera et al. (2016) [140]. They found that alumina and copper as sorbents for the accelerated solvent extraction (ASE) procedures yielded the best results for recoveries and matrix interferences for most compound classes, including PCBs. However, the extraction efficiency in their study remained low (<60%) for LMW PAHs, such as ACY, NAP, and ACE, while that of other PAHs and that of PCBs improved (>90%). Nevertheless, recoveries for these LMW PAHs were better in this study, particularly for NAP (91-107%) and ACE (94-103%), and were found to be appropriate for the purpose of this study. For a large number of analytes, including PHE, BbF, IND and PCB-28, slightly higher mean absolute recoveries were observable at the lower fortification level (50 ng mL^{-1}). One possible explanation for these findings may be effects resulting from matrix components, possibly leading to bias in recovery estimates [185]. A higher % positive matrix effect was noted for the lower fortification level (50 ng mL^{-1}) in comparison to effects from 100 ng mL^{-1} fortification level for most of the target analytes. This was particularly true for PAHs, such as BbF, BkF and BaP (see Sec. 4.3.4). Hence, the slightly higher mean absolute recoveries observed at 50 ng mL^{-1} fortification level may result from a more positive bias due to higher signal enhancement from matrix effects. A comparably high variation for the absolute and relative recoveries of NAP was observed at the lower fortification level, with RSD being 33% for the absolute recovery. This is likely caused by the variations observed for absolute and relative responses of this analyte at the 50 ng mL^{-1} fortification level. Precision of absolute and relative

values are displayed in Tab. 4.7. Similarly to improvements for the precision of analytical results (see Sec. 4.3.2), better recoveries of target analytes may be achieved by the internal standard method. By adding an internal standard at the beginning of the extraction procedures, losses during extraction and cleanup of samples as well as matrix effects may be compensated for to some extent [166, 185]. In fact, mean relative recoveries improved in comparison to mean absolute recoveries for low molecular weight (LMW) PAHs, such as NAP, ACY, ACE and FLU as well as for PCB target analytes. However, a rather opposite effect was observed for HMW PAHs, particularly for the ones where 3-fluorochrysene was used as internal standard, i.e. BaA, CHR, BbF, BkF, BaP, IND, DBA and BgP. As previously mentioned in Sec. 4.3.2, it was also observed that their precision did not improve by using the internal standard method. For future studies, it can be advantageous to test an additional fluorinated PAH internal standard for the HMW-PAHs where 3-fluorochrysene was used as internal standard. For instance, 9-fluoro-benzo[*b*]fluoranthene may serve this purpose. Using this compound as internal standard delivered satisfactory results for the quantification of PAHs in oil shale ash with GC-MS in a previous study [88].

Based on the improved recoveries for the majority of PAH and PCB target analytes at the 50 ng mL^{-1} fortification level, quantification of PAH and PCB target analytes in surface soil samples from Svalbard was carried out with a single-point matrix-matched calibration standard at 50 ng mL^{-1} fortification level. Moreover, the internal standard method was applied. The matrix-matched calibration standard was prepared by adding 50 ng PAH and PCB target analytes into a soil matrix prior to extraction. The appropriateness of the ISTD for quantification of a target compound was demonstrated by the achieved recoveries, precision and linearity.

Table 4.8 – Absolute and relative recoveries ($R_{abs.}$ and $R_{rel.}$, given in %) of PAH and PCB target compounds in soil matrix analyzed by GC-MS

	50 ng mL^{-1}				100 ng mL^{-1}			
	$R_{abs.}$ (%)		$R_{rel.}$ (%)		$R_{abs.}$ (%)		$R_{rel.}$ (%)	
Analyte	Mean	RSD	Mean	RSD	Mean	RSD	Mean	RSD
NAP	97	32.6	107	24.1	91	10.0	102	10.2
ACY	74	11.6	80	7.7	80	6.9	88	5.0
ACE	96	16.4	105	13.1	94	13.5	103	11.9
FLU	80	9.1	87	2.9	81	7.8	89	7.8
PHE	106	11.5	101	13.3	98	12.0	103	10.2
ANT	85	7.3	82	4.2	84	4.5	88	5.9
FLT	96	10.4	92	4.1	89	5.3	94	7.7
PYR	95	10.4	91	3.9	92	5.8	97	7.6
BaA	94	11.6	83	8.0	96	2.5	87	7.1
CHR	96	11.5	85	10.5	99	3.9	90	7.6
BbF	98	5.4	87	12.9	92	3.2	84	9.4
BkF	94	6.2	84	11.1	86	2.7	79	9.4
BaP	98	4.9	87	13.4	92	4.1	84	9.8
IND	100	3.2	90	17.2	98	1.3	89	7.5
DBA	96	4.9	86	17.2	98	4.1	89	8.7
BgP	109	4.4	98	18.2	93	8.1	85	8.0
PCB-28	89	6.9	93	3.7	86	3.2	98	4.4
PCB-52	89	5.6	92	3.7	86	2.2	98	4.5
PCB-101	91	8.3	99	7.6	89	1.7	101	5.8
PCB-118	94	9.0	102	3.5	92	3.0	104	8.2
PCB-138	92	10.1	100	1.8	91	4.6	103	10.4
PCB-153	92	9.1	100	3.0	91	3.6	103	8.8
PCB-180	93	6.7	100	5.2	92	2.8	103	8.7

4.3.4 Matrix effects

Matrix effects were evaluated by comparison of the instrumental response of the analytes in duplicates of post-extraction soil matrix spikes (also referred to as "matrix-match (MM) samples" in this study) with the instrumental response of the analyte in a pure solvent (ethyl acetate). The % matrix effects (ME %) are shown in Fig. 4.6. Values for matrix factors (MF) and ME % are listed in Tab. C.2 in the supplementary material. Importantly, it was observed that there were comparably large variations for the ME % of some compounds within a fortification level (indicated with error bars in Fig. 4.6), such as ACE and FLT, particularly at the lower fortification level, which complicates interpretations of matrix effects in relation to fortification levels.

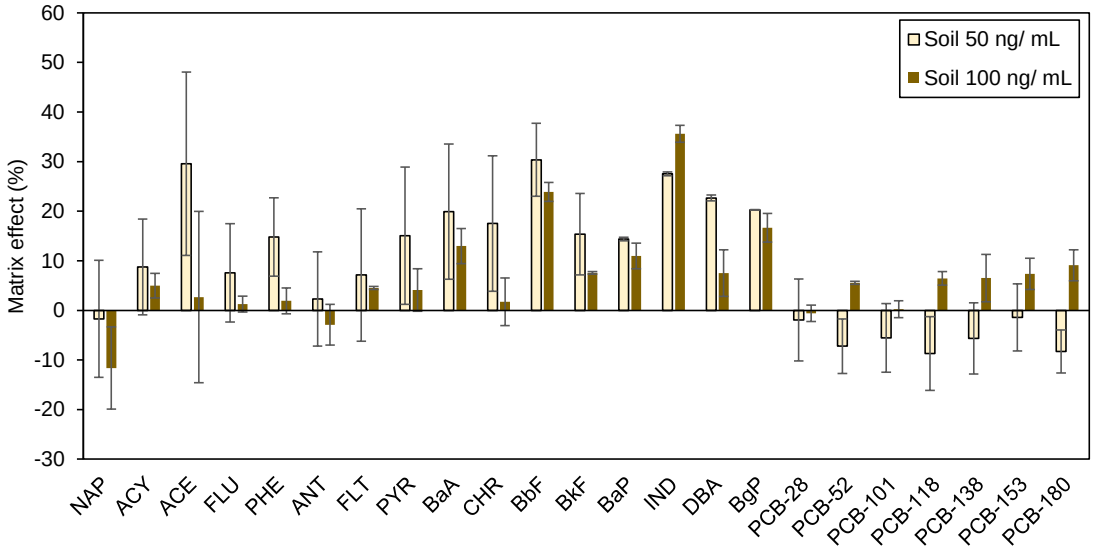

Figure 4.6 – Mean matrix effects (%) of 16 PAH and 7 PCB target analytes in soil extracts at 50 and 100 ng mL^{-1} fortification level. Error bars represent the standard deviation. See Tab. 2.1 for PAH compound abbreviations.

All PAHs but ANT at 100 ng mL^{-1} fortification level and NAP at both fortification levels, showed signal enhancement (ME>0%) due to matrix effects. In particular, HMW PAHs showed a comparably higher ME% than the lighter molecular weight PAHs, such as FLU, FLT and ANT. For instance, BbF and IND showed signal enhancement >20% at both fortification levels while it was <10% for FLU, FLT and ANT. Matrix effects have been investigated to a lesser extent in GC-MS than in LC-MS [161]. Signal enhancement in GC-MS due to the presence of matrix components is a common issue and has been described, particularly for pesticide analysis [56]. It is explained by competition mechanisms between target analytes and matrix constituents for active sites in the GC system, such as the column. As a consequence, a higher analyte amount arrives at the detector, leading to a higher chromatographic signal, in comparison to the signal of the analyte, dissolved in the pure solvent [57, 56]. For the analysis of PAHs and derivatives with GC-MS, signal enhancement effects have been reported, for instance for PAHs in cosmetic products [195]. Moreover, Qiao et al. (2017) observed signal enhancement for some chlorinated PAHs, such as 2-chloroanthrancene, in suspended particulate matrix samples from wastewater [144]. Interestingly, PCBs showed a different behavior than PAHs, concerning effects on the chromatographic signal due to presence of matrix constituents. In particular, the overall effect on the signal (enhancement or suppression) differed between the two fortification levels. All PCBs, but PCB-28, demonstrated signal suppression with ME being up to -9% at the lower fortification level and signal enhancement at the higher fortification level. Matrix suppression effects in GC-MS may be explained by matrix components that accumulate e.g. in the front part of the GC column and increase the number of active sites where analyte compounds bind to. As a consequence, less analyte arrives at the detector, leading to a diminished signal [71]. Moreover, dilution of samples may have an influence on the matrix effect as well. Takakuwa et al. (2018) found for the analysis of PCBs in reclaimed oil samples with

GC-triple quadrupole MS signal suppression effects for the ^{13}C-labeled PCB internal standards. Signal suppression was reduced or changed towards signal enhancement the more the samples were diluted. In particular, the ^{13}C-labeled PCB congeners with IUPAC numbers 28, 52, 101 and 118 showed signal suppression at 100-fold dilution which was reduced and/or changed to signal enhancement at 300- and 500-fold dilution [180]. Similar observations were made in this study. The samples that were fortified at 100 ng mL^{-1} level can be considered to be slightly more diluted, since the volume ratio between target analytes in solvent and matrix extract is slightly higher than for the matrix-matched samples at 50 ng mL^{-1} fortification level. The effect of dilution on matrix effects might be supported to some extent by observations for PAHs as well. For all PAHs, except NAP, ANT and IND, signal enhancement was reduced at the higher fortification level. One possibility to compensate for matrix effects when quantifying analytes in complex matrices is the application of internal standards [161]. In the study on PAHs in cosmetic products, analyzed with GC-MS, reduction of matrix effects after internal standard correction was successfully demonstrated. Hence, internal standard correction may improve the accuracy of analytical results [195]. Internal standards were applied in this study as well (see Sec. 4.5 for details).

4.4 Suspect screening of retene

Total ion chromatograms (TICs) and corresponding mass spectra of the analyzed soil extracts were examined for the presence of retene. Fig. 4.7 shows the TIC and corresponding mass spectrum of sample S5, which was one of the samples where the suspected peak of retene was observed. Moreover, the TIC of the external standard of retene and of matrix match samples spiked with retene external standard are shown in Fig. 4.7. One peak at RT=14.71 min was tentatively identified. The corresponding mass spectrum in some samples yielded a high match (879/912, i.e. 96%) to the mass spectrum of retene in the NIST library. Sunsequent GC-MS analysis of an external standard of retene at two different concentrations (100 and 200 ppb) showed a match in retention time and mass spectrum with that of the suspected peak in surface soil sample extracts. Moreover, analysis of a post extraction matrix-matched sample fortified with external retene standard at levels of approximately 50 and 200 ppb, showed an enhancement of the signal at RT=14.71 min in relation to the neighbouring signal at the higher fortification level. Thus, the identity of retene could be confirmed.

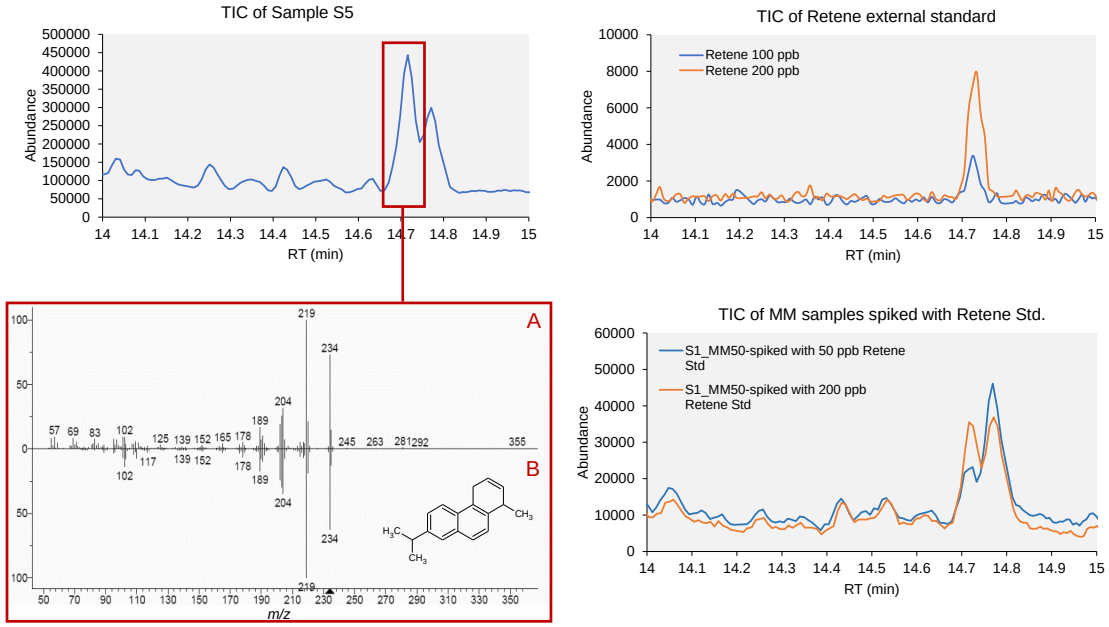

Figure 4.7 – Upper left panel: Total ion chromatogram (TIC) of sample S5, showing an intensive signal at RT=14.71 min, highlighted with a red box. Lower left panel: Corresponding mass spectrum in sample S5 at RT=14.71 min (A) and comparison to the mass spectrum of retene from the NIST library (B). The structural formula of Retene is included as well. Upper right panel: TIC of the retene external standard at two different concentrations (50 and 200 ppb), dissolved in ethyl acetate. Lower right panel: TIC of a post-extraction matrix spike sample (MM) sample which was fortified with retene external standard at two levels (50 and 200 ppb).

The retene signal with corresponding mass spectrum was observed only in samples collected from the three study areas in the vicinity of Ny-Ålesund settlement (BDE, BDW and GB). In total, 5 of 15 samples showed a retene peak (listed in the supplementary material, Tab. C.3). In a previous study, retene was detected and quantified in surface snow and seawater in the area of Ny-Ålesund at levels of 2.6 ng L^{-1}-1.8 µg L^{-1} and 1.2-55 ng L^{-1}, respectively [192]. The authors observed that retene levels in snow and seawater decreased with increasing distance from the settlement. Similarly, in this study, the retene peak appeared only in one sample from each of the study areas that were further away from Ny-Ålesund (BDW and GB), whereas in the location closest to the settlement (BDE) the peak was visible in all three samples (detection rates listed in Tab. 4.9). Another study investigated retene levels in soils close to Ny-Ålesund and on Mitrahalvøya and found retene only in samples in proximity to the settlement [96]. Likewise, in this study, the retene peak was only observed in soil samples from the vicinity of Ny-Ålesund. In the study on retene in Ny-Ålesund snow it was concluded that the high retene levels observed in seawater and surface snow are more likely attributable to coal dust from local sources rather than from wood burning from local or distant sources (long-range atmospheric transport) [192]. Moreover, they linked the relatively high levels of retene in snow and seawater in the vicinity of Ny-Ålesund to un-combusted coal dust being a major source of PAHs found in their samples [192]. Based on these findings, it is presumable that coal dust has been one contributor to retene and PAHs observed in soil samples from the vicinity of

Ny-Ålesund within this study. Moreover, the findings in the current study demonstrate that with the developed method, alkylated PAHs, such as retene can be detected as well.

4.5 Occurence of PAHs and PCBs in Svalbard soil

15 surface soil samples were analyzed for the presence of the 16 U.S. EPA priority PAHs and 7 indicator PCBs. The analytical results and discussion of PAH and PCB levels in studied surface soils are given in the following two sections.

4.5.1 Occurrence of PAHs

15 surface soil samples were analyzed for the presence of the 16 U.S. EPA priority PAHs. Spatial distribution of $\sum$PAHs levels is displayed in Fig. 4.9. 10 of the 16 PAH target compounds were above detection limits, namely NAP, FLU, PHE, ANT, FLT, PYR, BaA, CHR, BbF and BaP. PAH target analytes were detected and quantified in 11 of 15 samples in total. The analytical results of these PAHs and $\sum$PAHs for each study area are given in Tab. 4.9. The levels for the detected PAH target analytes are summarized for all 15 samples in Tab. C.3 and PAH-profiles for the 15 samples are displayed in Fig. C.23 in the supplementary material. Fig. 4.8 shows the average distribution of $\sum$PAHs between study areas. Importantly, it has to be noted that calculations of mean, median, min and max levels of $\sum$PAHs and single PAH target analytes were based on levels >LOD, which will have an impact on the representativeness of these values for study areas with samples that show levels <LOD. The amount of $\sum$PAHs in the 15 studied surface soil samples ranged between 12.5-533.6 ng g^{-1} (dw). $\sum$PAHs levels are approximately in a similar concentration range to levels reported in previous studies on PAHs in Ny-Ålesund soil (37-324 ng g^{-1} dw) [197] and lake sediment (27-711 ng g^{-1} dw) [87]. $\sum$PAHs concentrations in surface soils varied considerably between study areas as well as within study areas. The highest $\sum$PAHs levels were found in the study area BDE, that was closest to Ny-Ålesund settlement with mean $\sum$PAHs being 391.8 ng g^{-1}, followed by levels in samples from GB with a mean $\sum$PAHs concentration of 285.4 ng g^{-1} in surface soil.

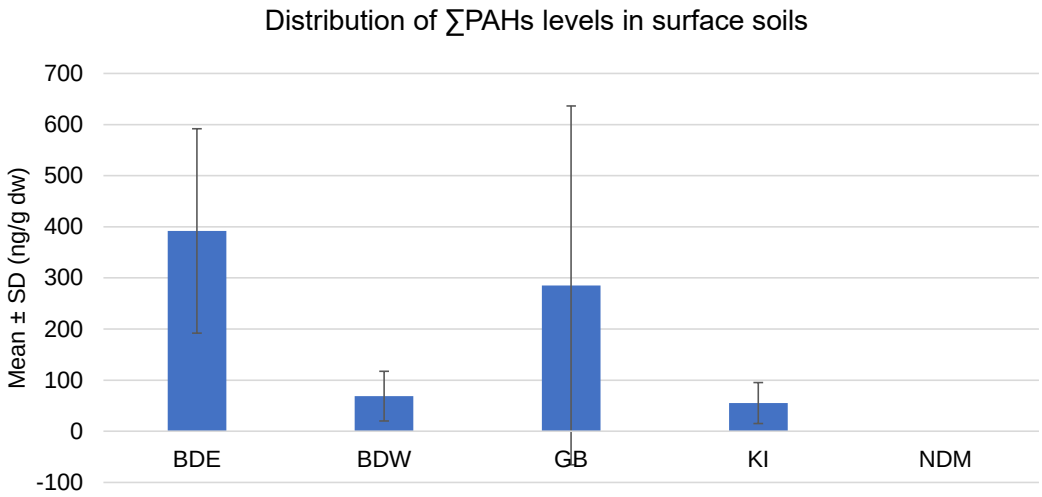

Figure 4.8 – Distribution of mean concentrations of ∑PAHs in ng g^{-1} (dw) between study areas. Error bars represent the standard deviation. Study areas are indicated with BDW=Brøggerdalen, west side of Bayelva, BDE=Brøggerdalen, west side of Bayelva, GB=Gåsebu, KI=Kiærstranda and NDM=Nordre Diesetvatnet (Mitrahalvøya).

Approximately 5 to 7-fold lower mean ∑PAHs levels compared to BDE were observed for the study areas BDW and KI, where the mean ∑PAHs concentration were 68.7 ng g^{-1} and 55.3 ng g^{-1}, respectively. All PAH compounds were found to be below LOD for the study area NDM (Nordre Diesetvatnet, Mitrahalvøya). A notably large variation in ∑PAHs concentrations was observed between samples from the study area GB where one sample showed a ∑PAHs content of 533.6 ng g^{-1} (sample S7), while the other sample contained 37.2 ng g^{-1} ∑PAHs and in the third sample the ∑PAHs concentration was found to be <LOD. It was also noted that the retene peak with mass spectrum was present in the samples with the highest ∑PAHs concentrations (except sample S1), which is highlighted with red letters in Fig. 4.9. Moreover, the sampling locations of these samples were comparably close to coal deposits from the Brøggerbreen Formation (Paleocene) within the Van Mijenfjorden Group according to the geoscience map of Svalbard [18]. Retene has been found to be a dominating compound in Svalbard coal [47]. In a previous study on seawater and surface snow in Ny-Ålesund snow, unburnt coal dust has been identified as one of the major sources for the occurence of PAHs in samples that contained retene at relatively high levels [192]. It may be presumed that unburnt coal dust has been contributed to PAH levels in samples that contained retene in this study as well. The absence of the retene peak in samples collected from Kiærstranda may indicate a different source than unburnt coal for PAHs in surface soils detected there.

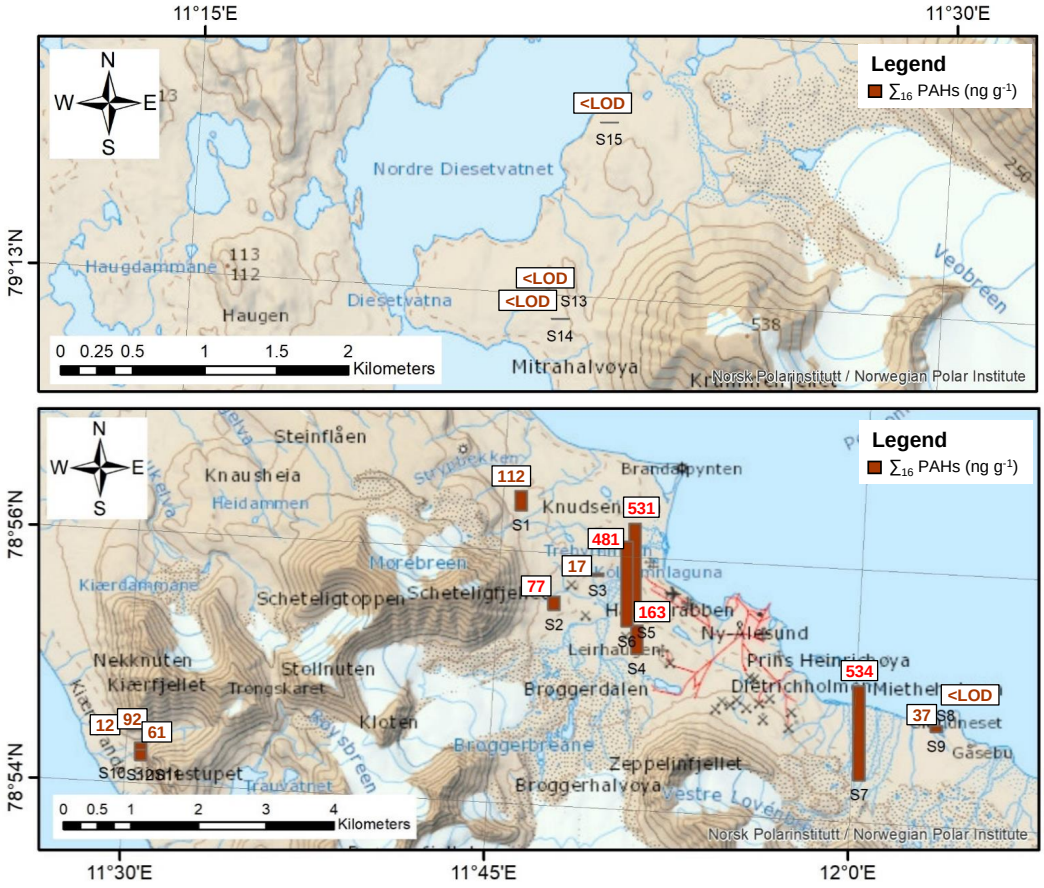

Figure 4.9 – Maps showing the ∑PAHs levels as bar chart for each sampling location. The number above the bar chart is the numerical value of the ∑PAHs level, expressed in ng g^{-1} soil (dw). For samples with values highlighted with a red color, the retene mass spectrum and peak in the total ion chromatogram was observed. The upper map shows the sampling locations with ∑PAHs levels of the study area Nordre Diesetvatnet (Mitrahalvøya), NDM. The lower map displays the sampling locations with ∑PAHs levels of the study areas Brøggerdalen, east and west of Bayelva (BDE, BDW) and Gåsebu (GB) as well as Kiærstranda (KI).

Table 4.9 – Detection rates (DR) and concentrations (mean, median, minimum and maximum) in ng g^{-1} (dw) of PAHs in soil samples, divided by study area (each study area with n=3). DR for each study area is expressed as ratio (number of samples above LOD/ total number of samples in the study area). ACY, ACE, BkF, IND, DBA and BgP were below LOD in all samples and are therefore not shown. Calculation of mean, median, minimum and maximum is based on values >LOD. Study areas are indicated with BDW=Brøggerdalen, west side of Bayelva, BDE=Brøggerdalen, west side of Bayelva, GB=Gåsebu, KI=Kiærstranda and NDM=Nordre Diesetvatnet (Mitrahalvøya). See Tab 2.1 for abbreviations of single PAH compounds.

Study area		NAP	FLU	PHE	ANT	FLT	PYR	BaA	CHR	BbF	BaP	∑PAHs	∑(carc. PAHs)	DR retene peak
BDE	DR	3/3	3/3	3/3	2/3	2/3	3/3	2/3	2/3	2/3	3/3	3/3	3/3	3/3
	Mean	116.6	20.1	119.2	32.4	30.9	23.6	12.0	34.2	17.3	27.8	391.8	70.1	
	Median	133.2	22.5	124.0	32.4	30.9	28.1	12.0	34.2	17.3	29.8	481.2	73.8	
	Min	39.3	12.8	82.4	31.2	21.9	7.6	6.7	25.2	12.1	21.0	163.1	21.0	
	Max	177.4	24.8	151.2	33.5	40.0	35.2	17.2	43.2	22.6	32.6	531.2	115.6	
BDW	DR	3/3	2/3	3/3	1/3	0/3	0/3	0/3	0/3	0/3	2/3	3/3	2/3	1/3
	Mean	10.8	4.8	16.7	10.4	<LOD	<LOD	<LOD	<LOD	<LOD	51.8	68.7	51.8	
	Median	8.0	4.8	21.2	-	-	-	-	-	-	51.8	77.4	51.8	
	Min	5.8	3.0	1.9	-	-	-	-	-	-	18.5	16.5	18.5	
	Max	18.7	6.6	26.9	-	-	-	-	-	-	85.1	112.1	85.1	
GB	DR	1/3	2/3	2/3	1/3	2/3	2/3	1/3	1/3	0/3	1/3	2/3	1/3	1/3
	Mean	88.2	9.5	104.9	23.1	33.0	30.2	25.4	47.6	<LOD	31.3	285.4	104.4	
	Median	-	9.5	104.9	-	33.0	30.2	-	-	-	-	285.4	-	
	Min	-	6.9	8.5	-	9.4	7.2	-	-	-	-	37.2	-	
	Max	-	12.1	201.2	-	56.6	53.2	-	-	-	-	533.6	-	
KI	DR	2/3	2/3	3/3	0/3	0/3	0/3	0/3	0/3	2/3	0/3	3/3	2/3	0/3
	Mean	21.4	10.3	25.8	<LOD	<LOD	<LOD	<LOD	<LOD	12.7	<LOD	55.3	12.7	
	Median	21.4	10.3	20.2	-	-	-	-	-	12.7	-	62.0	12.7	
	Min	14.0	6.0	12.4	-	-	-	-	-	12.1	-	12.4	12.1	
	Max	28.8	14.6	44.7	-	-	-	-	-	13.3	-	91.6	13.3	
NDM	DR	0/3	0/3	0/3	0/3	0/3	0/3	0/3	0/3	0/3	0/3	0/3	0/3	0/3
	Mean	<LOD	<LOD	<LOD	<LOD	<LOD	<LOD	<LOD	<LOD	<LOD	<LOD	<LOD	<LOD	
	Median	-	-	-	-	-	-	-	-	-	-	-	-	
	Min	-	-	-	-	-	-	-	-	-	-	-	-	
	Max	-	-	-	-	-	-	-	-	-	-	-	-	

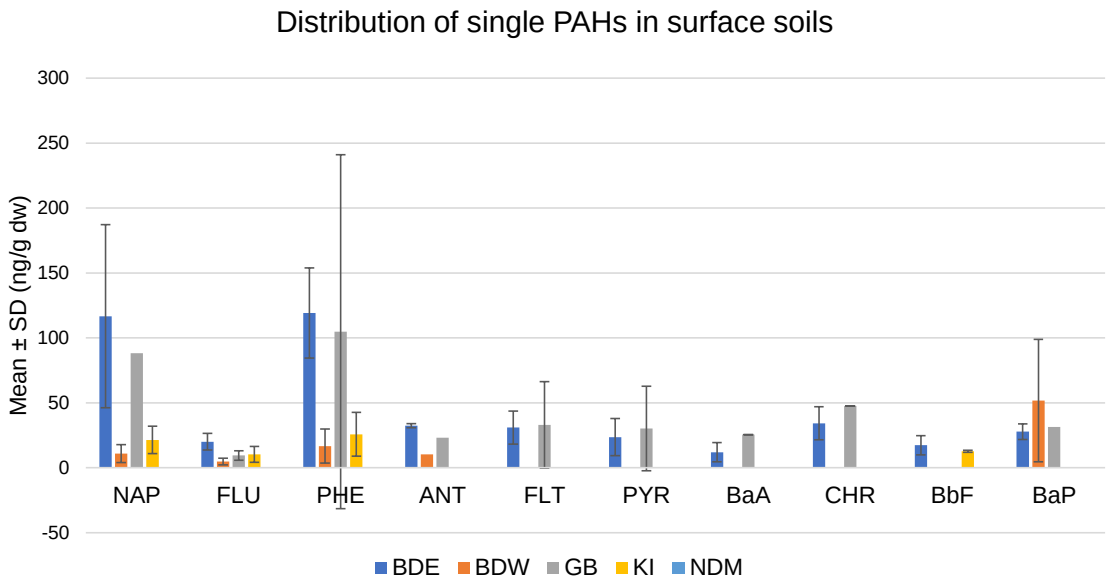

Figure 4.10 – Distribution of mean concentrations of the single PAH compounds in surface soil between study areas. Error bars represent the standard deviation. Study areas are indicated with BDW=Brøggerdalen, west side of Bayelva, BDE=Brøggerdalen, west side of Bayelva, GB=Gåsebu, KI=Kiærstranda and NDM=Nordre Diesetvatnet (Mitrahalvøya). See Tab 2.1 for abbreviations of single PAH compounds.

Fig. 4.10 shows the mean ± SD levels of single PAH compounds in surface soils compared between study areas. PHE was most abundant in samples. It was quantified in samples from all study areas except NDM with concentrations ranging between 1.9 and 201.2 ng g^{-1}. PHE concentrations were highest in surface soils from BDE with a mean level of 116.6 ng g^{-1}, followed by surface soils from GB with a mean level of 88.2 ng g^{-1}. Its concentration in surface soils varied considerably between study areas. For instance, surface soils from BDW and KI showed a respective 7- and 5-fold lower mean PHE level than surface soils from BDE. NAP dominated the PAH composition in surface soil samples as well. It was present in soil samples from all study areas except NDM. It was found in 9 of 15 samples at concentrations ranging from 5.8 to 177.4 ng g^{-1}. Comparably high variations of NAP concentrations were noted between samples from different study areas as well. For example, mean NAP levels at KI and BDW were approximately 5 and 11 times lower than the mean NAP level in surface soils from BDE. FLU was present in the 4 study areas BDE, BDW, GB and KI as well at levels in surface soils ranging between 3.0-24.8 ng g^{-1}. In comparison to PHE and NAP, lower variations in surface soil concentrations were observed for FLU between study areas. For example, mean concentrations of FLU were 2 and 4 times lower in surface soils from KI and BDW, compared to the mean FLU level in surface soils from BDE. The PAHs ACY and ACE were found to be below LOD for all 15 samples. ANT was above LOD only in samples collected from the three study areas in proximity of Ny-Ålesund settlement (BDE, BDW and GB). FLT and PYR were detected and quantified only in samples from BDE and GB. FLT levels ranged from 9.4 to 56.6 ng g^{-1}. PYR was found at concentrations ranging between 7.2-53.2 ng g^{-1}. Mean levels of FLT and PYR were similar between surface soils from BDE and GB. For instance, mean FLT concentration was 30.9

and 33.0 ng g^{-1} in surface soils from in BDE and GB, respectively. 4 of the 7 carcinogenic PAHs classified by the International Agency for Research on Cancer (IARC) [84] were detected in samples as well, namely BaA, CHR, BbF and BaP. BaA and CHR were detected in samples from BDE and GB, while BaP was found in samples from all three study areas close to Ny-Ålesund (BDE, BDW and GB). BbF was above LOD in samples from BDE and KI. The presence of BaP was notable. It is classified as group 1 carcinogen by IARC [84]. The highest amount of BaP was found to be 85.1 ng g^{-1} in sample S1 from the study area BDW. The HMW PAHs BkF, DBA, BgP and IND were <LOD in all 15 samples. Interestingly, it was observed that among the PAH compounds above LOD (except for BbF), the compounds with the lowest molecular weights NAP, FLU and PHE were detected and quantified in KI as well, while PAHs with a higher molecular weight, such as FLT, PYR and BaA were only above LOD at two locations in the proximity to Ny-Ålesund settlement (BDE and GB).

The found dominance of PHE and NAP over other PAH target analytes in surface soils from the present study is in accordance to findings from previous studies on Svalbard, such as in soils from Pyramiden and Ny-Ålesund [113, 197]. NAP, PHE and FLU were also noted as dominating PAHs, followed by FLT and PYR in emissions from a coal power plant in Longyearbyen, the main settlement on Svalbard [51]. Moreover, Yu et al. (2019) identified for PAHs detected in air at Zeppelin station at Ny-Ålesund that coal combustion was the main source (68% contribution) for PAHs detected there. They found that PHE, FLU, FLT, and PYR were the main contributing compounds of total PAHs [208]. Drotikova et al. (2020) concluded that the levels of these PAH target analytes in the air at Zeppelin station were most likely attributable to emissions from the Longyearbyen coal power plant which is located 115km southeast of Ny-Ålesund [51]. Interestingly NAP, PHE and FLU were detected in soils in Kiærstranda as well. However, it has to be noted that in Engelsbukta, which is situated in proximity to Kiærstranda, whaling activity has been taking place in the 17th century [89]. A more local source than the Longyearbyen coal power plant for PAHs found in KI would also be supported by the finding that the HMW-PAH BbF was above LOD for two samples in that study area. BbF has a comparably low vapour pressure and adsorbs to aerosol particles rather than being present in the gas phase, which favours a low mobility of this compounds in the atmosphere and a deposition relatively close to its emission source [95, 200]. ACE and ACY were below LOD in all surface soil samples from this study. Some previous studies found ACE and ACY at low levels, compared to other PAH compounds. For instance, ACY was reported to be at levels ranging between 0.3 and 5 ng g^{-1} and ACE was quantified at levels ranging between 0.1-0.9 ng g^{-1} in soil from Ny-Ålesund area, while that of FLU and PHE ranged between 2-20 and 11-133 ng g^{-1}, respectively [197]. Another study on surface snow from Ny-Ålesund found ACY to be below LOD as well [192]. Another possible explanation for ACE and ACY resulting below LOD for all samples is that it was noted during the method development that the presence of neighbour peaks was pronounced in the time window where these analytes eluted as it can be seen in the chromatogram in Fig. 4.2. These peaks might be attributable to matrix interferences and might have complicated quantification of ACY and ACE target analytes. Moreover, recoveries were lower for ACY, with absolute recoveries ranging between 74-80% and relative recoveries between 80-88%, while recoveries of most analytes ranged between 85 and 109%, in general (Tab. 4.8). BkF, DBA, BgP and IND were <LOD in all 15 samples. It is important to note that the detection limits with the current method were 1-2 orders of magnitude higher than in the other studies, such as in Ref. [113]. LOD of BkF, DBA, BgP and IND was 6.67 ng g^{-1} surface soil. One previous study on soil from Ny-Ålesund area reported levels of BkF, DBA, BgP and IND generally ranging from <1 to <20 ng g^{-1} in soils [197]. In another study on lake sediments from Ny-Ålesund area median levels of these compounds were within the range of a few ng g^{-1} [87].

For a further assessment of potential sources of PAHs to soils collected within this study, PAH indicator ratios were investigated, which have been frequently used to identify the potential origin of PAHs. Some PAH indicator ratios in soil samples were compared indicator ratios in some typical sources that were noted in Refs. [92, 209]. Based on selected diagnostic ratios and levels of respective PAH compounds being above LOD, diagnostic ratios could be obtained for samples from the study areas BDW, BDE and GB and are listed in Tab. 4.10.

Table 4.10 – PAH diagnostic ratios of soil samples collected in this study, in comparison to reported values for petrogenic (petrog.) and pyrogenic (pyrog.) origin, as well as different combustion (combust.) sources [92, 209]. Study areas are indicated with BDW=Brøggerdalen, west side of Bayelva, BDE=Brøggerdalen, west side of Bayelva and GB=Gåsebu.

Study area	BDW	BDE	BDE	GB	GB				
Diagnostic ratio/ sample ID	S2	S5	S6	S7	S9	Petrog.	Pyrog.	Fuel combust.	Grass/ coal/ wood combust.
ANT/ (ANT+PHE)	0.28	0.17	0.21	0.10		<0.1	>0.1		
FLT/ (FLT+PYR)		0.53	0.44	0.52	0.57	<0.4	>0.4	0.4–0.5	>0.5
BaA/ (BaA+CHR)		0.28	0.21	0.35		<0.2	>0.35		

The ratio ANT/ (ANT+PHE) ranged from 0.10 to 0.28, indicating that the detected PAHs are possibly originating from pyrogenic sources. Values for the ratio FLT/(FLT+PYR) in samples were ranging between 0.44-0.57, pointing towards a pyrogenic source as a main contributor to these PAHs. This ratio was >0.5 for three samples (S5, S7 and S9), possibly indicating grass, coal or wood combustion as a source. One sample (S6) showed a value ranging between 0.4-0.5 which may point towards fuel combustion being a potential source for these PAHs. The ratio BaA/(BaA+CHR) ranged in samples between 0.21-0.35, suggesting that PAHs detected in the respective samples might originate from a mixture of pyrogenic and petrogenic sources. Importantly, it has to be noted that these ratios should be regarded as an approximate indicator of a possible source, since degradation processes, such as biodegradation and photodegradation may alter PAH profiles in soils [186].

The presence of HMW-PAHs in surface soils, such as BaA, CHR, BbF and BaP in the three study areas in the vicinity of Ny-Ålesund as well as the presence of BbF at Kiærstranda may indicate that local sources contribute more likely than long-range atmospheric transport to PAH levels. It is known that HMW-PAHs show a lower likelihood to travel long distances via the atmosphere, since they have a comparably low vapor pressure and preferentially adsorb to aerosol particles rather than stay in the gas phase [95, 200]. These findings may also be supported by the fact that all PAH target analytes were below LOD in surface soils from Mitrahalvøya. It was used in this study as a reference location and is considered to be remote from local anthropogenic activities. The comparably large variations of total PAH levels in studied soil samples within and among the three study areas in the vicinity of Ny-Ålesund (BDE, BDW and GB) suggest the occurrence of local point sources that influence PAH levels in soils from these areas. The occurrence of retene, a dominating compound in Svalbard coal, the dominance of PHE, NAP and FLU as well as PAH indicator ratios point towards

a mixture of unburnt coal and combustion of coal and fuel being likely sources for PAHs found in soils from Ny-Alesund area. Moreover, emissions from cruise ships may have contributed to PAHs levels in surface soil samples from Ny-Alesund area as well, since aerosols from cruise ship emissions have been documented in air in a past study [211].

4.5.2 Occurrence of PCBs

15 surface soil samples were analyzed for the presence of the seven indicator PCBs (IUPAC numbers 28, 52, 101, 118, 138, 153 and 180). Analytical results for the seven indicator PCBs in surface soil on Svalbard are given in Tab 4.11. PCBs were detected and quantified in two samples from two different study areas (sample S9 from GB and sample S12 from KI). The $\sum_7$PCBs content in soil samples ranged from 37.9 to 45.9 ng g^{-1} (dw).

Table 4.11 – Analytical results for the indicator-PCBs in surface soil samples from Svalbard collected in this study, divided by study area. Values are reported and on dry weight (dw) basis. Only the single value is reported, since PCBs were detected in only one sample in two different study areas. Study areas are indicated with BDW=Brøggerdalen, west side of Bayelva, BDE=Brøggerdalen, west side of Bayelva, GB=Gåsebu, KI=Kiærstranda and NDM=Nordre Diesetvatnet (Mitrahalvøya).

Study area	BDE DR	Median (ng g^{-1})	BDW DR	Median (ng g^{-1})	GB DR	Median (ng g^{-1})	KI DR	Median (ng g^{-1})	NDM DR	Median (ng g^{-1})
PCB-28	0/3	<LOD	0/3	<LOD	1/3	11.7	0/3	<LOD	0/3	<LOD
PCB-52	0/3	<LOD	0/3	<LOD	1/3	11.7	0/3	<LOD	0/3	<LOD
PCB-101	0/3	<LOD	0/3	<LOD	0/3	<LOD	0/3	<LOD	0/3	<LOD
PCB-118	0/3	<LOD	0/3	<LOD	1/3	11.0	1/3	13.5	0/3	<LOD
PCB-138	0/3	<LOD	0/3	<LOD	1/3	11.4	1/3	13.4	0/3	<LOD
PCB-153	0/3	<LOD	0/3	<LOD	0/3	<LOD	1/3	10.9	0/3	<LOD
PCB-180	0/3	<LOD	0/3	<LOD	0/3	<LOD	0/3	<LOD	0/3	<LOD
$\sum$PCBs	0/3	<LOD	0/3	<LOD	1/3	45.9	1/3	37.9	0/3	<LOD

PCB-28 and PCB-52 were detected in one sample from GB and quantified to an amount of 11.7 ng g^{-1} for both congeners. PCB-118 and PCB-138 were found in surface soil samples from both study areas GB and KI. The congener PCB-153 was only detected and quantified with a concentration of 10.9 ng g^{-1} in the sample from KI. PCB-101 and PCB-180 were <LOD in all surface soil samples. Concentrations of single PCB congeners in surface soils were similar, potentially indicating a common source. Interestingly, $\sum$PCBs concentration in surface soils of this study was 1-2 orders of magnitude higher than in soils from Ny-Ålesund area reported in previous studies. For instance, Aslam et al. (2019) found $\sum_7$PCBs contents ranging between <1.0-8.1 ng g^{-1} [17]. Zhu et al. (2015) reported $\sum_7$PCBs levels in Ny-Ålesund soils being 0.07-1.92 ng g^{-1} [213] and Zhang et al. (2014) found $\sum_8$PCBs levels between 0.49-2.41 ng g^{-1} [212]. However, the $\sum$PCBs levels in this study were found to be not as elevated as reported in soils from the settlements Barentsburg and Pyramiden on Svalbard with median $\sum_7$PCBs levels being 268 and 172 ng g^{-1}, respectively [86]. PCB-28 and PCB-52 are relatively mobile in the atmosphere due to their comparably high volatility and low tendency to adsorb on aerosol particles [5, 199] (discussed in Sec. 2.4.1) and their presence in environmental samples is often associated with long-range atmospheric transport as a potential source [17]. However, heavier PCBs, such as PCB-138 and 153 were found in soil samples as well that more likely deposit closer to their emission source [5, 199]. Moreover, Ubl et al. (2012) found

higher concentrations of PCB-28 in air at Zeppelin station, Ny-Ålesund, during the years 1998–2009 in summer than in winter with a median value of 4 pg m^{-3} in summer and 2 pg m^{-3} in winter [189]. It has been documented that long-range atmospheric transport (LRAT) of pollutants to the Arctic is more dominant in winter and spring than in summer [51, 203]. Different mean atmospheric circulation directions across the Arctic between winter and summer as well as a lesser extent of wet deposition of aerosol particles during atmospheric transport in winter are factors contributing to enhanced LRAT in winter and spring [51, 203]. A previous study on PCBs in soils from Ny-Ålesund area noted a strong correlation between soil organic matter (SOM) and PCBs [212]. It would have been interesting to test a possible relationship between the analyzed soil organic carbon fractions TOC400 and ROC and PCBs concentrations. However, this relationship could not be tested with statistical methods due to a low number of samples (n=2), where PCBs were detected and quantified. It was observed that one of the two samples (S12) contained the highest amounts of TOC400 (272.1 mg g^{-1}) of all 15 studied samples. The relationship between organic carbon fractions and PCB concentrations in Svalbard surface soil samples has to be investigated further. It was also noted that both samples (S9 and S12) were comparably close to the shoreline. It is estimated that 30% of PCBs transported via long distances to Svalbard reach Svalbard by oceanic currents [108]. Arctic seabirds as potential vector of organic contaminants, such as dichlorodiphenyltrichloroethane (DDT) and hexachlorobenzene (HCB), have been discussed in the scientific literature as well [28]. One of the two samples (S12) was collected from Kiærstranda which seemed to be influenced by bird nesting activities as bird guano deposits were observed on the mountainside and sample S12 from that study area contained the highest total nitrogen (TN) amount (28.2 mg g^{-1}) of all 15 samples. Moreover, PCB-153, which was detected in the surface soil from KI, and PCB-138, which was found in surface soil samples from both KI and GB, were found to be dominating PCB compounds in the plasma of black guillemots, an Arctic seabird species that has its habitat on Svalbard [54].

4.6 Levels of pollution of Svalbard soils

For an assessment of pollution status in studied Svalbard surface soils, quantified levels of selected elements As, Cd, Cr, Cu, Ni, Pb and Zn as well as BaP, $\sum_{16}$ U.S. EPA priority PAHs and $\sum_{7}$ indicator PCBs were compared to the classification system for polluted soil (TA 2553/2009) by the Norwegian pollution control authority [73]. Tab. 4.12 shows the range of levels for the aforementioned elements, BaP, $\sum_{16}$PAHs and $\sum_{7}$PCBs grouped into five classes ('very good', 'good', 'moderate', 'bad' and 'very bad') according to the classification system [73]. Importantly, it has to be considered that this classification system is established mainly for urban areas and not for remote areas such as Svalbard [73]. Moreover, other factors, such as temperature, permafrost, lack of infrastructure and the occurrence of coal deposits in the bedrock will have influence on the classification of locations [69]. But to put the detected levels into an environmental context and since threshold levels for pollutant levels in Svalbard soil are lacking [113], the classification system was used for comparison purposes. Moreover, recent reports, for instance the report on PCB-contamination in soil from Kinnvika on Svalbard [59] discussed quantified levels with respect to this classification system.

Quantified levels for the elements Cu (3.1-35.6 µg g^{-1}), Pb (8.2-29.6 µg g^{-1}) and Zn (32.3-84.0 µg g^{-1}) corresponded to class 1 'very good' according to the classification system [73]. For As (1.59-35.42 µg g^{-1}) and Ni (4.5-99.9 µg g^{-1}), levels in all but one sample corresponded to class 1 'very good'. One sample from the study area NDM contained As at a level corresponding to class 3 'moderate' and Ni at a level that is considered within class 2 'good'. Cd levels in surface soils (0.10-4.49 µg g^{-1}) were within class 1 'very good' for samples from all study areas, except KI, where the levels corresponded to class 2 'good'. For Cr, whose concentrations in surface soil ranged between 8.5-65.3

µg g^{-1}, all samples from KI and NDM contained levels corresponding to class 1 'very good', while 1 sample from each of the study areas BDE, BDW and GB contained Cr-levels ranging within class 2 'good'. Importantly, it has to be noted that for detection and quantification of Cr levels in soils of the current study it was not distinguished between Cr(III) and Cr(VI) and that values are compared to the classification system for polluted soil (TA 2553/2009) for Cr(III). It cannot be excluded that samples may have contained Cr(VI) as well. In summary, the concentrations for the majority of elements and samples correspond to levels within class 1 which can be considered to be background levels, i.e. low pollution and low risk for ecosystem health [73]. Levels above class 1 can indicate pollution and can pose a risk to ecosystems health [73].

According to the classification system for polluted soil by the Norwegian pollution control authority, the levels found for BaP (18.5-85.1 ng g^{-1}) as well as $\sum$PAHs levels in this study (12.4-533.6 ng g^{-1}) are within class 1 'very good', which can be considered to be background pollution [73]. The $\sum$PCBs contents in surface soils (37.9-45.9 ng g^{-1}) corresponded to Class 2 - Good of the reported guidelines for Norwegian soil quality which can be considered to be slightly above background concentrations which can indicate pollution and can pose a risk to ecosystems health [73].

Table 4.12 – Classification system for polluted soil (TA 2553/2009) reported for elements, the sum of 16 U.S. EPA priority PAHs and the sum of the 7 indicator PCBs (IUPAC numbers 28, 52, 101, 118, 138, 153 and 180). Concentrations for elements are given in µg g^{-1} dry weight. Concentrations for BaP, $\sum_{16}$PAHs and $\sum_{7}$PCBs are given in ng g^{-1} dry weight.

	Class 1 Very good	Class 2 Good	Class 3 Moderate	Class 4 Bad	Class 5 Very bad
As	<8	8-20	20-50	50-600	600-1000
Cd	<1.5	1.5-10	10-15	15-30	30-1000
Cr (III)	<50	50-200	200-500	500-2800	2800-25,000
Cu	<100	100-200	200-1000	1000-8500	8500-25,000
Ni	<60	60-135	135-200	200-1200	1200-2500
Pb	<60	60-100	100-300	300-700	700-2500
Zn	<200	200-500	500-1000	1000-5000	5000-25,000
Benzo[*a*]pyrene	<100	100-500	500-5000	5000-15,000	15,000-100,000
$\sum_{16}$PAHs	<2000	2000-8000	8000-50,000	50,000-150,000	150,000-2,500,000
$\sum_{7}$PCBs	<10	10-500	500-1000	1000-5000	5000-50,000

CHAPTER 5

Conclusion

Surface soils were collected at different areas on Svalbard: in the vicinity of Ny-Ålesund as well as on Kiærstranda and Mitrahalvøya, which are two remote locations that are considered to be devoid of local sources of anthropogenic pollution. Surface soils were analyzed for TC, TN, TOC400, ROC and TIC900, elements (As, Cd, Cr, Cu, Ni, P, Pb and Zn). A method for the simultaneous extraction, cleanup, separation and quantification of PAHs and PCBs was developed.

Analysis of carbon and nitrogen fraction in surface soils revealed that TN content was significantly higher in surface soils from Kiærstranda, an area influenced by the occurrence of seabirds. Analysis of elements showed approximately 10-fold elevated concentrations of Cd in surface soils from Kiærstranda as well, compared to other study areas. Paired with the observation of significantly higher TN and P levels, these findings may suggest that seabird guano deposits potentially have been one contributor to pronounced levels of this element. Moreover, these findings highlight the importance of additional vectors of pollutant transfer that may deserve more attention in future studies. At the same time, these findings suggest that local sources of anthropogenic pollution seem to be negligible for Cd in studied soils as levels between the three study areas in proximity to Ny-Ålesund and Mitrahalvøya were similar. Other elements than Cd and P did not show statistically significant differences between study areas. Mean As, Cr, Cu and Ni levels in surface soils from this study were higher than reported values in surface soils from Norway. Different sources may have contributed to levels of these elements in surface soils in the present study, such as the local bedrock as it has been documented in previous studies on Svalbard surface soils. Levels for most elements in the majority of samples were below the suggested guideline values for polluted soil in Norway. One exception from this were Cd levels in surface soils from Kiærstranda, which was in class 2 'good'.

The developed method for the simultaneous extraction, cleanup, separation and quantification of PAHs and PCBs proved to be successful. Recoveries were between 80-106% for PAH and PCB target analytes. An acceptable precision with RSD < 15% was achieved for the majority of target analytes. Limits of detection ranged between 0.67 and 6.67 ng g^{-1}. The developed method was applied to analysis of sampled surface soils for 16 U.S. EPA PAHs and 7 indicator PCBs.

10 of 16 U.S. EPA PAHs were detected and quantified in samples, with NAP and PHE showing greatest abundance. Levels for PAHs and Benzo[*a*]pyrene were below the suggested guideline values for polluted soil in Norway. Moreover, the presence of alkylated PAH compound, retene, was confirmed, which has been documented to be a dominating compound in Svalbard coal. Moreover, these findings indicate the capacity to detect alkylated PAHs in soils with the developed methodology. The presence of HMW-PAHs in soils in the three study areas in the vicinity of

Ny-Ålesund as well as at Kiærstranda indicate that local sources potentially contribute more likely than long-range atmospheric transport to PAHs levels quantified in soils from these study areas. These findings may also be supported by the fact that all PAH target analytes were below LOD at Mitrahalvøya. It was used in this study as a reference location and is considered to be remote from local anthropogenic activities. Moreover, comparably high spatial variations in PAH concentrations were found between study areas in the vicinity of Ny-Ålesund settlement (study areas BDE, BDW and GB) which potentially indicate the presence of local point sources. The occurrence of retene, the dominance of PHE, NAP and FLU as well as PAH indicator ratios point towards a mixture of unburnt coal and combustion of coal and fuel being potential sources for PAHs found in soils from Ny-Alesund.

In addition, 5 of the 7 PCB target analytes (IUPAC numbers 28, 52, 118, 138 and 153) were detected and quantified. Two samples from two distinct study areas (GB and KI) contained PCBs. Interestingly, levels of the PCBs compounds were markedly higher than in previous studies reported. Levels for the total PCB concentration in the two samples within class 2 'good' of the suggested guideline values for polluted soil in Norway. PCB congeners were detected at similar levels, which may indicate a common source. Moreover, the presence of heavier PCBs, including PCB-118 and PCB-138 in samples potentially suggest another source than atmospheric deposition. The proximity to the shore of the two sampling locations may indicate oceanic currents or the transfer from the marine food web by seabirds to these locations as possible sources for PCBs found there. These influences on PCB levels in Arctic coastal areas should be further investigated.

The findings in this study suggest that local sources of pollution should not be disregarded when carrying out a study on long-range atmospheric transported pollutants in the vicinity of considerably remote Arctic settlements. Moreover, the transfer of pollutants from the marine food web to the terrestrial environment by seabirds as a potential source of pollutants to remote areas should receive more attention in future studies.

With the findings in this study, it was possible to identify a possible additional important source to remote Arctic regions: the transport of contaminants from the marine food web by seabirds to coastal areas. Moreover, it was possible to obtain a clearer picture about distribution patterns and potential contamination sources of PAHs in Ny-Ålesund area. This will help future studies in choosing less affected locations by local sources for the investigation of long-range atmospheric transport of contaminants, such as PAHs in Ny-Ålesund area. Moreover, Mitrahalvøya was identified as a study area that may be suitable for evaluating the impact of long-range atmospheric transport on terrestrial ecosystems for future studies. With the developed method for the simultaneous extraction, cleanup, detection and quantification of PAHs and PCBs in soil, this study has contributed to a new methodology that will be time-efficient and cost-saving for future environmental screening studies of PAHs and PCBs in surface soil.

Bibliography

[1] Christine Achten and Jan T. Andersson. 'Overview of Polycyclic Aromatic Compounds (PAC)'. In: *Polycyclic Aromatic Compounds* 35.2-4 (Mar. 2015), pp. 177–186. ISSN: 15635333. DOI: 10.1080/10406638.2014.994071. URL: https://www.tandfonline.com/doi/full/10.1080/10406638.2014.994071.

[2] Christine Achten and Jan T. Andersson. 'Overview of Polycyclic Aromatic Compounds (PAC)'. In: *Polycyclic Aromatic Compounds* 35.2-4 (Mar. 2015), pp. 177–186. ISSN: 15635333. DOI: 10.1080/10406638.2014.994071.

[3] Jason M.E. Ahad et al. *Polycyclic aromatic compounds (PACs) in the Canadian environment: A review of sampling techniques, strategies and instrumentation*. Nov. 2020. DOI: 10.1016/j.envpol.2020.114988.

[4] G R Aiken et al. 'Humic Substances in Soil, Sediment, and Water'. In: *Soil Science* 142.5 (1986). ISSN: 0038-075X. URL: https://journals.lww.com/soilsci/Fulltext/1986/11000/Humic_Substances_in_Soil,_Sediment,_and_Water_.11.aspx.

[5] Benoit Van Aken, Paola A Correa and Jerald L Schnoor. 'Phytoremediation of Polychlorinated Biphenyls: New Trends and Promises'. In: *Environmental Science & Technology* 44.8 (Apr. 2010), pp. 2767–2776. ISSN: 0013-936X. DOI: 10.1021/es902514d. URL: https://doi.org/10.1021/es902514d.

[6] Oluwadara Oluwaseun Alegbeleye, Beatrice Oluwatoyin Opeolu and Vanessa Angela Jackson. 'Polycyclic Aromatic Hydrocarbons: A Critical Review of Environmental Occurrence and Bioremediation'. In: *Environmental Management* 60.4 (Oct. 2017), pp. 758–783. ISSN: 14321009. DOI: 10.1007/s00267-017-0896-2. URL: https://link.springer.com/article/10.1007/s00267-017-0896-2.

[7] Philip N Anderson and Ronald A Hites. 'OH Radical Reactions: The Major Removal Pathway for Polychlorinated Biphenyls from the Atmosphere'. In: *Environmental Science & Technology* 30.5 (Apr. 1996), pp. 1756–1763. ISSN: 0013-936X. DOI: 10.1021/es950765k. URL: https://doi.org/10.1021/es950765k.

[8] Jan T Andersson and Uwe Weis. 'Gas chromatographic determination of polycyclic aromatic compounds with fluorinated analogues as internal standards'. In: *Journal of Chromatography A* 659.1 (1994), pp. 151–161. ISSN: 0021-9673. DOI: https://doi.org/10.1016/0021-9673(94)85017-8. URL: https://www.sciencedirect.com/science/article/pii/0021967394850178.

[9] Arctic Monitoring and Assessment Programme (AMAP). *AMAP Assessment 2002: Heavy Metals in the Arctic. Arctic*. Tech. rep. Oslo, Norway, 2005, xvi + 265 pp.

[10] Arctic Monitoring and Assessment Programme (AMAP). *AMAP Assessment 2002: Persistent Organic Pollutants in the Arctic*. Tech. rep. Oslo, Norway: Arctic Monitoring and Assessment Programme (AMAP), 2004, xvi +310 pp. URL: https://www.amap.no/documents/doc/amap-assessment-2002-persistent-organic-pollutants-in-the-arctic/96.

[11] Arctic Monitoring and Assessment Programme (AMAP). *AMAP Assessment 2011: Mercury in the Arctic.* Oslo, Norway, 2011. URL: https://www.amap.no/documents/doc/amap-assessment-2011-mercury-in-the-arctic/90.

[12] David A Armbruster and Terry Pry. 'Limit of blank, limit of detection and limit of quantitation'. eng. In: *The Clinical biochemist. Reviews* 29 Suppl 1.Suppl 1 (Aug. 2008), S49–S52. ISSN: 0159-8090. URL: https://pubmed.ncbi.nlm.nih.gov/18852857%20https://www.ncbi.nlm.nih.gov/pmc/articles/PMC2556583/.

[13] Hans Peter H Arp et al. 'The presence, emission and partitioning behavior of polychlorinated biphenyls in waste, leachate and aerosols from Norwegian waste-handling facilities'. In: *Science of The Total Environment* 715 (2020), p. 136824. ISSN: 0048-9697. DOI: https://doi.org/10.1016/j.scitotenv.2020.136824. URL: https://www.sciencedirect.com/science/article/pii/S004896972030334X.

[14] Johannes Asheim et al. 'Benzotriazoles, benzothiazoles and trace elements in an urban road setting in Trondheim, Norway: Re-visiting the chemical markers of traffic pollution'. In: *Science of The Total Environment* 649 (2019), pp. 703–711. ISSN: 0048-9697. DOI: https://doi.org/10.1016/j.scitotenv.2018.08.299. URL: https://www.sciencedirect.com/science/article/pii/S0048969718332704.

[15] Alexandros G Asimakopoulos et al. 'A multi-class bioanalytical methodology for the determination of bisphenol A diglycidyl ethers, p-hydroxybenzoic acid esters, benzophenone-type ultraviolet filters, triclosan, and triclocarban in human urine by liquid chromatography–tandem mass spectromet'. In: *Journal of Chromatography A* 1324 (2014), pp. 141–148. ISSN: 0021-9673. DOI: https://doi.org/10.1016/j.chroma.2013.11.031. URL: https://www.sciencedirect.com/science/article/pii/S0021967313018025.

[16] Alexandros G Asimakopoulos et al. 'Occurrence and removal efficiencies of benzotriazoles and benzothiazoles in a wastewater treatment plant in Greece'. In: *Science of The Total Environment* 452-453 (2013), pp. 163–171. ISSN: 0048-9697. DOI: https://doi.org/10.1016/j.scitotenv.2013.02.041. URL: https://www.sciencedirect.com/science/article/pii/S0048969713002234.

[17] Shazia N. Aslam et al. 'Trace elements and polychlorinated biphenyls (PCBs) in terrestrial compartments of Svalbard, Norwegian Arctic'. In: *Science of The Total Environment* 685 (Oct. 2019), pp. 1127–1138. ISSN: 0048-9697. DOI: 10.1016/J.SCITOTENV.2019.06.060. URL: https://www.sciencedirect.com/science/article/pii/S0048969719326282?via%3Dihub#bb0085.

[18] K. Atakan et al. *Geoscience Atlas of Svalbard*. Ed. by W.K. Dallmann. Norsk Polarinstitutt, 2015, pp. 1–292. ISBN: 978 82 7666-312-9. URL: https://www.npolar.no/produkt/geoscience-atlas-of-svalbard/.

[19] Olav Leiros Bakkerud. 'Profiles of bisphenols and benzophenone-type UV filters concentrations in sediment from Trondheimsfjorden: Associations with PAHs and trace elements'. PhD thesis. Norwegian University of Science and Technology (NTNU), 2019, pp. 38–39.

[20] K Ballschmiter and M Zell. 'Analysis of polychlorinated biphenyls (PCB) by glass capillary gas chromatography'. In: *Fresenius' Zeitschrift für analytische Chemie* 302.1 (1980), pp. 20–31. ISSN: 1618-2650. DOI: 10.1007/BF00469758. URL: https://doi.org/10.1007/BF00469758.

[21] J. Balmer and D. Muir. 'Polycyclic aromatic hydrocarbons (PAHs)'. In: *AMAP Assessment 2016: Chemicals of emerging Arctic concern*. Ed. by H. Hung, R. Letcher and Y. Yu. Oslo, Norway: Arctic Monitoring and Assessment Programme (AMAP), 2017, pp. 219–238.

[22] Jennifer E. Balmer et al. 'Sources and environmental fate of pyrogenic polycyclic aromatic hydrocarbons (PAHs) in the Arctic'. In: *Emerging Contaminants* 5 (Jan. 2019), pp. 128–142. ISSN: 2405-6650. DOI: 10.1016/J.EMCON.2019.04.002. URL: https://www.sciencedirect.com/science/article/pii/S2405665018300684.

[23] L.A. Barrie et al. 'Arctic contaminants: sources, occurrence and pathways'. In: *Science of The Total Environment* 122.1-2 (July 1992), pp. 1–74. ISSN: 0048-9697. DOI: 10.1016/0048-9697(92)90245-N. URL: https://www.sciencedirect.com/science/article/pii/004896979290245N?via%3Dihub.

[24] Andrea Bazzano et al. 'Source assessment of atmospheric lead measured at Ny-Ålesund, Svalbard'. In: *Atmospheric Environment* 113 (July 2015), pp. 20–26. ISSN: 1352-2310. DOI: 10.1016/J.ATMOSENV.2015.04.053. URL: https://www.sciencedirect.com/science/article/pii/S1352231015300558.

[25] Torunn Berg et al. 'Atmospheric trace metal concentrations at Norwegian background sites during 25 years and its relation to European emissions'. In: *Atmospheric Environment* 42.32 (2008), pp. 7494–7501. ISSN: 1352-2310. DOI: https://doi.org/10.1016/j.atmosenv.2008.05.020. URL: https://www.sciencedirect.com/science/article/pii/S1352231008005360.

[26] T Berg et al. 'Ten-year trends in atmospheric mercury concentrations, meteorological effects and climate variables at Zeppelin, Ny-Ålesund'. In: *Atmospheric Chemistry and Physics* 13.13 (2013), pp. 6575–6586. DOI: 10.5194/acp-13-6575-2013. URL: https://www.atmos-chem-phys.net/13/6575/2013/.

[27] Ambavaram Vijaya Bhaskar Reddy et al. *Modern approaches in separation, identification and quantification of polychlorinated biphenyls*. Dec. 2020. DOI: 10.1016/j.coesh.2020.06.003.

[28] Jules M Blais et al. 'Arctic Seabirds Transport Marine-Derived Contaminants'. In: *Science* 309.5733 (July 2005), p. 445. DOI: 10.1126/science.1112658. URL: http://science.sciencemag.org/content/309/5733/445.abstract.

[29] L.C. Bliss. 'Vascular plant vegetation of the southern circumpolar region in relation to the Antarctic, alpine and Arctic vegetation.' In: *Canadian Journal of Botany* 57 (1979).

[30] James G Bockheim. 'Cryosols as a Three-Part System'. In: *Cryopedology*. Ed. by James G Bockheim. Cham: Springer International Publishing, 2015, pp. 7–21. ISBN: 978-3-319-08485-5. DOI: 10.1007/978-3-319-08485-5{_}2. URL: https://doi.org/10.1007/978-3-319-08485-5_2.

[31] Jacob de Boer and Robin J Law. 'Developments in the use of chromatographic techniques in marine laboratories for the determination of halogenated contaminants and polycyclic aromatic hydrocarbons'. In: *Journal of Chromatography A* 1000.1 (2003), pp. 223–251. ISSN: 0021-9673. DOI: https://doi.org/10.1016/S0021-9673(03)00309-1. URL: https://www.sciencedirect.com/science/article/pii/S0021967303003091.

[32] J Boike et al. 'A 20-year record (1998–2017) of permafrost, active layer and meteorological conditions at a high Arctic permafrost research site (Bayelva, Spitsbergen)'. In: *Earth Syst. Sci. Data* 10.1 (Mar. 2018), pp. 355–390. ISSN: 1866-3516. DOI: 10.5194/essd-10-355-2018. URL: https://essd.copernicus.org/articles/10/355/2018/.

[33] J.T. Borlakoglu and J.P.G. Wilkins. 'Correlations between the molecular structures of polyhalogenated biphenyls and their metabolism by hepatic microsomal monooxygenases'. In: *Comparative Biochemistry and Physiology Part C: Comparative Pharmacology* 105.1 (May 1993), pp. 113–117. ISSN: 0306-4492. DOI: 10.1016/0742-8413(93)90066-T. URL: https://www.sciencedirect.com/science/article/pii/074284139390066T.

[34] Marion Børresen. *Miljøundersøkelse av forurensede lokaliteter, Ny-Ålesund*. Tech. rep. Oslo, Norway: Norwegian Geotechnical Institiute, 2003.

[35] Gijs D. Breedveld. *Svalbard - Terrestriske bakgrunnsverdier i Longyearbyen*. Tech. rep. Oslo, Norway: Norwegian Geotechnical Institiute, 2000.

[36] Gijs D. Breedveld and Paul Sverdrup Cappelen. *Bakgrunnsverdier rundt Longyearbyen - sammenstilling av tilgjengelige data fra undersøkelser av bakgrunnsverdier på Svalbard*. Tech. rep. Oslo, Norway: Norges Geotekniske Institutt, 2019, pp. 1–19.

[37] Gijs D. Breedveld, Martin Skedsmo and Reidar Otter. *Svalbard - Undersøkelse av forurensede lokaliteter, Ny Ålesund*. Tech. rep. Oslo, Norway: Norwegian Geotechnical Institiute, 1999, p. 38.

[38] Knut Breivik et al. 'Towards a global historical emission inventory for selected PCB congeners — a mass balance approach: 1. Global production and consumption'. In: *Science of The Total Environment* 290.1 (2002), pp. 181–198. ISSN: 0048-9697. DOI: https://doi.org/10.1016/S0048-9697(01)01075-0. URL: https://www.sciencedirect.com/science/article/pii/S0048969701010750.

[39] Knut Breivik et al. 'Towards a global historical emission inventory for selected PCB congeners — A mass balance approach: 3. An update'. In: *Science of The Total Environment* 377.2 (2007), pp. 296–307. ISSN: 0048-9697. DOI: https://doi.org/10.1016/j.scitotenv.2007.02.026. URL: https://www.sciencedirect.com/science/article/pii/S0048969707002926.

[40] J. M. Bremner. 'Nitrogen-Total'. In: *Methods of Soil Analysis*. Ed. by D. Sparks et al. John Wiley & Sons, Ltd, 1996. Chap. 37, pp. 1085–1121. DOI: 10.2136/sssabookser5.3.c37. URL: http://doi.wiley.com/10.2136/sssabookser5.3.c37.

[41] Samantha K Brimble et al. 'High arctic ponds receiving biotransported nutrients from a nearby seabird colony are also subject to potentially toxic loadings of arsenic, cadmium, and zinc'. In: *Environmental Toxicology and Chemistry* 28.11 (Nov. 2009), pp. 2426–2433. ISSN: 0730-7268. DOI: https://doi.org/10.1897/09-235.1. URL: https://doi.org/10.1897/09-235.1.

[42] J Brown et al. *Circum-Arctic map of permafrost and ground-ice conditions*. ENGLISH. Tech. rep. 1997. DOI: 10.3133/cp45. URL: http://pubs.er.usgs.gov/publication/cp45.

[43] Andrea H Buckman et al. 'Organochlorine contaminants in seven species of Arctic seabirds from northern Baffin Bay'. In: *Environmental Pollution* 128.3 (2004), pp. 327–338. ISSN: 0269-7491. DOI: https://doi.org/10.1016/j.envpol.2003.09.017. URL: https://www.sciencedirect.com/science/article/pii/S0269749103003762.

[44] Banu Cetin et al. 'Ambient concentrations and source apportionment of PCBs and trace elements around an industrial area in Izmir, Turkey'. In: *Chemosphere* 69.8 (2007), pp. 1267–1277. ISSN: 0045-6535. DOI: https://doi.org/10.1016/j.chemosphere.2007.05.064. URL: https://www.sciencedirect.com/science/article/pii/S004565350700687X.

[45] A. Chatterjee et al. 'Evaluation of Different Soil Carbon Determination Methods'. In: *Critical Reviews in Plant Sciences* 28.3 (Apr. 2009), pp. 164–178. ISSN: 0735-2689. DOI: 10.1080/07352680902776556. URL: http://www.tandfonline.com/doi/abs/10.1080/07352680902776556.

[46] Erik R. Christensen, Eiliv Steinnes and Ola Anfin Eggen. 'Anthropogenic and geogenic mass input of trace elements to moss and natural surface soil in Norway'. In: *Science of the Total Environment* 613-614 (Feb. 2018), pp. 371–378. ISSN: 18791026. DOI: 10.1016/j.scitotenv.2017.09.094.

[47] Stanisław R Ćmiel and Monika J Fabiańska. 'Geochemical and petrographic properties of some Spitsbergen coals and dispersed organic matter'. In: *International Journal of Coal Geology* 57.2 (2004), pp. 77–97. ISSN: 0166-5162. DOI: https://doi.org/10.1016/j.coal.2003.09.002. URL: https://www.sciencedirect.com/science/article/pii/S0166516203001630.

[48] Christine M. Davidson. 'Methods for the Determination of Heavy Metals and Metalloids in Soils'. In: Springer, Dordrecht, 2013, pp. 97–140. DOI: 10.1007/978-94-007-4470-7{_}4. URL: https://link.springer.com/chapter/10.1007/978-94-007-4470-7_4.

[49] Silvia Diez Fernández et al. 'Determination of low B/Ca ratios in carbonates using ICP-QQQ'. In: *Geochemistry, Geophysics, Geosystems* 16.6 (June 2015), pp. 2005–2014. ISSN: 1525-2027. DOI: https://doi.org/10.1002/2015GC005817. URL: https://doi.org/10.1002/2015GC005817.

[50] DIN Standards Committee Water Practice. 'DIN 19539, Investigation of solids - Temperature-dependent differentiation of total carbon (TOC400, ROC, TIC900)'. Beuth, Berlin, Germany, 2016.

[51] Tatiana Drotikova et al. 'Polycyclic aromatic hydrocarbons (PAHs) and oxy- and nitro-PAHs in ambient air of the Arctic town Longyearbyen, Svalbard'. In: *Atmospheric Chemistry and Physics* 20.16 (Aug. 2020), pp. 9997–10014. ISSN: 1680-7324. DOI: 10.5194/acp-20-9997-2020. URL: https://acp.copernicus.org/articles/20/9997/2020/.

[52] John L Durant et al. 'Human cell mutagenicity of oxygenated, nitrated and unsubstituted polycyclic aromatic hydrocarbons associated with urban aerosols'. In: *Mutation Research/Genetic Toxicology* 371.3 (1996), pp. 123–157. ISSN: 0165-1218. DOI: https://doi.org/10.1016/S0165-1218(96)90103-2. URL: https://www.sciencedirect.com/science/article/pii/S0165121896901032.

[53] Bohuslav Dušek, Jana Hajšlová and Vladimir Kocourek. 'Determination of nitrated polycyclic aromatic hydrocarbons and their precursors in biotic matrices'. In: *Journal of Chromatography A* 982.1 (2002), pp. 127–143. ISSN: 0021-9673. DOI: https://doi.org/10.1016/S0021-9673(02)01340-7. URL: https://www.sciencedirect.com/science/article/pii/S0021967302013407.

[54] Norith Eckbo et al. 'Individual variability in contaminants and physiological status in a resident Arctic seabird species'. In: *Environmental Pollution* 249 (2019), pp. 191–199. ISSN: 0269-7491. DOI: https://doi.org/10.1016/j.envpol.2019.01.025. URL: https://www.sciencedirect.com/science/article/pii/S0269749118336972.

[55] Mitchell D. Erickson. *Analytical Chemistry of PCBs*. 2nd ed. Boca Raton, FL, USA: CRC Press LLC, 1997, pp. 1–448. ISBN: 0-87371-923-9.

[56] D Ronald Erney, Tina M Pawlowski and Colin F Poole. 'Matrix-induced peak enhancement of pesticides in gas chromatogrtaphy: Is there a solution?' In: *Journal of High Resolution Chromatography* 20.7 (July 1997), pp. 375–378. ISSN: 0935-6304. DOI: https://doi.org/10.1002/jhrc.1240200706. URL: https://doi.org/10.1002/jhrc.1240200706.

[57] D R Erney et al. 'Explanation of the matrix-induced chromatographic response enhancement of organophosphorus pesticides during open tubular column gas chromatography with splitless or hot on-column injection and flame photometric detection'. In: *Journal of Chromatography A* 638.1 (1993), pp. 57–63. ISSN: 0021-9673. DOI: https://doi.org/10.1016/0021-9673(93)85007-T. URL: https://www.sciencedirect.com/science/article/pii/002196739385007T.

[58] ESRI. *ArcGIS Desktop: Release 10*. Redlands, CA, 2011.

[59] Anita Evenset and Guttorm N. Christensen. *Miljøgifter i jord, marine sedimenter og fisk fra Kinnvika, Nordaustlandet, Svalbard, 2011*. Tech. rep. Tromsø, Norway: Akvaplan niva, 2012, p. 85.

[60] Antonio Finizio et al. 'Octanol-air partition coefficient as a predictor of partitioning of semi-volatile organic chemicals to aerosols'. In: *Atmospheric Environment* 31.15 (1997), pp. 2289–2296. ISSN: 1352-2310. DOI: https://doi.org/10.1016/S1352-2310(97)00013-7. URL: https://www.sciencedirect.com/science/article/pii/S1352231097000137.

[61] E Forgács and T Cserháti. 'CHROMATOGRAPHY | Principles'. In: *Encyclopedia of Food Sciences and Nutrition*. Ed. by Benjamin Caballero, Paul Finglas and Fidel Toldrá. Second Edi. Oxford: Academic Press, 2003, pp. 1259–1267. ISBN: 978-0-12-227055-0. DOI: https://doi.org/10.1016/B0-12-227055-X/00230-3. URL: https://www.sciencedirect.com/science/article/pii/B012227055X002303.

[62] David A. Freedman. *Statistical Models: Theory and Practice*. 2nd Ed. Cambridge: Cambridge University Press, 2009. ISBN: 9780521743853.

[63] Carey L. Friedman and Noelle E. Selin. 'Long-range atmospheric transport of polycyclic aromatic hydrocarbons: A global 3-D model analysis including evaluation of arctic sources'. In: *Environmental Science and Technology* 46.17 (Sept. 2012), pp. 9501–9510. ISSN: 0013936X. DOI: 10.1021/es301904d. URL: https://pubs.acs.org/sharingguidelines.

[64] Tomoharu Fujiyoshi et al. 'Evaluation of the matrix effect on gas chromatography – mass spectrometry with carrier gas containing ethylene glycol as an analyte protectant'. In: *Journal of Chromatography A* 1434 (2016), pp. 136–141. ISSN: 0021-9673. DOI: https://doi.org/10.1016/j.chroma.2015.12.085. URL: https://www.sciencedirect.com/science/article/pii/S0021967315018841.

[65] Antonia Garrido Frenich et al. 'Compensation for matrix effects in gas chromatography–tandem mass spectrometry using a single point standard addition'. In: *Journal of Chromatography A* 1216.23 (2009), pp. 4798–4808. ISSN: 0021-9673. DOI: https://doi.org/10.1016/j.chroma.2009.04.018. URL: https://www.sciencedirect.com/science/article/pii/S0021967309005536.

[66] Raouf Ghavami and S Mohammad Sajadi. 'Semi-Empirical Topological Method for Prediction of the Relative Retention Time of Polychlorinated Biphenyl Congeners on 18 Different HR GC Columns'. In: *Chromatographia* 72.5 (2010), pp. 523–533. ISSN: 1612-1112. DOI: 10.1365/s10337-010-1696-5. URL: https://doi.org/10.1365/s10337-010-1696-5.

[67] Chiara Giorio et al. 'Prospects for reconstructing paleoenvironmental conditions from organic compounds in polar snow and ice'. In: *Quaternary Science Reviews* 183 (2018), pp. 1–22. ISSN: 0277-3791. DOI: https://doi.org/10.1016/j.quascirev.2018.01.007. URL: https://www.sciencedirect.com/science/article/pii/S0277379117307850.

[68] T. Gouin et al. 'Evidence for the "grasshopper" effect and fractionation during long-range atmospheric transport of organic contaminants'. In: *Environmental Pollution* 128.1-2 (Mar. 2004), pp. 139–148. ISSN: 0269-7491. DOI: 10.1016/J.ENVPOL.2003.08.025. URL: https://www.sciencedirect.com/science/article/pii/S0269749103003385.

[69] Maria E Granberg, Amalie V Ask and Geir Wing Gabrielsen. *Local contamination in Svalbard: overview and suggestions for remediation actions*. Tech. rep. Tromsø: Norsk Polarinstitutt, 2017, pp. 1–48.

[70] J. Gulińska et al. 'Soil Contamination in High Arctic Areas of Human Impact, Central Spitsbergen, Svalbard'. In: *Polish Journal of Environmental Studies* 12.6 (2003), pp. 701–707. ISSN: 1230-1485. URL: http://www.pjoes.com/Soil-Contamination-in-High-Arctic-Areas-r-nof-Human-Impact-Central-Spitsbergen-Svalbard,87609,0,2.html.

[71] Jana Hajšlová and Tomáš Čajka. 'Gas chromatography–mass spectrometry (GC–MS)'. In: *Food Toxicants Analysis: Techniques, Strategies and Developments*. Ed. by Yolanda B T - Food Toxicants Analysis Picó. Amsterdam: Elsevier, 2007, pp. 419–473. ISBN: 978-0-444-52843-8. DOI: https://doi.org/10.1016/B978-044452843-8/50013-4. URL: https://www.sciencedirect.com/science/article/pii/B9780444528438500134.

[72] Katharina Halbach et al. 'The presence of mercury and other trace metals in surface soils in the Norwegian Arctic'. In: *Chemosphere* 188 (Dec. 2017), pp. 567–574. ISSN: 0045-6535. DOI: 10.1016/J.CHEMOSPHERE.2017.09.012. URL: https://www.sciencedirect.com/science/article/pii/S0045653517314285?via%3Dihub.

[73] H. J. Hansen and A. Danielsberg. *Helsebaserte tilstandsklasser for forurenset grunn*. Tech. rep. Oslo, Norway: Statens forurensningstilsyn, 2009, pp. 1–28. URL: https://www.miljodirektoratet.no/globalassets/publikasjoner/klif2/publikasjoner/2553/ta2553.pdf.

[74] Zhi Ling Hao, Feng Wang and Hai Zhen Yang. 'Baseline values for heavy metals in soils on Ny-Alesund, Spitsbergen Island, Arctic: The extent of anthropogenic pollution'. In: *Advanced Materials Research*. Vol. 779. Trans Tech Publications Ltd, 2013, pp. 1260–1265. ISBN: 9783037858042. DOI: 10.4028/www.scientific.net/AMR.779-780.1260. URL: https://www.scientific.net/AMR.779-780.1260.

[75] Stuart J Harrad et al. 'Polychlorinated biphenyls (PCBs) in the British environment: Sinks, sources and temporal trends'. In: *Environmental Pollution* 85.2 (1994), pp. 131–146. ISSN: 0269-7491. DOI: https://doi.org/10.1016/0269-7491(94)90079-5. URL: https://www.sciencedirect.com/science/article/pii/0269749194900795.

[76] F Hernández et al. 'Current use of high-resolution mass spectrometry in the environmental sciences'. In: *Analytical and Bioanalytical Chemistry* 403.5 (2012), pp. 1251–1264. ISSN: 1618-2650. DOI: 10.1007/s00216-012-5844-7. URL: https://doi.org/10.1007/s00216-012-5844-7.

[77] D Brynn Hibbert. *Quality Assurance in the Analytical Chemistry Laboratory*. New York, USA: Oxford University Press, 2007, pp. 1–321. ISBN: 978-0-19-516212-7.

[78] Alain Hildebrandt, Sílvia Lacorte and Damià Barceló. 'Sampling of water, soil and sediment to trace organic pollutants at a river-basin scale'. In: *Analytical and Bioanalytical Chemistry* 386.4 (2006), pp. 1075–1088. ISSN: 1618-2650. DOI: 10.1007/s00216-006-0486-2. URL: https://doi.org/10.1007/s00216-006-0486-2.

[79] Juliane Hollender et al. 'Nontarget Screening with High Resolution Mass Spectrometry in the Environment: Ready to Go?' In: *Environmental Science & Technology* 51.20 (Oct. 2017), pp. 11505–11512. ISSN: 0013-936X. DOI: 10.1021/acs.est.7b02184. URL: https://doi.org/10.1021/acs.est.7b02184.

[80] E. B. Holm, P. J. Brandvik and E. Steinnes. 'Pollution in acid mine drainage from mine tailings in Svalbard, Norwegian Arctic'. In: *Journal de Physique IV (Proceedings)* 107.I (May 2003), pp. 625–628. ISSN: 1155-4339. DOI: 10.1051/jp4:20030381. URL: http://www.edpsciences.org/10.1051/jp4:20030381.

[81] M. J.J. Hoogsteen et al. 'Estimating soil organic carbon through loss on ignition: Effects of ignition conditions and structural water loss'. In: *European Journal of Soil Science* 66.2 (2015), pp. 320–328. ISSN: 13652389. DOI: 10.1111/ejss.12224.

[82] Weilin Huang et al. 'Effects of organic matter heterogeneity on sorption and desorption of organic contaminants by soils and sediments'. In: *Applied Geochemistry* 18.7 (2003), pp. 955–972. ISSN: 0883-2927. DOI: https://doi.org/10.1016/S0883-2927(02)00205-6. URL: https://www.sciencedirect.com/science/article/pii/S0883292702002056.

[83] O. Hutzinger, S. Safe and V. Zitko. *The Chemistry of PCB's*. 1th Ed. CRC Press, 1974, p. 279. ISBN: 9781351070591. URL: https://www.taylorfrancis.com/books/mono/10.1201/9781351070591/chemistry-pcb-hutzinger-safe-zitko.

[84] International Agency for Research on Cancer (IARC). *Some non-heterocyclic polycyclic aromatic hydrocarbons and some related exposures.* English. Ed. by International Agency for Research on Cancer. Lyon, 2010.

[85] International Standard. *ISO 18400-104 Soil quality - Sampling Part 104: Strategies*. Tech. rep. 2018, pp. 1–140. URL: https://www.standard.no/no/Nettbutikk/produktkatalogen/Produktpresentasjon/?ProductID=998926.

[86] Morten Jartun et al. 'Local Sources of Polychlorinated Biphenyls (PCB) in Russian and Norwegian Settlements on Spitsbergen Island, Norway'. In: *Journal of Toxicology and Environmental Health, Part A* 72.3-4 (Jan. 2009), pp. 284–294. ISSN: 1528-7394. DOI: 10.1080/15287390802539426. URL: https://doi.org/10.1080/15287390802539426.

[87] Liping Jiao et al. 'Persistent toxic substances in remote lake and coastal sediments from Svalbard, Norwegian Arctic: Levels, sources and fluxes'. In: *Environmental Pollution* 157.4 (2009), pp. 1342–1351. ISSN: 0269-7491. DOI: https://doi.org/10.1016/j.envpol.2008.11.030. URL: https://www.sciencedirect.com/science/article/pii/S0269749108006490.

[88] K Joa et al. 'Determination of polycyclic aromatic hydrocarbons (PAHs) in oil shale processing wastes: Current practice and new trends'. In: *Oil Shale* 26.1 (Jan. 2009), pp. 59–72. DOI: 10.3176/oil.2009.1.07. URL: https://kirj.ee/oil-shale-publications/?filter[year]=2009&filter[issue]=69&filter[publication]=471.

[89] B F Johansen, K Prestvold and Ø Overrein. *Cruise Handbook for Svalbard*. 2011, pp. 1–252. ISBN: 9788276662863. URL: https://www.npolar.no/produkt/cruise-handbook-for-svalbard/.

[90] R. Kallenborn et al. *Effects of Selected Pollutants and Climate Change in the Arctic Environment*. Oslo: AMAP Technical Report No. 5, 2011, p. 108.

[91] Roland Kallenborn, Eliza Harris and Bartek Luks. 'Historical contamination from earlier IPY Research: The Kinnvika Story'. In: June 2010.

[92] Athanasios Katsoyiannis, Andrew J Sweetman and Kevin C Jones. 'PAH Molecular Diagnostic Ratios Applied to Atmospheric Sources: A Critical Evaluation Using Two Decades of Source Inventory and Air Concentration Data from the UK'. In: *Environmental Science & Technology* 45.20 (Oct. 2011), pp. 8897–8906. ISSN: 0013-936X. DOI: 10.1021/es202277u. URL: https://doi.org/10.1021/es202277u.

[93] Lawrence H Keith. 'The Source of U.S. EPA's Sixteen PAH Priority Pollutants'. In: *Polycyclic Aromatic Compounds* 35.2-4 (Mar. 2015), pp. 147–160. ISSN: 1040-6638. DOI: 10.1080/10406638.2014.892886. URL: https://doi.org/10.1080/10406638.2014.892886.

[94] A. Kettle. 'Use of Accelerated Solvent Extraction With In-Cell Cleanup to Eliminate Sample Cleanup During Sample Preparation'. In: *Thermo Fisher Scientific* White Paper 70632 (2013), pp. 1–7.

[95] Ian J. Keyte, Roy M. Harrison and Gerhard Lammel. *Chemical reactivity and long-range transport potential of polycyclic aromatic hydrocarbons-a review*. Dec. 2013. DOI: 10.1039/c3cs60147a. URL: www.rsc.org/csr.

[96] J.-H. Kim et al. 'Large ancient organic matter contributions to Arctic marine sediments (Svalbard)'. In: *Limnology and Oceanography* 56.4 (July 2011), pp. 1463–1474. ISSN: 00243590. DOI: 10.4319/lo.2011.56.4.1463. URL: http://doi.wiley.com/10.4319/lo.2011.56.4.1463.

[97] Ki Hyun Kim et al. *A review of airborne polycyclic aromatic hydrocarbons (PAHs) and their human health effects*. Oct. 2013. DOI: 10.1016/j.envint.2013.07.019.

[98] Fulton G Kitson, Barbara S Larsen and Charles N McEwen. 'Chapter 1 - What Is GC/MS?' In: ed. by Fulton G Kitson et al. San Diego: Academic Press, 1996, pp. 3–23. ISBN: 978-0-12-483385-2. DOI: https://doi.org/10.1016/B978-012483385-2/50002-6. URL: https://www.sciencedirect.com/science/article/pii/B9780124833852500026.

[99] P R S Kodavanti et al. 'Comparative Effects of Two Polychlorinated Biphenyl Congeners on Calcium Homeostasis in Rat Cerebellar Granule Cells'. In: *Toxicology and Applied Pharmacology* 123.1 (1993), pp. 97–106. ISSN: 0041-008X. DOI: https://doi.org/10.1006/taap.1993.1226. URL: https://www.sciencedirect.com/science/article/pii/S0041008X83712263.

[100] K.J. Kristiansen and J.L. Sollid. 'Svalbard - jordartskart (Map of supericial materials)'. In: *National Atlas of Norway, sheet 2.3.6*. 1987.

[101] Gerhard Lammel et al. 'Long-range Atmospheric Transport of Polycyclic Aromatic Hydrocarbons is Worldwide Problem - Results from Measurements at Remote Sites and Modelling.' eng. In: *Acta chimica Slovenica* 62.3 (2015), pp. 729–735. ISSN: 1580-3155 (Electronic). DOI: 10.17344/acsi.2015.1387.

[102] Béatrice Lauby-Secretan et al. 'Carcinogenicity of polychlorinated biphenyls and polybrominated biphenyls'. In: *The Lancet Oncology* 14.4 (2013), pp. 287–288. ISSN: 1470-2045. DOI: https://doi.org/10.1016/S1470-2045(13)70104-9. URL: https://www.sciencedirect.com/science/article/pii/S1470204513701049.

[103] Kathy S Law and Andreas Stohl. 'Arctic Air Pollution: Origins and Impacts'. In: *Science* 315.5818 (Mar. 2007), 1537 LP –1540. DOI: 10.1126/science.1137695. URL: http://science.sciencemag.org/content/315/5818/1537.abstract.

[104] Nanqin Li et al. 'A Comprehensive and Critical Compilation, Evaluation, and Selection of Physical–Chemical Property Data for Selected Polychlorinated Biphenyls'. In: *Journal of Physical and Chemical Reference Data* 32.4 (Oct. 2003), pp. 1545–1590. ISSN: 0047-2689. DOI: 10.1063/1.1562632. URL: https://doi.org/10.1063/1.1562632.

[105] Ana Lúcia C. Lima, John W. Farrington and Christopher M. Reddy. 'Combustion-Derived Polycyclic Aromatic Hydrocarbons in the Environment—A Review'. In: *Environmental Forensics* 6.2 (June 2005), pp. 109–131. ISSN: 1527-5922. DOI: 10.1080/15275920590952739. URL: http://www.tandfonline.com/doi/abs/10.1080/15275920590952739.

[106] Maria Lorenzo and Yolanda Pico. 'Chapter 2 - Gas Chromatography and Mass Spectroscopy Techniques for the Detection of Chemical Contaminants and Residues in Foods'. In: *Woodhead Publishing Series in Food Science, Technology and Nutrition*. Ed. by Dieter Schrenk, Alexander B T - Chemical Contaminants Cartus and Residues in Food (Second Edition). Woodhead Publishing, 2017, pp. 15–50. ISBN: 978-0-08-100674-0. DOI: https://doi.org/10.1016/B978-0-08-100674-0.00002-3. URL: https://www.sciencedirect.com/science/article/pii/B9780081006740000023.

[107] Elsa Lundanes, Léon Reubsaet and Tyge Greibrokk. *Chromatography: Basic Principles, Sample Preparations and Related Methods*. Weinheim: Wiley-VCH, 2013, pp. 1–224. ISBN: 978-3-527-33620-3.

[108] Qno Lundkvist et al. *PCBs on Svalbard (Report 2008): Governor of Svalbard. PCBs on Svalbard: Status of Knowledge and Management*. Tech. rep. 2008. URL: https://brage.npolar.no/npolar-xmlui/bitstream/handle/11250/173172/PCBSvalbard2008english.pdf?sequence=1.

[109] Staffan Lundstedt et al. 'Pressurised liquid extraction of polycyclic aromatic hydrocarbons from contaminated soils'. In: *Journal of Chromatography A* 883.1-2 (June 2000), pp. 151–162. ISSN: 00219673. DOI: 10.1016/S0021-9673(00)00419-2.

[110] Gregor M Luthe, Benjamin G Schut and Jon Erik Aaseng. 'Monofluorinated analogues of polychlorinated biphenyls (F-PCBs): Synthesis using the Suzuki-coupling, characterization, specific properties and intended use'. In: *Chemosphere* 77.9 (2009), pp. 1242–1248. ISSN: 0045-6535. DOI: https://doi.org/10.1016/j.chemosphere.2006.02.029. URL: https://www.sciencedirect.com/science/article/pii/S0045653506002190.

[111] G Luthe et al. 'Monofluorinated analogues of polycyclic aromatic hydrocarbons as internal standards for GC-MS in environmental analysis'. In: *Chromatographia* 57.5 (2003), pp. 379–383. ISSN: 1612-1112. DOI: 10.1007/BF02492411. URL: https://doi.org/10.1007/BF02492411.

[112] Daniel. MacDougall, Warren B Crummett and et al. 'Guidelines for data acquisition and data quality evaluation in environmental chemistry'. In: *Analytical Chemistry* 52.14 (Dec. 1980), pp. 2242–2249. ISSN: 0003-2700. DOI: 10.1021/ac50064a004. URL: https://doi.org/10.1021/ac50064a004.

[113] Montse Marquès et al. 'Concentrations of polycyclic aromatic hydrocarbons and trace elements in Arctic soils: A case-study in Svalbard'. In: *Environmental Research* 159 (Nov. 2017), pp. 202–211. ISSN: 0013-9351. DOI: 10.1016/J.ENVRES.2017.08.003. URL: https://www.sciencedirect.com/science/article/pii/S0013935117309519?via%3Dihub.

[114] S. N. Meijer et al. 'Global distribution and budget of PCBs and HCB in background surface soils: Implications for sources and environmental processes'. In: *Environmental Science and Technology* 37.4 (Feb. 2003), pp. 667–672. ISSN: 0013936X. DOI: 10.1021/es025809l. URL: https://pubs.acs.org/sharingguidelines.

[115] James N. Miller and Jane C. Miller. *Statistics and Chemometrics for Analytical Chemistry*. Fifth Edit. Harlow, England: Pearson Education Limited, 2005.

[116] Philip E. Miller and M. Bonner Denton. 'The quadrupole mass filter: Basic operating concepts'. In: *Journal of Chemical Education* 63.7 (1986), pp. 617–622. ISSN: 00219584. DOI: 10.1021/ed063p617. URL: https://pubs.acs.org/sharingguidelines.

[117] Elizabeth A. Mishalanie et al. *Validation and Peer Review of U.S. Environmental Protection Agency Chemical Methods of Analysis*. Tech. rep. EPA Forum on Environmental Measurements (FEM), 2016, pp. 1–18. URL: https://www.epa.gov/sites/production/files/2016-02/documents/chemical_method_guide_revised_020316.pdf.

[118] Arctic Monitoring, (AMAP) and Assessment Programme. *AMAP Assessment 2015: Temporal Trends in Persistent Organic Pollutants in the Arctic*. Tech. rep. Oslo, Norway: Arctic Monitoring and Assessment Programme (AMAP), 2015, p. 71.

[119] Akbar Montaser. *Inductively Coupled Plasma Mass Spectrometry*. Ed. by Akbar Montaser. Wiley-VCH, 1998, pp. 266–267. ISBN: 0-471-18620-1.

[120] Derek C. G. Muir, Ross J. Norstrom and Mary. Simon. 'Organochlorine contaminants in arctic marine food chains: accumulation of specific polychlorinated biphenyls and chlordane-related compounds'. In: *Environmental Science & Technology* 22.9 (May 2002), pp. 1071–1079. DOI: 10.1021/es00174a012. URL: https://pubs.acs.org/doi/abs/10.1021/es00174a012.

[121] Derek Muir and Ed Sverko. 'Analytical methods for PCBs and organochlorine pesticides in environmental monitoring and surveillance: a critical appraisal'. In: *Analytical and Bioanalytical Chemistry* 386.4 (2006), pp. 769–789. ISSN: 1618-2650. DOI: 10.1007/s00216-006-0765-y. URL: https://doi.org/10.1007/s00216-006-0765-y.

[122] Brett Murphy et al. 'Simultaneous Extraction of PAHs and PCBs from Environmental Samples Using Accelerated Solvent Extraction'. In: Thermo Fisher Scientific, Application Note 1025 (2012), pp. 1–5.

[123] Martí Nadal, Marta Schuhmacher and José L Domingo. 'Levels of metals, PCBs, PCNs and PAHs in soils of a highly industrialized chemical/petrochemical area: Temporal trend'. In: *Chemosphere* 66.2 (2007), pp. 267–276. ISSN: 0045-6535. DOI: https://doi.org/10.1016/j.chemosphere.2006.05.020. URL: https://www.sciencedirect.com/science/article/pii/S0045653506006473.

[124] Martí Nadal et al. 'Climate change and environmental concentrations of POPs: A review'. In: *Environmental Research* 143 (2015), pp. 177–185. ISSN: 0013-9351. DOI: https://doi.org/10.1016/j.envres.2015.10.012. URL: https://www.sciencedirect.com/science/article/pii/S0013935115301109.

[125] W.M.A. (Ed.) Niessen. *Current Practice of Gas Chromatography-Mass Spectrometry*. 1st Ed. CRC Press, 2001. DOI: https://doi.org/10.1201/9780367801274.

[126] Hongsen Niu and R. S. Houk. 'Fundamental aspects of ion extraction in inductively coupled plasma mass spectrometry'. In: *Spectrochimica Acta - Part B Atomic Spectroscopy* 51.8 PART B (July 1996), pp. 779–815. ISSN: 05848547. DOI: 10.1016/0584-8547(96)01506-6.

[127] NLM. *ChemIDplus - National Library of Medicine*. URL: chem.sis.nlm.nih.gov/chemidplus/.

[128] Norwegian Polar Institute; Norsk institutt for naturforskning. *Vegetation map Svalbard - 22 classes*. 2014. URL: https://geodata.npolar.no/arcgis/rest/services/Temadata/F_Vegetation_Map_22cl_Svalbard/MapServer.

[129] NPI. *Norwegian Polar Institute: Map Data and Services*. 2020. URL: http://geodata.npolar.no/.

[130] Jerome O Nriagu. 'Global inventory of natural and anthropogenic emissions of trace metals to the atmosphere'. In: *Nature* 279.5712 (1979), pp. 409–411. ISSN: 1476-4687. DOI: 10.1038/279409a0. URL: https://doi.org/10.1038/279409a0.

[131] C. Nuth et al. 'Decadal changes from a multi-temporal glacier inventory of Svalbard'. In: *The Cryosphere* 7.5 (Oct. 2013), pp. 1603–1621. ISSN: 1994-0424. DOI: 10.5194/tc-7-1603-2013. URL: https://tc.copernicus.org/articles/7/1603/2013/.

[132] Tord Nygård, Eiliv Steinnes and Oddvar Røyset. 'Distribution of 32 elements in organic surface soils: Contributions from atmospheric transport of pollutants and natural sources'. In: *Water, Air, and Soil Pollution* 223.2 (Feb. 2012), pp. 699–713. ISSN: 00496979. DOI: 10.1007/s11270-011-0895-5. URL: https://link.springer.com/article/10.1007/s11270-011-0895-5.

[133] Wendy A. Ockenden et al. 'The global re-cycling of persistent organic pollutants is strongly retarded by soils'. In: *Environmental Pollution* 121.1 (Jan. 2003), pp. 75–80. ISSN: 02697491. DOI: 10.1016/S0269-7491(02)00204-X.

[134] Takeshi Ohno et al. 'Determination of strontium 90 in environmental samples by triple quadrupole ICP-MS and its application to Fukushima soil samples'. In: *Journal of Analytical Atomic Spectrometry* 33.6 (2018), pp. 1081–1085. ISSN: 0267-9477. DOI: 10.1039/C8JA00017D. URL: http://dx.doi.org/10.1039/C8JA00017D.

[135] Jaakko Paasivirta et al. 'Estimation of vapor pressures, solubilities and Henry's law constants of selected persistent organic pollutants as functions of temperature'. In: *Chemosphere* 39.5 (1999), pp. 811–832. ISSN: 0045-6535. DOI: https://doi.org/10.1016/S0045-6535(99)00016-8. URL: https://www.sciencedirect.com/science/article/pii/S0045653599000168.

[136] Aneta Dorota Pacyna-Kuchta et al. 'A screening of select toxic and essential elements and persistent organic pollutants in the fur of Svalbard reindeer'. In: *Chemosphere* 245 (Apr. 2020), p. 125458. ISSN: 18791298. DOI: 10.1016/j.chemosphere.2019.125458.

[137] J M Pacyna and E G Pacyna. 'An assessment of global and regional emissions of trace metals to the atmosphere from anthropogenic sources worldwide'. In: *Environmental Reviews* 9.4 (Dec. 2001), pp. 269–298. ISSN: 1181-8700. DOI: 10.1139/a01-012. URL: https://doi.org/10.1139/a01-012.

[138] R. Steven Pappas. *Sample preparation problem solving for inductively coupled plasma-mass spectrometry with liquid introduction systems: Solubility, chelation, and memory effects*. May 2012. URL: /pmc/articles/PMC4550584/?report=abstract%20https://www.ncbi.nlm.nih.gov/pmc/articles/PMC4550584/.

[139] R G Petersen and L D Calvin. 'Sampling'. In: *Methods of Soil Analysis*. Ed. by D. Sparks et al. SSSA Book Series. Jan. 1996, pp. 1–17. ISBN: 9780891188667. DOI: https://doi.org/10.2136/sssabookser5.3.c1. URL: https://doi.org/10.2136/sssabookser5.3.c1.

[140] Marina G. Pintado-Herrera, Eduardo González-Mazo and Pablo A. Lara-Martín. 'In-cell clean-up pressurized liquid extraction and gas chromatography-tandem mass spectrometry determination of hydrophobic persistent and emerging organic pollutants in coastal sediments'. In: *Journal of Chromatography A* 1429 (Jan. 2016), pp. 107–118. ISSN: 18733778. DOI: 10.1016/j.chroma.2015.12.040.

[141] Jeffry B Plomley, Mila Lauševic and Raymond E March. 'Determination of dioxins/furans and PCBs by quadrupole ion-trap gas chromatography–mass spectrometry'. In: *Mass Spectrometry Reviews* 19.5 (Jan. 2000), pp. 305–365. ISSN: 0277-7037. DOI: https://doi.org/10.1002/1098-2787(2000)19:5<305::AID-MAS4>3.0.CO;2-T. URL: https://analyticalsciencejournals.onlinelibrary.wiley.com/doi/abs/10.1002/1098-2787%282000%2919%3A5%3C305%3A%3AAID-MAS4%3E3.0.CO%3B2-T.

[142] Colin F Poole. 'Chapter 9 - Spectroscopic Detectors for Identification and Quantification'. In: ed. by Colin F B T - The Essence of Chromatography Poole. Amsterdam: Elsevier Science, 2003, pp. 719–792. ISBN: 978-0-444-50198-1. DOI: https://doi.org/10.1016/B978-044450198-1/50022-7. URL: https://www.sciencedirect.com/science/article/pii/B9780444501981500227.

[143] Dianne L. Poster et al. *Analysis of polycyclic aromatic hydrocarbons (PAHs) in environmental samples: A critical review of gas chromatographic (GC) methods*. Oct. 2006. DOI: 10.1007/s00216-006-0771-0. URL: http://www.ospar.org.

[144] Meng Qiao et al. 'Simultaneous detection of chlorinated polycyclic aromatic hydrocarbons with polycyclic aromatic hydrocarbons by gas chromatography–mass spectrometry'. In: *Analytical and Bioanalytical Chemistry* 409.13 (2017), pp. 3465–3473. ISSN: 1618-2650. DOI: 10.1007/s00216-017-0290-1. URL: https://doi.org/10.1007/s00216-017-0290-1.

[145] R Core Team. *R: A Language and Environment for Statistical Computing*. Vienna, Austria, 2020. URL: https://www.r-project.org/.

[146] Amal Al-Rashdan et al. 'Determination of the Levels of Polycyclic Aromatic Hydrocarbons in Toasted Bread Using Gas Chromatography Mass Spectrometry'. In: *International Journal of Analytical Chemistry* 2010 (2010). Ed. by Shoji Motomizu, p. 821216. ISSN: 1687-8760. DOI: 10.1155/2010/821216. URL: https://doi.org/10.1155/2010/821216.

[147] Khaiwal Ravindra, Ranjeet Sokhi and René Van Grieken. *Atmospheric polycyclic aromatic hydrocarbons: Source attribution, emission factors and regulation*. Apr. 2008. DOI: 10.1016/j.atmosenv.2007.12.010.

[148] Andriy Rebryk and Peter Haglund. 'Non-targeted screening workflows for gas chromatography–high-resolution mass spectrometry analysis and identification of biomagnifying contaminants in biota samples'. In: *Analytical and Bioanalytical Chemistry* 413.2 (2021), pp. 479–501. ISSN: 1618-2650. DOI: 10.1007/s00216-020-03018-4. URL: https://doi.org/10.1007/s00216-020-03018-4.

[149] Eric J Reiner. 'The analysis of dioxins and related compounds'. In: *Mass Spectrometry Reviews* 29.4 (July 2010), pp. 526–559. ISSN: 0277-7037. DOI: https://doi.org/10.1002/mas.20255. URL: https://doi.org/10.1002/mas.20255.

[150] Brace E. Richter et al. 'Accelerated solvent extraction: A technique for sample preparation'. In: *Analytical Chemistry* 68.6 (1996), pp. 1033–1039. ISSN: 00032700. DOI: 10.1021/ac9508199. URL: https://pubs.acs.org/sharingguidelines.

[151] N. L. Rose et al. 'Lake-sediment evidence for local and remote sources of atmospherically deposited pollutants on Svalbard'. In: *Journal of Paleolimnology* 31.4 (May 2004), pp. 499–513. ISSN: 09212728. DOI: 10.1023/B:JOPL.0000022548.97476.39. URL: https://link.springer.com/article/10.1023/B:JOPL.0000022548.97476.39.

[152] R Rubio and A M Ure. 'Approaches to Sampling and Sample Pretreatments for Metal Speciation in Soils and Sediments'. In: *International Journal of Environmental Analytical Chemistry* 51.1-4 (June 1993), pp. 205–217. ISSN: 0306-7319. DOI: 10.1080/03067319308027626. URL: https://doi.org/10.1080/03067319308027626.

[153] Stephen H Safe. 'Polychlorinated Biphenyls (PCBs): Environmental Impact, Biochemical and Toxic Responses, and Implications for Risk Assessment'. In: *Critical Reviews in Toxicology* 24.2 (Jan. 1994), pp. 87–149. ISSN: 1040-8444. DOI: 10.3109/10408449409049308. URL: https://doi.org/10.3109/10408449409049308.

[154] Stephen Safe and Otto Hutzinger. 'Polychlorinated Biphenyls (PCBs) and Polybrominated Biphenyls (PBBs): Biochemistry, Toxicology, and Mechanism of Action'. In: *CRC Critical Reviews in Toxicology* 13.4 (Jan. 1984), pp. 319–395. ISSN: 0045-6446. DOI: 10.3109/10408448409023762. URL: https://doi.org/10.3109/10408448409023762.

[155] James Sangster. 'Octanol-Water Partition Coefficients of Simple Organic Compounds'. In: *Journal of Physical and Chemical Reference Data* 18.3 (July 1989), pp. 1111–1229. ISSN: 0047-2689. DOI: 10.1063/1.555833. URL: https://doi.org/10.1063/1.555833.

[156] Randall J. Schaetzl and Michael L. Thompson. *Soils - Genesis and Geomorphology*. 2nd ed. New York, USA: Cambridge University Press, 2015, p. 8. ISBN: 9781107016934.

[157] P.J. Schoeneberger et al. *Field book for describing and sampling soils, Version 3.0*. Lincoln, NE: Natural Resources Conservation Service, National Soil Survey Center, 2012, pp. 1–300.

[158] Maria Schönbächler. 'Inductively Coupled Plasma Mass Spectrometry (ICP-MS)'. In: *Encyclopedia of Geochemistry. Encyclopedia of Earth Sciences Series.* Ed. by W. White. Springer, Cham, 2016, pp. 1–6. DOI: 10.1007/978-3-319-39193-9{_}111-1. URL: http://link.springer.com/10.1007/978-3-319-39193-9_111-1.

[159] Secretariat of the Stockholm Convention. *The 12 initial POPs under the Stockholm Convention*. 2001. URL: http://chm.pops.int/TheConvention/ThePOPs/The12InitialPOPs/tabid/296/Default.aspx.

[160] Wan Ying Shiu and Donald Mackay. 'A Critical Review of Aqueous Solubilities, Vapor Pressures, Henry's Law Constants, and Octanol–Water Partition Coefficients of the Polychlorinated Biphenyls'. In: *Journal of Physical and Chemical Reference Data* 15.2 (Apr. 1986), pp. 911–929. ISSN: 0047-2689. DOI: 10.1063/1.555755. URL: https://doi.org/10.1063/1.555755.

[161] Luigi Silvestro, Isabela Tarcomnicu and Simona Rizea Savu. 'Matrix Effects in Mass Spectrometry Combined with Separation Methods - Comparison HPLC, GC and Discussion on Methods to Control these Effects'. In: *Tandem Mass Spectrometry - Molecular Characterization*. Ed. by Ana Varela Coelho and Catarina de Matos Ferraz Franco. IntechOpen, 2013. Chap. 1. ISBN: 978-953-51-1136-8. DOI: 10.5772/55982.

[162] Skalar Analytical. 'Skalar methods - total carbon/ total nitrogen in soil (lab protocol description)'. Breda, The Netherlands.

[163] Douglas A. Skoog et al. *Fundamentals of Analytical Chemistry*. 9th. Boston (USA): Brooks/Cole Cengage Learning, 2014. ISBN: 978-0-495-55828-6.

[164] Anna Sobek and Örjan Gustafsson. 'Deep Water Masses and Sediments Are Main Compartments for Polychlorinated Biphenyls in the Arctic Ocean'. In: *Environmental Science & Technology* 48.12 (June 2014), pp. 6719–6725. DOI: 10.1021/es500736q.

[165] Silvia de Sousa Freitas and Fernando M Lanças. 'Matrix effects observed during pesticides residue analysis in fruits by GC'. In: *Journal of Separation Science* 32.21 (Nov. 2009), pp. 3698–3705. ISSN: 1615-9306. DOI: https://doi.org/10.1002/jssc.200900358. URL: https://doi.org/10.1002/jssc.200900358.

[166] O David Sparkman, Zelda E Penton and Fulton G Kitson. 'Chapter 6 - Quantitation with GC/MS'. In: ed. by O David Sparkman et al. Amsterdam: Academic Press, 2011, pp. 207–218. ISBN: 978-0-12-373628-4. DOI: https://doi.org/10.1016/B978-0-12-373628-4.00006-X. URL: https://www.sciencedirect.com/science/article/pii/B978012373628400006X.

[167] K Srogi. 'Monitoring of environmental exposure to polycyclic aromatic hydrocarbons: a review'. In: *Environmental Chemistry Letters* 5.4 (2007), pp. 169–195. ISSN: 1610-3661. DOI: 10.1007/s10311-007-0095-0. URL: https://doi.org/10.1007/s10311-007-0095-0.

[168] Standard Norge. 'NS-EN 15934:2012, Sludge, treated biowaste, soil and waste - Calculation of dry matter fraction after determination of dry residue or water content'. 2012. URL: https://www.standard.no/no/Nettbutikk/produktkatalogen/Produktpresentasjon/?ProductID=595831.

[169] Eric Stauffer, Julia A Dolan and Reta Newman. 'CHAPTER 8 - Gas Chromatography and Gas Chromatography—Mass Spectrometry'. In: ed. by Eric Stauffer, Julia A Dolan and Reta B T - Fire Debris Analysis Newman. Burlington: Academic Press, 2008, pp. 235–293. ISBN: 978-0-12-663971-1. DOI: https://doi.org/10.1016/B978-012663971-1.50012-9. URL: https://www.sciencedirect.com/science/article/pii/B9780126639711500129.

[170] Eiliv Steinnes, T. Berg and Hilde Thelle Uggerud. 'Three decades of atmospheric metal deposition in Norway as evident from analysis of moss samples'. In: *Science of the Total Environment* 412-413 (Dec. 2011), pp. 351–358. ISSN: 00489697. DOI: 10.1016/j.scitotenv.2011.09.086.

[171] Eiliv Steinnes and Andrew J. Friedland. *Metal contamination of natural surface soils from long-range atmospheric transport: Existing and missing knowledge*. 2006. DOI: 10.1139/A06-002.

[172] Eiliv Steinnes and Syverin Lierhagen. 'Geographical distribution of trace elements in natural surface soils: Atmospheric influence from natural and anthropogenic sources'. In: *Applied Geochemistry* 88 (Jan. 2018), pp. 2–9. ISSN: 18729134. DOI: 10.1016/j.apgeochem.2017.03.013.

[173] Safe Stephen et al. 'PCBs: structure–function relationships and mechanism of action'. In: *Environmental Health Perspectives* 60 (May 1985), pp. 47–56. DOI: 10.1289/ehp.856047. URL: https://doi.org/10.1289/ehp.856047.

[174] Frank J. Stevenson. *Humus chemistry: genesis, composition, reactions*. 2nd ed. John Wiley & Sons, 1994.

[175] Scott A Stout et al. 'Beyond 16 Priority Pollutant PAHs: A Review of PACs used in Environmental Forensic Chemistry'. In: *Polycyclic Aromatic Compounds* 35.2-4 (Mar. 2015), pp. 285–315. ISSN: 1040-6638. DOI: 10.1080/10406638.2014.891144. URL: https://doi.org/10.1080/10406638.2014.891144.

[176] Ken Sutherland. 'Gas chromatography/mass spectrometry techniques for the characterisation of organic materials in works of art'. In: *Physical Sciences Reviews* 4.6 (2019). DOI: doi:10.1515/psr-2018-0010. URL: https://doi.org/10.1515/psr-2018-0010.

[177] Harald Svendsen et al. 'The physical environment of Kongsfjorden–Krossfjorden, an Arctic fjord system in Svalbard'. In: *Polar Research* 21.1 (June 2002), pp. 133–166. ISSN: 0800-0395. DOI: https://doi.org/10.1111/j.1751-8369.2002.tb00072.x. URL: https://doi.org/10.1111/j.1751-8369.2002.tb00072.x.

[178] Michael E. Swartz and Ira S. Krull. *Analytical Method Development and Validation*. First Edit. Boca Raton, USA: CRC Press, 1997, pp. 1–96. ISBN: 978-0-8247-0115-4.

[179] Małgorzata Szopińska et al. 'Determination of polycyclic aromatic hydrocarbons (PAHs) and other organic pollutants in freshwaters on the western shore of Admiralty Bay (King George Island, Maritime Antarctica)'. In: *Environmental Science and Pollution Research* 26.18 (2019), pp. 18143–18161. ISSN: 1614-7499. DOI: 10.1007/s11356-019-05045-w. URL: https://doi.org/10.1007/s11356-019-05045-w.

[180] Hiroshi Takakuwa et al. 'Analysis method for PCBs in reclaimed oil using a fast-GC triple stage quadrupole mass spectrometer with the 13-component quantitation method'. In: *Environmental Science and Pollution Research* 25.17 (2018), pp. 16300–16308. ISSN: 1614-7499. DOI: 10.1007/s11356-017-0533-x. URL: https://doi.org/10.1007/s11356-017-0533-x.

[181] Takumi Takasuga et al. 'Isotope dilution analysis of polychlorinated biphenyls (PCBs) in transformer oil and global commercial PCB formulations by high resolution gas chromatography–high resolution mass spectrometry'. In: *Chemosphere* 62.3 (2006), pp. 469–484. ISSN: 0045-6535. DOI: https://doi.org/10.1016/j.chemosphere.2005.04.034. URL: https://www.sciencedirect.com/science/article/pii/S0045653505005710.

[182] Charles Tarnocai. 'Arctic Permafrost Soils BT - Permafrost Soils'. In: ed. by Rosa Margesin. Berlin, Heidelberg: Springer Berlin Heidelberg, 2009, pp. 3–16. ISBN: 978-3-540-69371-0. DOI: 10.1007/978-3-540-69371-0{_}1. URL: https://doi.org/10.1007/978-3-540-69371-0_1.

[183] R. Thomas. *Practical Guide to ICP-MS: A Tutorial for Beginners, Second Edition (2nd ed.)* CRC Press, 2008. DOI: https://doi.org/10.1201/9781420067873.

[184] Michael Thompson, Stephen Ellison and Roger Wood. 'Harmonized guidelines for single-laboratory validation of methods of analysis (IUPAC Technical Report)'. In: *Pure and Applied Chemistry* 74 (Jan. 2002), pp. 835–855. DOI: 10.1351/pac200274050835.

[185] Michael Thompson et al. *Harmonised guidelines for the use of recovery information in analytical measurement*. Tech. rep. Orlando, USA: IUPAC, 1996, pp. 1–17. URL: https://www.eurachem.org/images/stories/Guides/pdf/recovery.pdf.

[186] Marek Tobiszewski and Jacek Namieśnik. 'PAH diagnostic ratios for the identification of pollution emission sources'. In: *Environmental Pollution* 162 (Mar. 2012), pp. 110–119. ISSN: 0269-7491. DOI: 10.1016/J.ENVPOL.2011.10.025. URL: https://www.sciencedirect.com/science/article/pii/S0269749111006051?via%3Dihub.

[187] U.S. EPA. 'Method 3545A (SW-846): Pressurized Fluid Extraction (PFE)'. Washington, DC, 2007.

[188] U.S. EPA. 'Method 3660B: Sulfur cleanup'. Washington, DC, 1996.

[189] Sandy Ubl et al. 'Primary source regions of polychlorinated biphenyls (PCBs) measured in the Arctic'. In: *Atmospheric Environment* 62 (2012), pp. 391–399. ISSN: 1352-2310. DOI: https://doi.org/10.1016/j.atmosenv.2012.07.061. URL: https://www.sciencedirect.com/science/article/pii/S1352231012007479.

[190] UNECE. *The 1998 Aarhus Protocol on Persistent Organic Pollutants (POPs)*. 2014. URL: http://www.unece.org/env/lrtap/pops_h1.html.

[191] Sílvio Vaz Jr. 'The Main Environmental Matrices: Air, Soil, and Water'. In: *Analytical Chemistry Applied to Emerging Pollutants*. Ed. by Sílvio Vaz Jr. Cham: Springer International Publishing, 2018, pp. 79–101. ISBN: 978-3-319-74403-2. DOI: 10.1007/978-3-319-74403-2{_}4. URL: https://doi.org/10.1007/978-3-319-74403-2_4.

[192] Marco Vecchiato et al. 'Fragrances and PAHs in snow and seawater of Ny-Ålesund (Svalbard): Local and long-range contamination'. In: *Environmental Pollution* 242 (Nov. 2018), pp. 1740–1747. ISSN: 0269-7491. DOI: 10.1016/J.ENVPOL.2018.07.095. URL: https://www.sciencedirect.com/science/article/pii/S0269749118322346#bib2.

[193] G Wagner. 'Basic approaches and methods for quality assurance and quality control in sample collection and storage for environmental monitoring'. In: *Science of The Total Environment* 176.1 (1995), pp. 63–71. ISSN: 0048-9697. DOI: https://doi.org/10.1016/0048-9697(95)04830-8. URL: https://www.sciencedirect.com/science/article/pii/0048969795048308.

[194] G Wagner et al. 'Objectives, concept and design of the CEEM soil project'. In: *Science of The Total Environment* 264.1 (2001), pp. 3–15. ISSN: 0048-9697. DOI: https://doi.org/10.1016/S0048-9697(00)00608-2. URL: https://www.sciencedirect.com/science/article/pii/S0048969700006082.

[195] Sheng-Wei Wang et al. 'Determination of polycyclic aromatic hydrocarbons (PAHs) in cosmetic products by gas chromatography-tandem mass spectrometry'. In: *Journal of Food and Drug Analysis* 27.3 (2019), pp. 815–824. ISSN: 1021-9498. DOI: https://doi.org/10.1016/j.jfda.2019.01.003. URL: https://www.sciencedirect.com/science/article/pii/S102194981930016X.

[196] Zhen Wang et al. 'Correlations between physicochemical properties of PAHs and their distribution in soil, moss and reindeer dung at Ny-Ålesund of the Arctic'. In: *Environmental Pollution* 157.11 (Nov. 2009), pp. 3132–3136. ISSN: 02697491. DOI: 10.1016/j.envpol.2009.05.014.

[197] Zhen Wang et al. 'Correlations between physicochemical properties of PAHs and their distribution in soil, moss and reindeer dung at Ny-Ålesund of the Arctic'. In: *Environmental Pollution* 157.11 (Nov. 2009), pp. 3132–3136. ISSN: 0269-7491. DOI: 10.1016/J.ENVPOL.2009.05.014. URL: https://www.sciencedirect.com/science/article/pii/S0269749109002450.

[198] F. Wania and D. Mackay. 'Global fractionation and cold condensation of low volatility organochlorine compounds in polar regions'. In: *Ambio* 22.1 (1993), pp. 10–18. DOI: 10.2307/4314030.

[199] Frank Wania and Donald MacKay. 'Tracking the Distribution of Persistent Organic Pollutants'. In: *Environmental Science & Technology* 30.9 (Aug. 1996), 390A–396A. ISSN: 0013-936X. DOI: 10.1021/es962399q. URL: https://pubs.acs.org/sharingguidelines.

[200] Frank Wania and Donald Mackay. *The Global Fractionation of Persistent Organic Pollutants*. Kjeller (NO), 1996, pp. 1–28. ISBN: 82-425-0772-4.

[201] Greg Wells, Harry Prest and Charles William Russ. 'Signal, Noise and Detection Limits in Mass Spectrometry'. Wilmington, US, 2011. URL: https://www.agilent.com/cs/library/technicaloverviews/Public/5990-7651EN.pdf.

[202] Simon R Wild and Kevin C Jones. 'Polynuclear aromatic hydrocarbons in the United Kingdom environment: A preliminary source inventory and budget'. In: *Environmental Pollution* 88.1 (1995), pp. 91–108. ISSN: 0269-7491. DOI: https://doi.org/10.1016/0269-7491(95)91052-M. URL: https://www.sciencedirect.com/science/article/pii/026974919591052M.

[203] Megan D Willis, W Richard Leaitch and Jonathan P D Abbatt. 'Processes Controlling the Composition and Abundance of Arctic Aerosol'. In: *Reviews of Geophysics* 56.4 (Dec. 2018), pp. 621–671. ISSN: 8755-1209. DOI: https://doi.org/10.1029/2018RG000602. URL: https://doi.org/10.1029/2018RG000602.

[204] Scott Wilschefski and Matthew Baxter. 'Inductively Coupled Plasma Mass Spectrometry: Introduction to Analytical Aspects'. In: *Clinical Biochemist Reviews* 40.3 (Aug. 2019), pp. 115–133. ISSN: 0159-8090. DOI: 10.33176/aacb-19-00024. URL: /pmc/articles/PMC6719745/?report=abstract%20https://www.ncbi.nlm.nih.gov/pmc/articles/PMC6719745/.

[205] Coby S. C. Wong and Xiangdong Li. 'Analysis of Heavy Metal Contaminated Soils'. In: *Practice Periodical of Hazardous, Toxic, and Radioactive Waste Management* 7.1 (Jan. 2003), pp. 12–18. DOI: 10.1061/(ASCE)1090-025X(2003)7:1(12). URL: https://doi.org/10.1061/(ASCE)1090-025X(2003)7:1(12).

[206] Fiona Wong et al. 'Time trends of persistent organic pollutants (POPs) and Chemicals of Emerging Arctic Concern (CEAC) in Arctic air from 25 years of monitoring'. In: *Science of The Total Environment* 775 (2021), p. 145109. ISSN: 0048-9697. DOI: https://doi.org/10.1016/j.scitotenv.2021.145109. URL: https://www.sciencedirect.com/science/article/pii/S0048969721001753.

[207] Jon W Wong et al. 'Multiresidue Pesticide Analysis by Capillary Gas Chromatography-Mass Spectrometry'. In: *Mass Spectrometry in Food Safety: Methods and Protocols, vol 747*. Ed. by Jerry Zweigenbaum. Totowa, NJ: Humana Press, 2011, pp. 131–172. ISBN: 978-1-61779-136-9. DOI: 10.1007/978-1-61779-136-9{_}6. URL: https://doi.org/10.1007/978-1-61779-136-9_6.

[208] Yong Yu et al. 'Polycyclic Aromatic Hydrocarbons Not Declining in Arctic Air Despite Global Emission Reduction'. In: *Environmental Science and Technology* 53.5 (Mar. 2019), pp. 2375–2382. ISSN: 15205851. DOI: 10.1021/acs.est.8b05353. URL: https://pubs.acs.org/sharingguidelines.

[209] Mark B Yunker et al. 'PAHs in the Fraser River basin: a critical appraisal of PAH ratios as indicators of PAH source and composition'. In: *Organic Geochemistry* 33.4 (2002), pp. 489–515. ISSN: 0146-6380. DOI: https://doi.org/10.1016/S0146-6380(02)00002-5. URL: https://www.sciencedirect.com/science/article/pii/S0146638002000025.

[210] Sema Yurdakul et al. 'Levels, temporal/spatial variations and sources of PAHs and PCBs in soil of a highly industrialized area'. In: *Atmospheric Pollution Research* 10.4 (July 2019), pp. 1227–1238. ISSN: 13091042. DOI: 10.1016/j.apr.2019.02.006.

[211] Jianqiong Zhan et al. 'Effects of ship emissions on summertime aerosols at Ny–Alesund in the Arctic'. In: *Atmospheric Pollution Research* 5.3 (2014), pp. 500–510. ISSN: 1309-1042. DOI: https://doi.org/10.5094/APR.2014.059. URL: https://www.sciencedirect.com/science/article/pii/S1309104215303081.

[212] Peng Zhang et al. 'Distribution and transfer pattern of Polychlorinated Biphenyls (PCBs) among the selected environmental media of Ny-Ålesund, the Arctic: As a case study'. In: *Marine Pollution Bulletin* 89.1-2 (Dec. 2014), pp. 267–275. ISSN: 18793363. DOI: 10.1016/j.marpolbul.2014.09.050.

[213] Chaofei Zhu et al. 'Polychlorinated biphenyls (PCBs) and polybrominated biphenyl ethers (PBDEs) in environmental samples from Ny-Ålesund and London Island, Svalbard, the Arctic'. In: *Chemosphere* 126 (2015), pp. 40–46. ISSN: 0045-6535. DOI: https://doi.org/10.1016/j.chemosphere.2015.01.043. URL: https://www.sciencedirect.com/science/article/pii/S0045653515000831.

[214] Marta Ziółek, Piotr Bartmiński and Alfred Stach. 'The Influence of Seabirds on the Concentration of Selected Heavy Metals in Organic Soil on the Bellsund Coast, Western Spitsbergen'. In: *Arctic, Antarctic, and Alpine Research* 49.4 (Nov. 2017), pp. 507–520. ISSN: 1523-0430. DOI: 10.1657/AAAR0016-024. URL: https://www.tandfonline.com/doi/full/10.1657/AAAR0016-024.

Appendices

APPENDIX A

Sample data

A.1 Sample details

Table A.1 – Soil sample location details and analysis strategy. Sampling date is given above the respective samples. Samples indicated with the letter "M" are mineral soil samples. Sample areas are indicated with BDW=Brøggerdalen (west side), BDE=Brøggerdalen (east side), NDM=Nordre Diesetvatnet (Mitrahalvøya), KI=Kiærstranda, GB=Gåsebu. Samples with identical GPS coordinates are samples that were collected within 10-20 m distance from each other. See section 3.2 for further description.

Sample ID	Area	Latitude	Longitude
August 2020, week 33			
S4	BDE	78°55.248′N	11°50.882′E
S5	BDE	78°55.537′N	11°50.737′E
S6	BDE	78°55.462′N	11°50.411′E
S1	BDW	78°56.333′N	11°45.784′E
S2	BDW	78°55.562′N	11°47.364′E
S3	BDW	78°55.849′N	11°49.093′E
S13	NDM	79°12.915′N	11°22.429′E
S14	NDM	79°12.915′N	11°22.429′E
S15	NDM	79°13.656′N	11°23.164′E
August 2020, week 34			
S10	KI	78°54.197′N	11°30.651′E
S11	KI	78°54.183′N	11°30.656′E
S12	KI	78°54.184′N	11°30.646′E
S7	GB	78°54.341′N	12°00.339′E
S8	GB	78°54.765′N	12°03.396′E
S9	GB	78°54.755′N	12°03.420′E

APPENDIX B

Soil carbon, nitrogen and element content in surface soils

B.1 Nitrogen and carbon content in surface soil samples

Table B.1 – Dataset of TC, TN, TIC900, TOC400 and ROC composition of surface soil samples investigated in this study. Study areas are indicated with BDE=Brøggerdalen, east side of Bayelva, BDW=Brøggerdalen, west side of Bayelva, GB=Gåsebu, KI=Kiærstranda and NDM=Nordre Diesetvatnet (Mitrahalvøya).

sample ID	Study area	Unit	TC	TN	TIC	TOC400	ROC
S4	BDE	mg g^{-1}	140.6	10.1	1.3	114.9	16.6
S5	BDE	mg g^{-1}	104.2	6.2	0.3	82.5	10.7
S6	BDE	mg g^{-1}	132.2	10.6	0.4	117.3	8.9
S1	BDW	mg g^{-1}	279.2	17.1	3.7	223.9	21.8
S2	BDW	mg g^{-1}	83.0	5.9	0.3	52.6	12.2
S3	BDW	mg g^{-1}	202.2	12.5	1.4	229.9	13.6
S7	GB	mg g^{-1}	45.0	2.7	0.1	21.4	4.2
S8	GB	mg g^{-1}	343.6	17.9	2.2	237.4	17.1
S9	GB	mg g^{-1}	210.4	13.1	2.6	151.5	22.1
S10	KI	mg g^{-1}	292.1	23.0	7.5	238.2	24.6
S11	KI	mg g^{-1}	317.0	27.2	3.2	255.8	22.1
S12	KI	mg g^{-1}	326.3	28.2	3.6	272.1	16.8
S13	NDM	mg g^{-1}	282.5	10.9	63.3	166.2	28.7
S14	NDM	mg g^{-1}	161.7	3.3	103.8	49.6	13.3
S15	NDM	mg g^{-1}	161.2	11.7	2.0	124.8	11.1

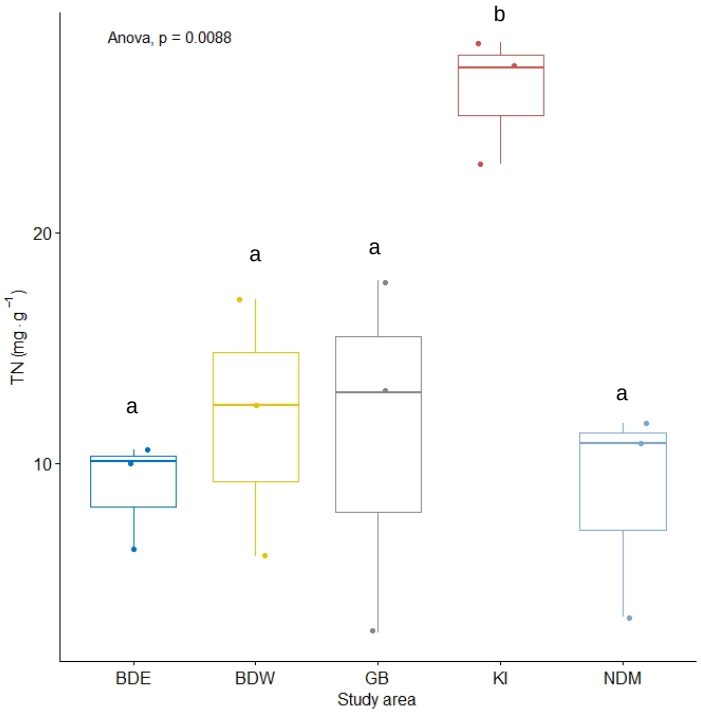

Figure B.1 – Boxplot for total nitrogen (TN) content in soil (mg g^{-1}) at different study areas. The median is displayed by the line inside the box. The interquartile range (IQR) is displayed as a box. The whisker is determined by the 1st/ 3rd quartile $\pm$ 1.5 $\cdot$ IQR. Single data points are visualized as well. There are no outliers due to the low number of data points for each study area (n=3). Study areas sharing the same letter code were not significantly different from each other (one-way Anova and Tukey's post hoc test, $p < 0.05$).

B.2 Profile of trace elements in Svalbard surface soil samples

Table B.2 – Dataset of element composition of surface soil samples investigated in this study. Study areas are indicated with BDE=Brøggerdalen, east side of Bayelva, BDW=Brøggerdalen, west side of Bayelva, GB=Gåsebu, KI=Kiærstranda and NDM=Nordre Diesetvatnet (Mitrahalvøya).

Study area	Sample ID	Unit	P	Cr	Ni	Cu	Zn	As	Cd	Pb
BDE	S4	$\mu g\ g^{-1}$	904	42.9	21.4	18.5	59.7	3.56	0.35	15.7
BDE	S5	$\mu g\ g^{-1}$	849	62.8	27.9	20.0	69.4	5.31	0.12	16.9
BDE	S6	$\mu g\ g^{-1}$	1288	44.2	19.6	15.1	48.1	3.89	0.10	17.0
BDW	S1	$\mu g\ g^{-1}$	1158	21.4	10.5	7.5	32.3	1.92	0.27	8.2
BDW	S2	$\mu g\ g^{-1}$	821	65.3	35.7	25.3	84.0	5.43	0.32	21.8
BDW	S3	$\mu g\ g^{-1}$	739	22.2	12.4	9.5	57.7	2.02	0.51	8.8
GB	S7	$\mu g\ g^{-1}$	560	53.8	40.6	33.2	78.5	6.04	0.39	20.8
GB	S8	$\mu g\ g^{-1}$	918	13.4	6.5	8.7	34.1	1.78	0.31	13.6
GB	S9	$\mu g\ g^{-1}$	795	21.8	10.0	10.6	58.7	2.26	0.20	10.1
KI	S10	$\mu g\ g^{-1}$	2123	41.6	31.5	15.8	83.6	7.06	4.15	12.9
KI	S11	$\mu g\ g^{-1}$	2372	49.1	36.6	19.2	80.8	7.30	4.31	10.6
KI	S12	$\mu g\ g^{-1}$	2256	43.1	35.4	16.8	77.3	7.03	4.49	10.0
NDM	S13	$\mu g\ g^{-1}$	382	8.5	4.5	3.3	80.3	1.59	0.25	13.2
NDM	S14	$\mu g\ g^{-1}$	234	10.0	5.8	3.1	69.7	2.32	0.21	18.0
NDM	S15	$\mu g\ g^{-1}$	1377	46.2	99.9	35.6	71.4	35.42	0.32	29.6

APPENDIX C

Analysis of PAHs and PCBs and method development

C.1 Extraction protocol

Table C.1 – Comparison of estimated absolute and relative recoveries for target analytes between extracts, resulting from different sample amounts: 1 g and 0.5 g. The fortification level was 100 ng mL^{-1}.

	Estimated $R_{abs.}$ (%)		Estimated $R_{rel.}$ (%)	
	Sample amount		Sample amount	
Analyte	0.5 g	1 g	0.5 g	1 g
NAP	88	46	163	119
ACY	57	49	72	79
ACE	51	74	64	117
FLU	75	56	97	93
PHE	85	67	94	104
ANT	24	103	25	136
FLT	83	59	91	89
PYR	81	62	88	88
BaA	61	68	64	81
CHR	79	64	82	76
BbF	83	63	86	74
BkF	80	55	84	65
BaP	24	85	25	97
IND	73	66	75	76
DBA	82	65	85	75
BgP	98	53	102	61
PCB-28	75	62	104	94
PCB-52	81	60	113	92
PCB-101	81	57	115	86
PCB-118	81	64	115	96
PCB-138	76	62	108	93
PCB-153	80	63	113	95
PCB-180	72	60	102	90

C.2 Calibration curves of PAH target analytes

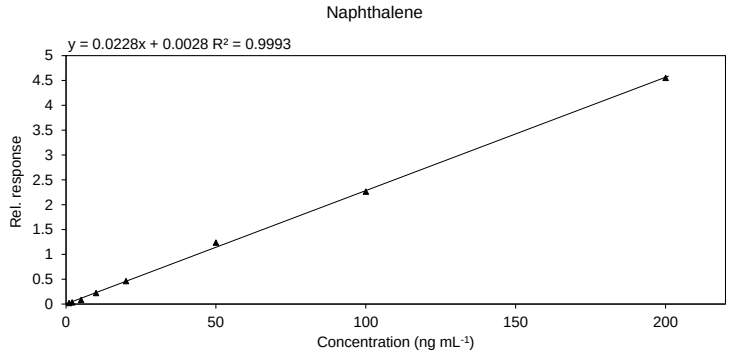

Figure C.1 – Calibration curve of naphthalene based on relative response. All standards contained 50 ng mL^{-1} internal standard.

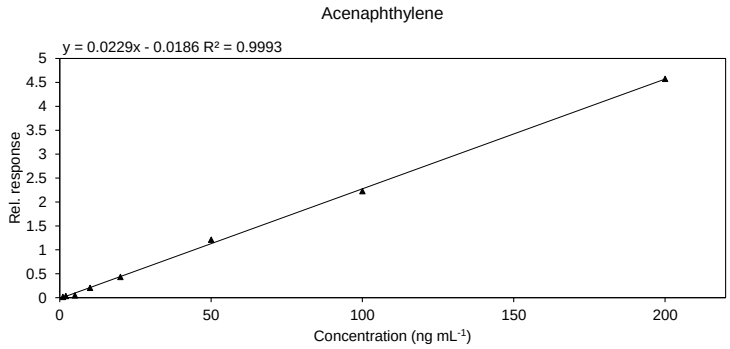

Figure C.2 – Calibration curve of acenaphthylene based on relative response. All standards contained 50 ng mL^{-1} internal standard.

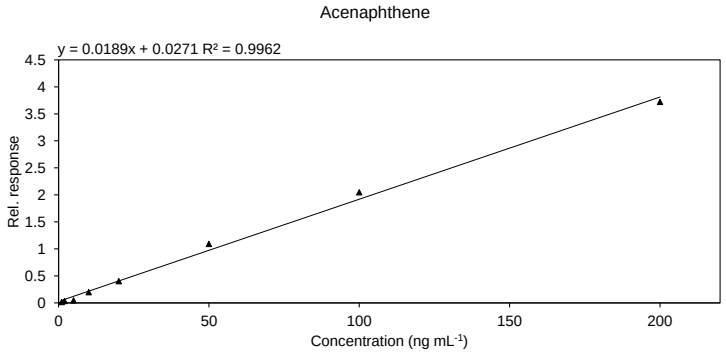

Figure C.3 – Calibration curve of acenaphthene based on relative response. All standards contained 50 ng mL^{-1} internal standard.

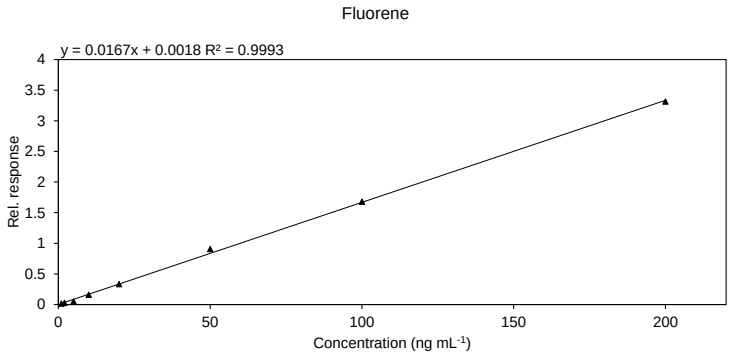

Figure C.4 – Calibration curve of fluorene based on relative response. All standards contained 50 ng mL^{-1} internal standard.

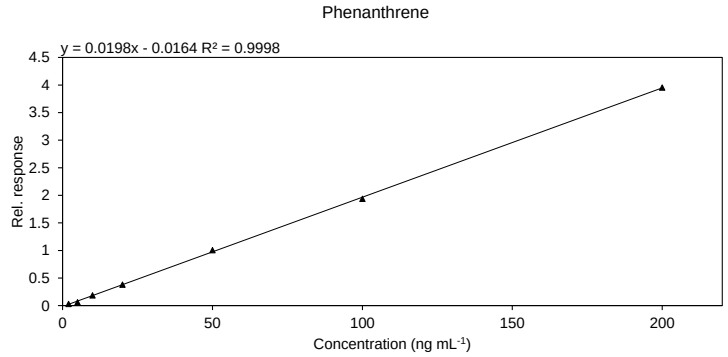

Figure C.5 – Calibration curve of phenanthrene based on relative response. All standards contained 50 ng mL^{-1} internal standard.

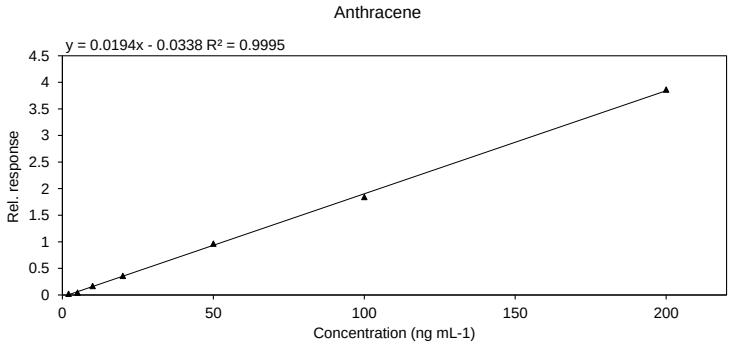

Figure C.6 – Calibration curve of anthracene based on relative response. All standards contained 50 ng mL^{-1} internal standard.

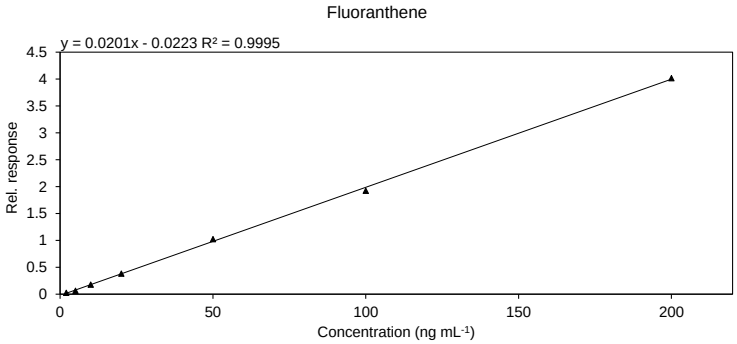

Figure C.7 – Calibration curve of fluoranthene based on relative response. All standards contained 50 ng mL^{-1} internal standard.

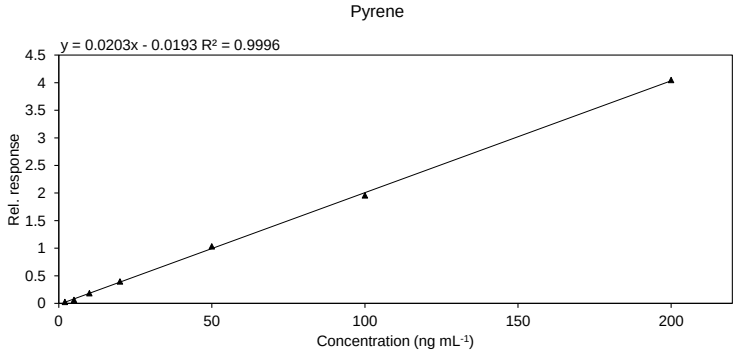

Figure C.8 – Calibration curve of pyrene based on relative response. All standards contained 50 ng mL^{-1} internal standard.

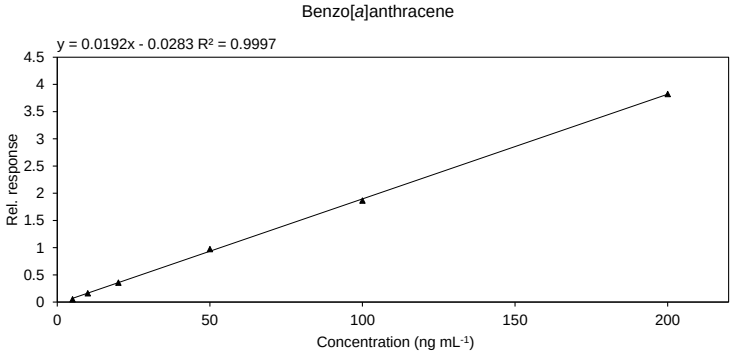

Figure C.9 – Calibration curve of benzo[*a*]anthracene based on relative response. All standards contained 50 ng mL^{-1} internal standard.

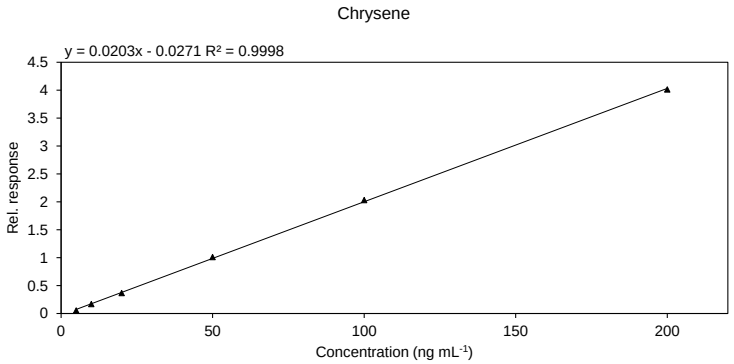

Figure C.10 – Calibration curve of chrysene based on relative response. All standards contained 50 ng mL^{-1} internal standard.

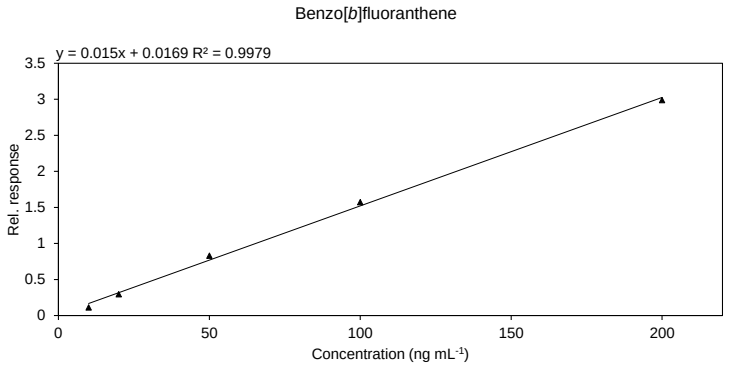

Figure C.11 – Calibration curve of benzo[*b*]fluoranthene based on relative response. All standards contained 50 ng mL^{-1} internal standard.

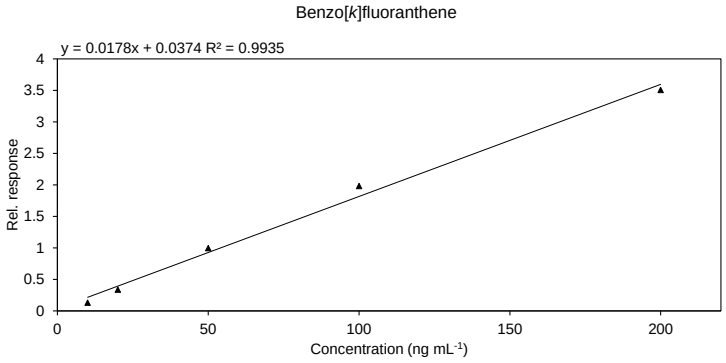

Figure C.12 – Calibration curve of benzo[k]fluoranthene based on relative response. All standards contained 50 ng mL^{-1} internal standard.

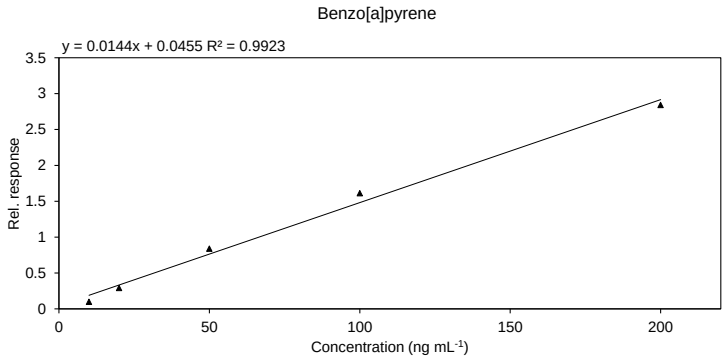

Figure C.13 – Calibration curve of benzo[a]pyrene based on relative response. All standards contained 50 ng mL^{-1} internal standard.

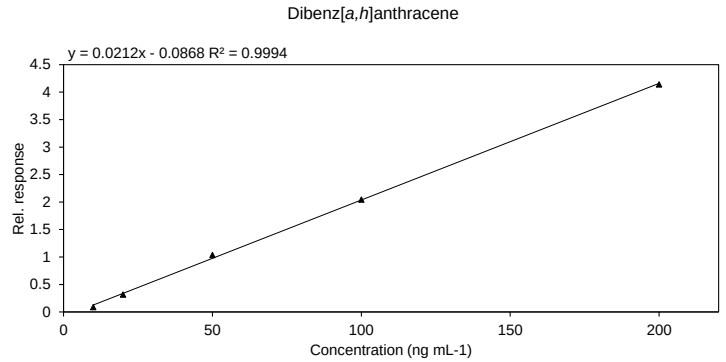

Figure C.14 – Calibration curve of dibenz[a,h]anthracene based on relative response. All standards contained 50 ng mL^{-1} internal standard.

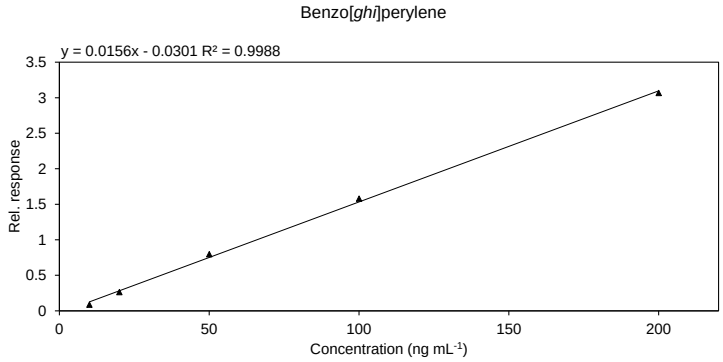

Figure C.15 – Calibration curve of benzo[*ghi*]perylene based on relative response. All standards contained 50 ng mL^{-1} internal standard.

C.3 Calibration curves of PCB target analytes

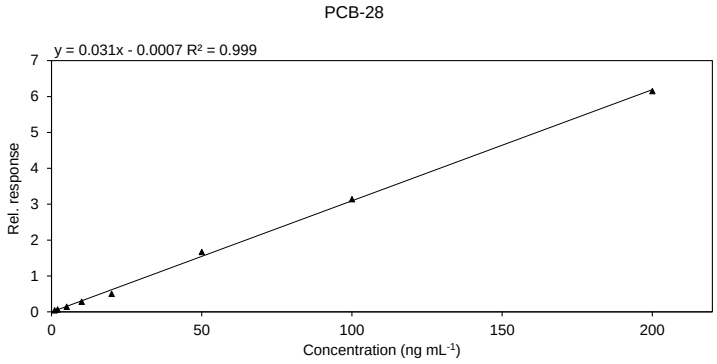

Figure C.16 – Calibration curve of PCB-28 based on relative response. All standards contained 50 ng mL^{-1} internal standard.

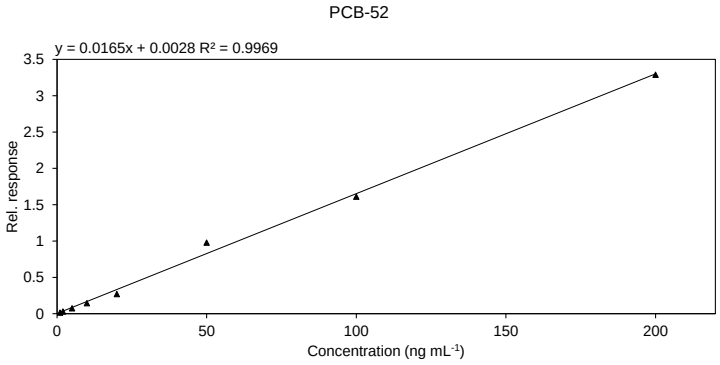

Figure C.17 – Calibration curve of PCB-52 based on relative response. All standards contained 50 ng mL^{-1} internal standard.

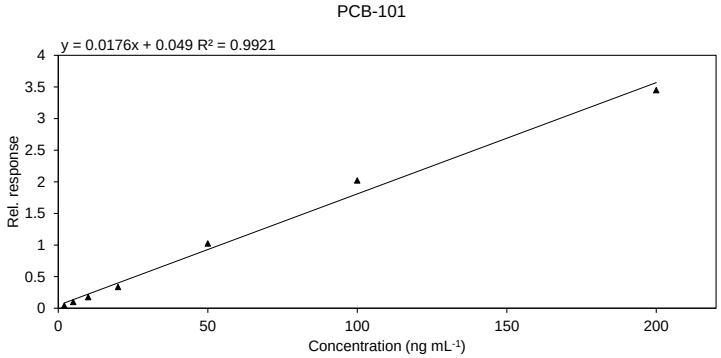

Figure C.18 – Calibration curve of PCB-101 based on relative response. All standards contained 50 ng mL^{-1} internal standard.

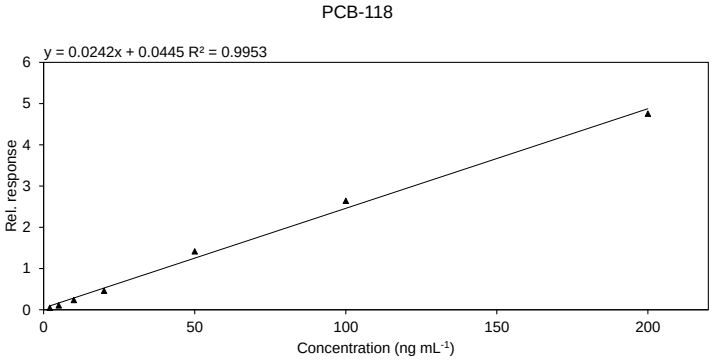

Figure C.19 – Calibration curve of PCB-118 based on relative response. All standards contained 50 ng mL^{-1} internal standard.

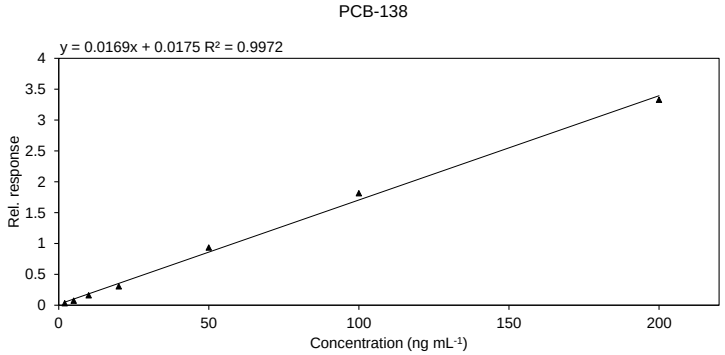

Figure C.20 – Calibration curve of PCB-138 based on relative response. All standards contained 50 ng mL^{-1} internal standard.

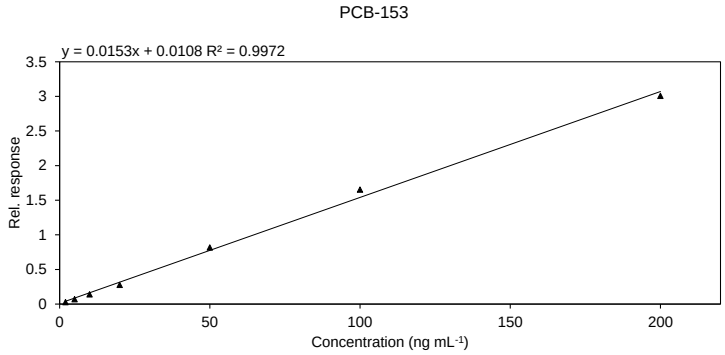

Figure C.21 – Calibration curve of PCB-153 based on relative response. All standards contained 50 ng mL^{-1} internal standard.

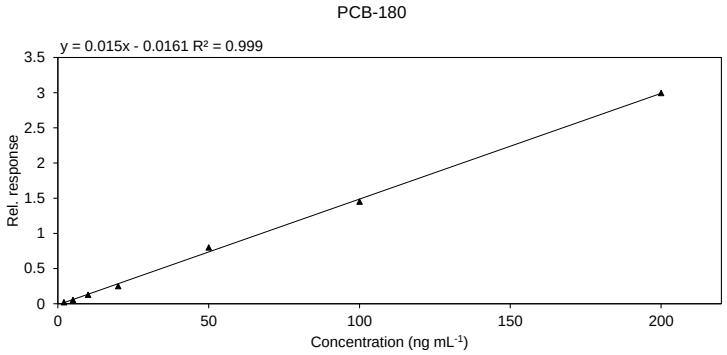

Figure C.22 – Calibration curve of PCB-180 based on relative response. All standards contained 50 ng mL^{-1} internal standard.

C.4 Matrix effects

Table C.2 – Matrix factors (MF) and matrix effects (ME%) of 16 PAH and 7 PCB target analytes in extracted soil samples.

	50 ng mL^{-1}		100 ng mL^{-1}	
Analyte	**MF**	**ME (%)**	**MF**	**ME (%)**
NAP	0.98	-2	0.88	-12
ACY	1.09	9	1.05	5
ACE	1.30	30	1.03	3
FLU	1.08	8	1.01	1
PHE	1.15	15	1.02	2
ANT	1.02	2	0.97	-3
FLT	1.07	7	1.05	5
PYR	1.15	15	1.04	4
BaA	1.20	20	1.13	13
CHR	1.18	18	1.02	2
BbF	1.30	30	1.24	24
BkF	1.15	15	1.08	8
BaP	1.14	14	1.11	11
IND	1.28	28	1.36	36
DBA	1.23	23	1.08	8
BgP	1.20	20	1.17	17
PCB-28	0.98	-2	0.99	-1
PCB-52	0.93	-7	1.06	6
PCB-101	0.92	-8	1.00	0
PCB-118	0.91	-9	1.06	6
PCB-138	0.94	-6	1.07	7
PCB-153	0.99	-1	1.07	7
PCB-180	0.92	-8	1.09	9

C.5 Dataset of PAHs concentration in surface soils

Table C.3 – Detection rates (DR), mean, median, minimum and maximum detected concentrations in ng g^{-1} of 10 PAHs in Svalbard surface soils for the total number of analyzed samples in this study (n=15). DR is expressed as ratio (number of samples above LOD/ total number of samples). Only concentrations above LOD are displayed. Calculation of mean, median, minimum and maximum is based on values >LOD.

	DR	Mean (ng g^{-1})	Median (ng g^{-1})	Min (ng g^{-1})	Max (ng g^{-1})
NAP	9/15	57.0	28.8	5.8	177.4
FLU	9/15	12.1	12.1	3.0	24.8
PHE	11/15	63.1	26.9	1.9	201.2
ANT	4/15	24.6	27.2	10.4	33.5
FLT	4/15	32.0	30.9	9.4	56.6
PYR	5/15	26.2	28.1	7.2	53.2
BaA	3/15	16.4	17.2	6.7	25.4
CHR	5/15	38.7	43.2	25.2	47.6
BbF	4/15	15.0	12.7	12.1	22.6
BaP	6/15	36.4	30.6	18.5	85.1
$\sum$PAHs	11/15	192.6	91.6	12.4	533.6
$\sum$carcinogenic PAHs[1]	8/15	69.7	79.5	18.5	115.6
Retene signal	5/15				

[1] = $\sum$(BaA, CHR, BbF, BkF, BaP, IND, DBA)

Table C.4 – Dataset of PAHs composition of surface soil samples investigated in this study. Only PAHs where concentrations were > LOD are presented. Concentrations are given in ng g^{-1} surface soil. Study areas are indicated with BDE=Brøggerdalen, east side of Bayelva, BDW=Brøggerdalen, west side of Bayelva, GB=Gåsebu, KI=Kiærstranda and NDM=Nordre Diesetvatnet (Mitrahalvøya). See Tab 2.1 for abbreviations of single PAH compounds.

Study area	Sample ID	NAP	FLU	PHE	ANT	FLT	PYR	BaA	CHR	BbF	BaP	∑PAHs
BDE	S4	39.3	12.8	82.4	<LOD	<LOD	7.6	<LOD	<LOD	<LOD	21.0	163.1
BDE	S5	133.2	24.8	151.2	31.2	40.0	35.2	17.2	43.2	22.6	32.6	531.2
BDE	S6	177.4	22.5	124.0	33.5	21.9	28.1	6.7	25.2	12.1	29.8	481.2
BDW	S1	5.8	<LOD	21.2	<LOD	<LOD	<LOD	<LOD	<LOD	<LOD	85.1	112.1
BDW	S2	18.7	3.0	26.9	10.4	<LOD	<LOD	<LOD	<LOD	<LOD	18.5	77.4
BDW	S3	8.0	6.6	1.9	<LOD	<LOD	<LOD	<LOD	<LOD	<LOD	<LOD	16.5
GB	S7	88.2	6.9	201.2	23.1	56.6	53.2	25.4	47.6	<LOD	31.3	533.6
GB	S8	<LOD	<LOD	<LOD	<LOD	<LOD	<LOD	<LOD	<LOD	<LOD	<LOD	<LOD
GB	S9	<LOD	12.1	8.5	<LOD	9.4	7.2	<LOD	<LOD	<LOD	<LOD	37.2
KI	S10	28.8	6.0	44.7	<LOD	<LOD	<LOD	<LOD	<LOD	12.1	<LOD	91.6
KI	S11	<LOD	<LOD	12.4	<LOD	<LOD	<LOD	<LOD	<LOD	<LOD	<LOD	12.4
KI	S12	14.0	14.6	20.2	<LOD	<LOD	<LOD	<LOD	<LOD	13.3	<LOD	62.0
NDM	S13	<LOD	<LOD	<LOD	<LOD	<LOD	<LOD	<LOD	<LOD	<LOD	<LOD	<LOD
NDM	S14	<LOD	<LOD	<LOD	<LOD	<LOD	<LOD	<LOD	<LOD	<LOD	<LOD	<LOD
NDM	S15	<LOD	<LOD	<LOD	<LOD	<LOD	<LOD	<LOD	<LOD	<LOD	<LOD	<LOD

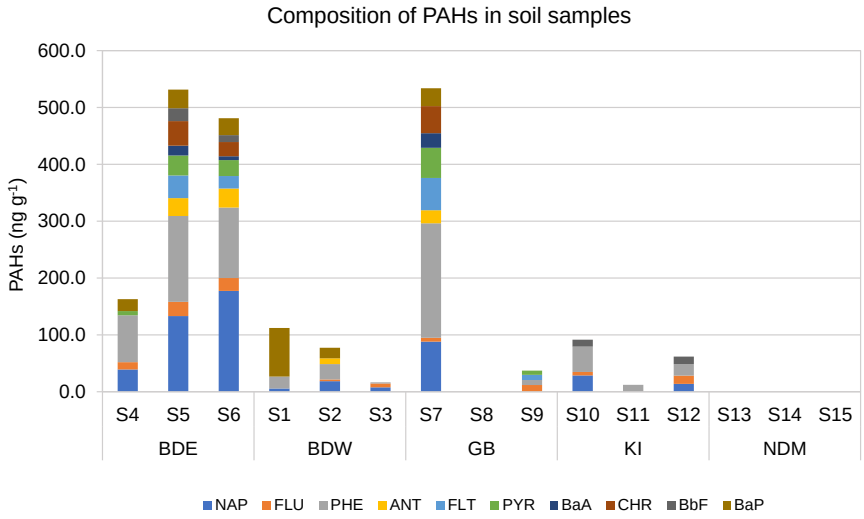

Figure C.23 – Composition of PAHs in the 15 surface soil samples collected in this study. Study areas are indicated with BDE=Brøggerdalen, east side of Bayelva, BDW=Brøggerdalen, west side of Bayelva, GB=Gåsebu, KI=Kiærstranda and NDM=Nordre Diesetvatnet (Mitrahalvøya). See Tab 2.1 for abbreviations of single PAH compounds.

Sylvia Weging

NTNU
Norwegian University of
Science and Technology

UNIS
The University Centre in Svalbard